



**UNIVERSITÉ  
DE GENÈVE**

**FACULTÉ DES SCIENCES**

Département de physique  
nucléaire et corpusculaire



# First Results from the DAMPE Mission

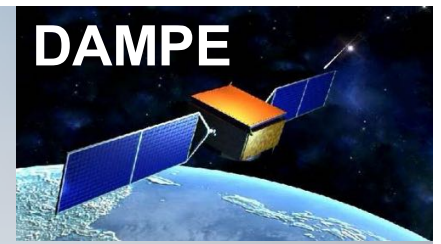
**Xin Wu**

*Department of Nuclear and Particle Physics  
University of Geneva, Switzerland*

**Seminar at Laboratoire de l'Accélérateur Linéaire (LAL)  
Univ. Paris-Sud, CNRS/IN2P3  
June 1, 2018**

**Launched >2 years ago, 17/12/2015**

**High energy particle physics  
experiment in space**



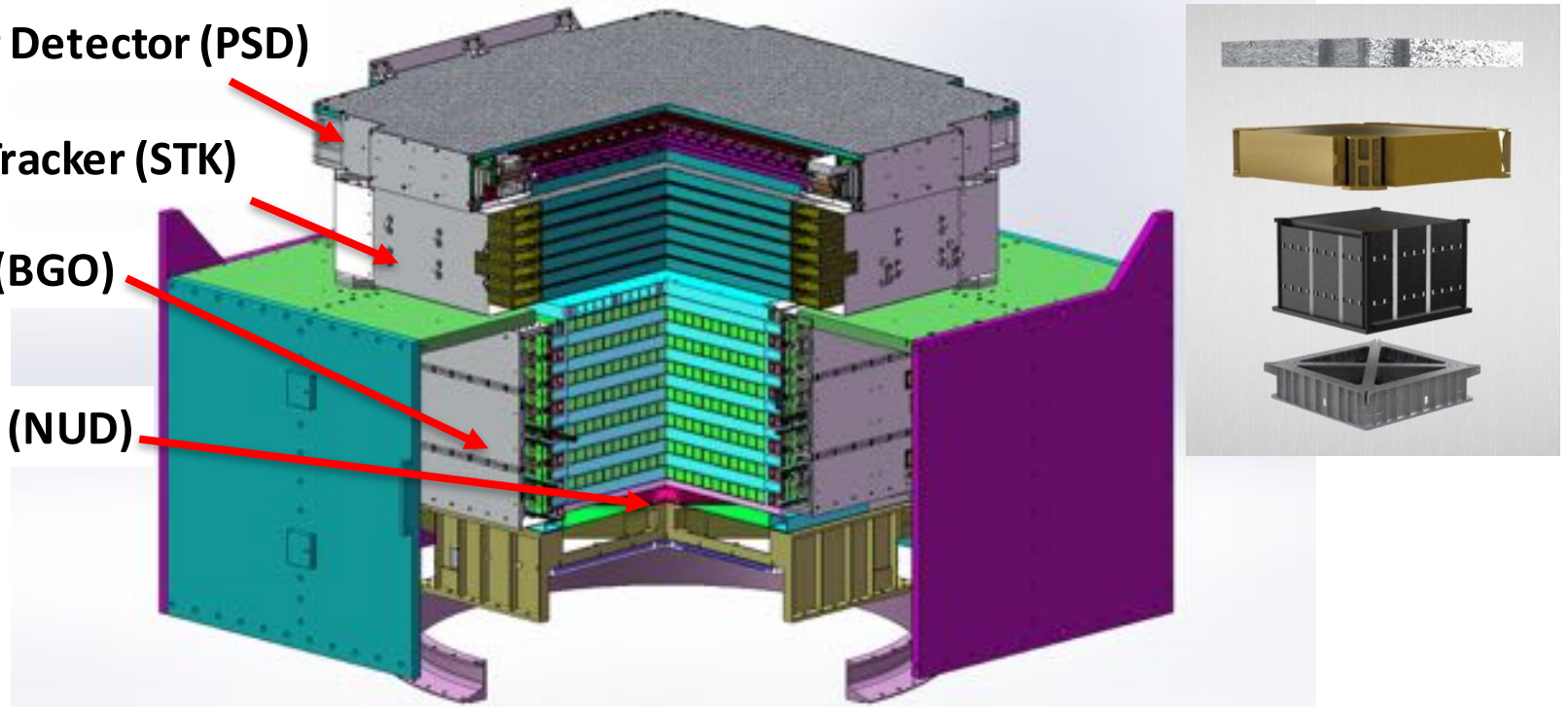
# The Detector

Plastic Scintillator Detector (PSD)

Silicon-Tungsten Tracker (STK)

BGO Calorimeter (BGO)

Neutron Detector (NUD)



- ✓ Charge measurements (PSD and STK)
- ✓ Precise tracking with Si strip detectors (STK)
- ✓ Tungsten photon converters in tracker (STK)
- ✓ Thick imaging calorimeter (BGO of  $32 X_0$ )
- ✓ Extra hadron rejection (NUD)

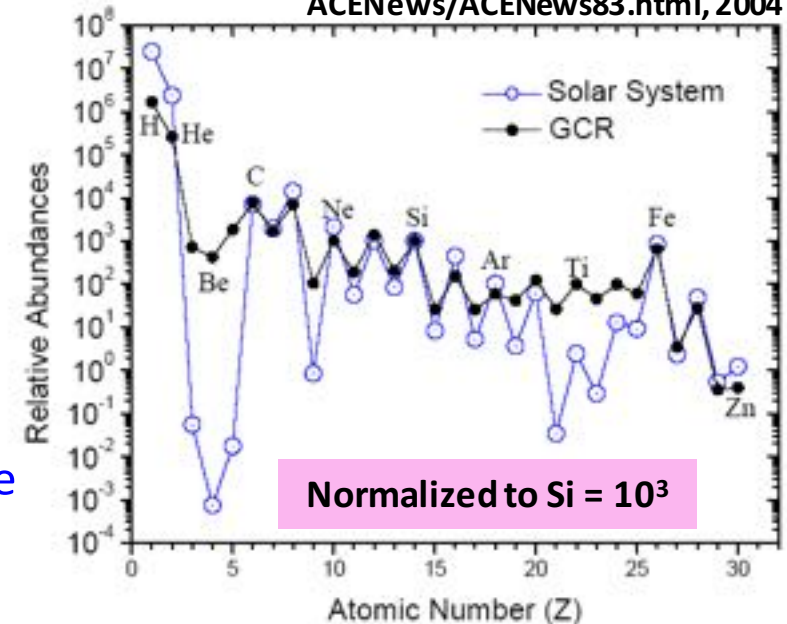


high energy  $\gamma$ -ray,  
electron and cosmic ray  
nuclei telescope

# Why study particles in space?

- Our Galaxy is immersed in a halo of high energy **charged particles** (Cosmic Rays)
  - Mainly nuclei consistent with stellar material: p (90%), He, C, O, ... Fe, ...
    - But also secondary ions: Li, Be, B, sub-Fe, pbar, ...
    - and electrons, positrons ( $\lesssim 1\%$ )
- Gamma-rays, neutrinos (not covered here)
  - Source pointing capability
    - gamma-ray/neutrino astronomy
- Observed particles with energy up to  $\sim 10^{20}$  eV (=100 Million TeV = 100 EeV)
  - Up to PeV, best measured in space, above the atmosphere, for precision and composition

<http://www.srl.caltech.edu/ACE/ACENews/ACENews83.html>, 2004



Cosmic particles are messengers of high energy processes  
("cosmic particle accelerators")  $\Rightarrow$  fundamental  
implications on astronomy, cosmology and particle physics

Essential ingredient of the Multi-messenger high energy astrophysics

# All started with the leaking charge ...

- In 1785 Charles-Augustin Coulomb observed isolated charge leaking out in air



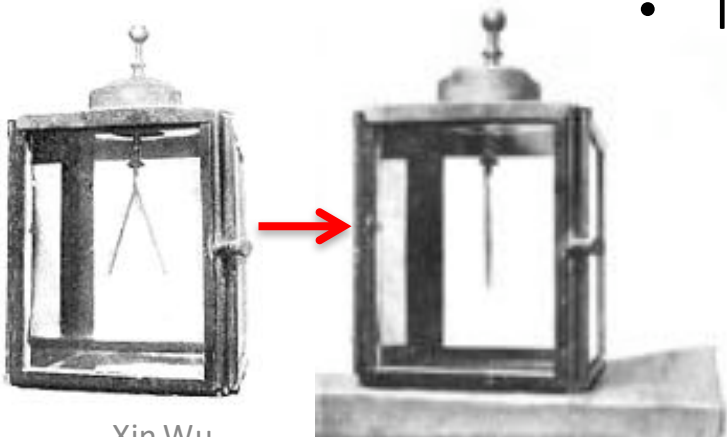
612 MÉMOIRES DE L'ACADÉMIE ROYALE

*TROISIÈME MÉMOIRE  
SUR L'ÉLECTRICITÉ ET LE MAGNÉTISME.  
De la quantité d'Électricité qu'un corps isolé perd  
dans un temps donné, soit par le contact de l'air  
plus ou moins humide, soit le long des soutiens  
plus ou moins idio-électriques.*

Par M. COULOMB.

... so there is  
“radioactivity”  
in the air, but  
where does  
this radiation  
come from?

- In 1896 Becquerel discovered radioactivity, also ...



Xin Wu



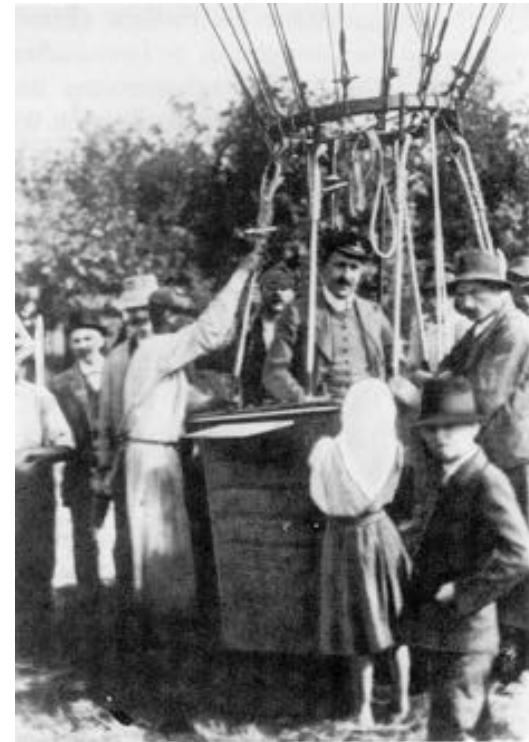
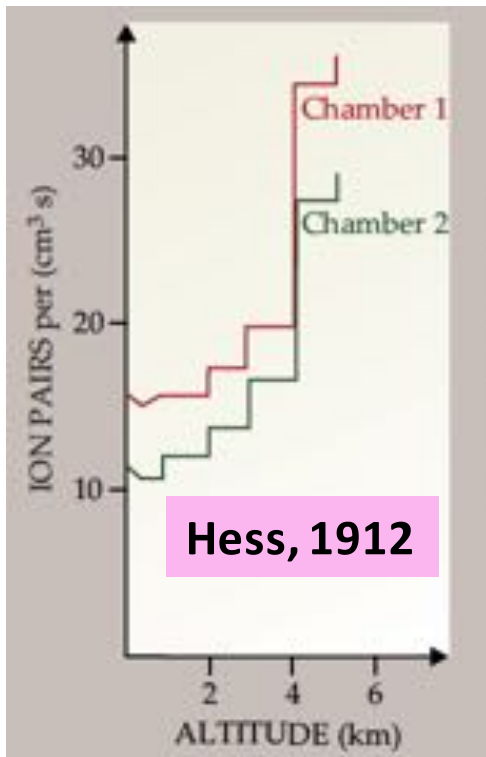
LAL,

Electroscope can be  
discharged by  
radioactivity!

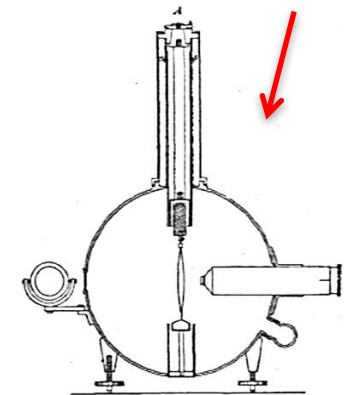
# The Discovery of “Cosmic Radiation”

- Many searches ... Elster & Geitel (1899), **metal box**; C.T.R. Wilson (1901), **railway tunnel**; Wulf (1909), **Eiffel tower**; Gockel (1910), **balloon**; Pacini (1911), **lake** ... led to the **discovery by V. Hess (1912)** in a balloon up to 5000 m
  - Conclusive evidence of increasing penetrating radiation with rising altitude  
→ extraterrestrial origin!

Space particle physics was born!



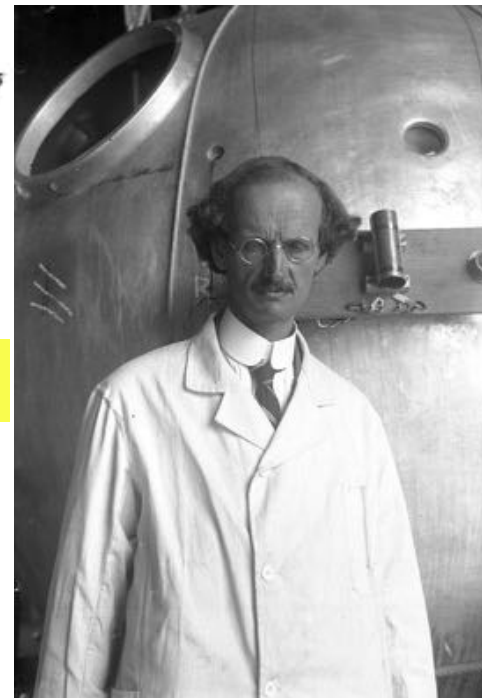
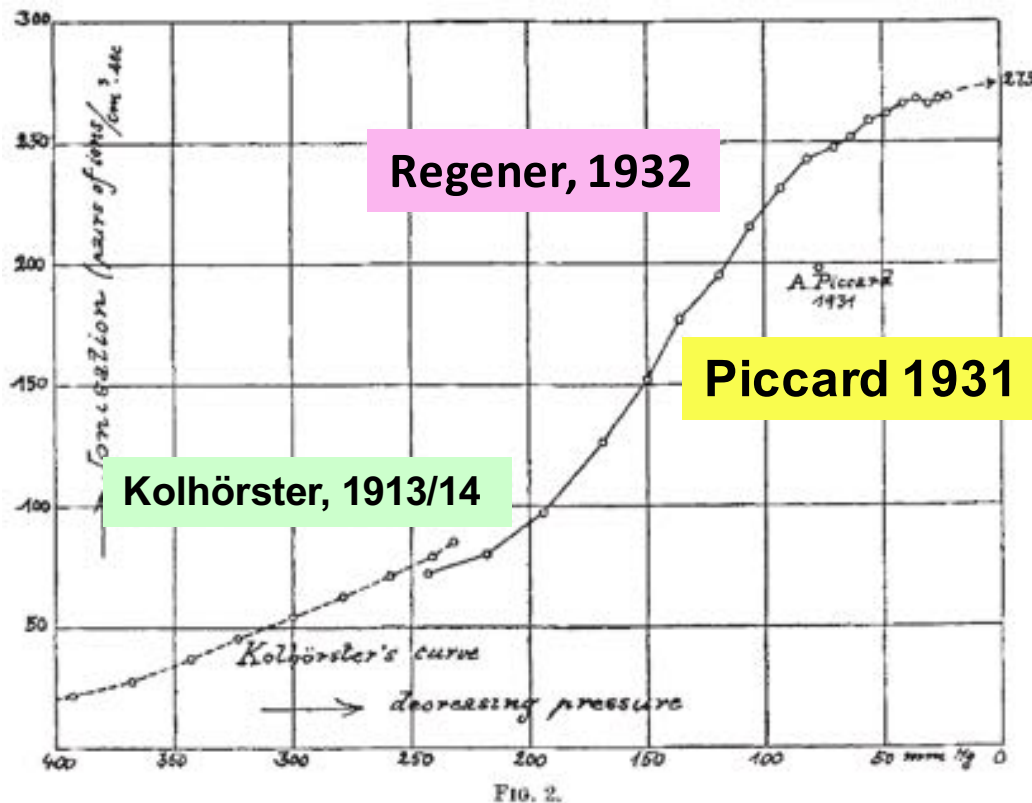
Detector!



Wulf Electroscope

# Going to the Stratosphere

- Auguste Piccard developed a **pressured aluminum cabin**
  - Measured cosmic rays up to the stratosphere (**~16 km**) in 1931
- Erich Regener extended the measurement to an altitude of **28km** in 1932 with small unmanned rubber-balloons



First "space-lab"!



First "astronauts"!



Studies of cosmic rays on ground led to the discoveries of: positron (1932), muon (1936), charged pion (1947),  $K$ ,  $\Lambda$ ,  $\Sigma$ ,  $\Xi$ , ... (1950's)

# From balloons to satellites and space stations

- **Many discoveries with balloons in 1930-40's**
  - Geomagnetic effects (1927), CR mainly charged particles (1929)  $\Rightarrow$  mainly positively charged (1933)  $\Rightarrow$  mainly protons (1940), heavy nuclei observed (1948)
- **Space age: particle detectors were key elements on first satellites**
  - Sputnik-2: launched Nov. 3, 1957 carried 2 Geiger counters
    - Indication of the Van Allen radiation belt
  - Explorer-1 (First US satellite): launched in Jan. 1, 1958
    - Discovery of the Van Allen belt with a Geiger counter
- **1960: First evidences of cosmic ray electrons ( $\sim 0.5$  GeV) in 2 balloon experiments, with multi-plate cloud chamber and NaI/scintillator counters**
  - 1963: First  $e^+/e^-$  ratio (0.1 – 1 GeV) with magnet in balloon experiments
- **Magnetic spectrometers** continues with balloons and satellites, leading to the high precision **AMS-02** experiment, launched in **2011**
- A long series of balloons and satellites experiments based on **calorimeters**, leading to the high precision **DAMPE** mission, launched in Dec. **2015**
- **Gamma-ray** detection technologies successfully deployed in space, leading to the high precision and large acceptance **FERMI** observatory launched in **2008**

Xi **Particle physics in space has entered a precision measurement era!**



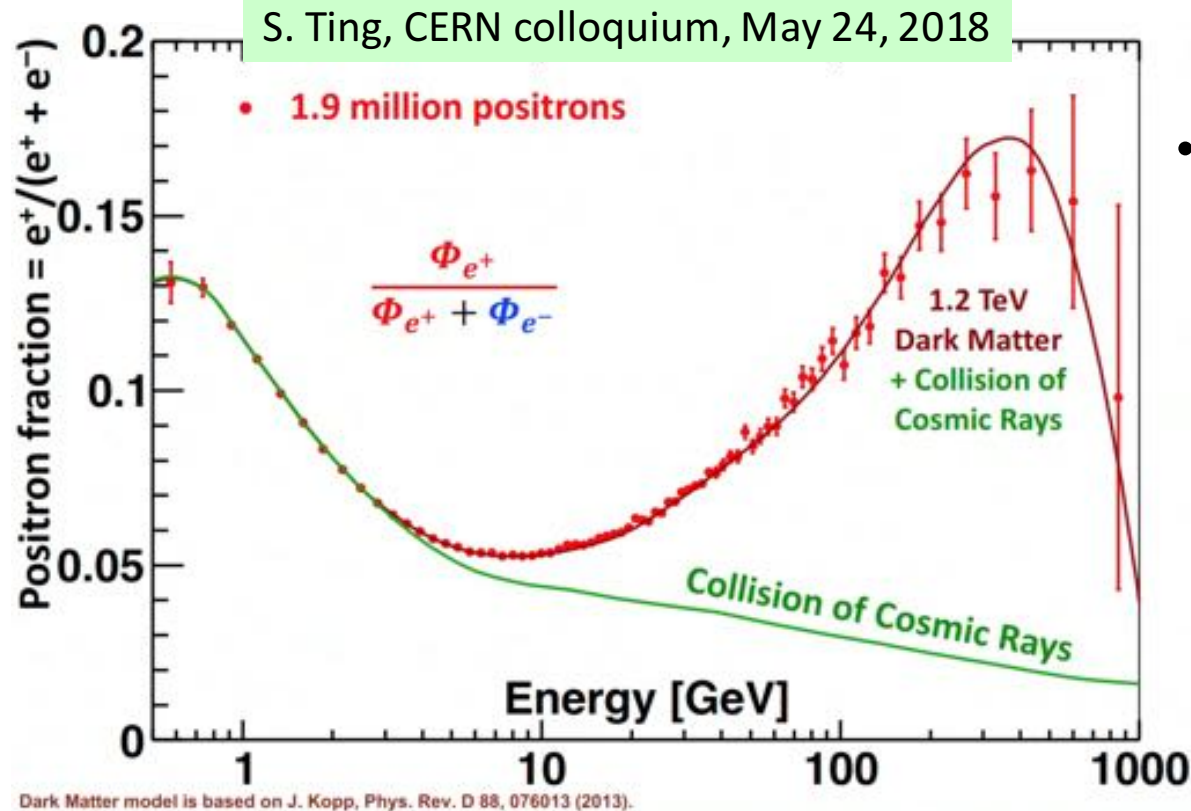
# Many surprises!

- **Spectra do not follow the simple power law, as observed with lower precision data**
- **Many new spectral features observed with high precision data, reflecting the complex nature of cosmic rays**
  - Particles can be produced from different sources at different times at different distances, with different acceleration mechanisms, then travel through different paths to the Earth
    - Astrophysical sources (eg. SNR, Pulsar, AGN) or exotic sources (eg. DM)
    - Propagation/secondary production effects
- **Non-exhaustive list of new and “unexpected” observations**
  - Cosmic ray positron fraction “anomaly”
  - Cosmic ray electron + positron spectral breaks
  - Proton and light nuclei spectral breaks
  - Flattening antiproton fraction
  - GeV gamma-ray excess at the Galactic Center
  - ...

**Still a long way from a “Standard Model of Cosmic Ray Physics”!**

# Positron fraction “anomaly”

- Positrons were thought to be mainly secondary  $\Rightarrow$  single power law
  - Secondary: from cosmic rays interacting with Interstellar medium



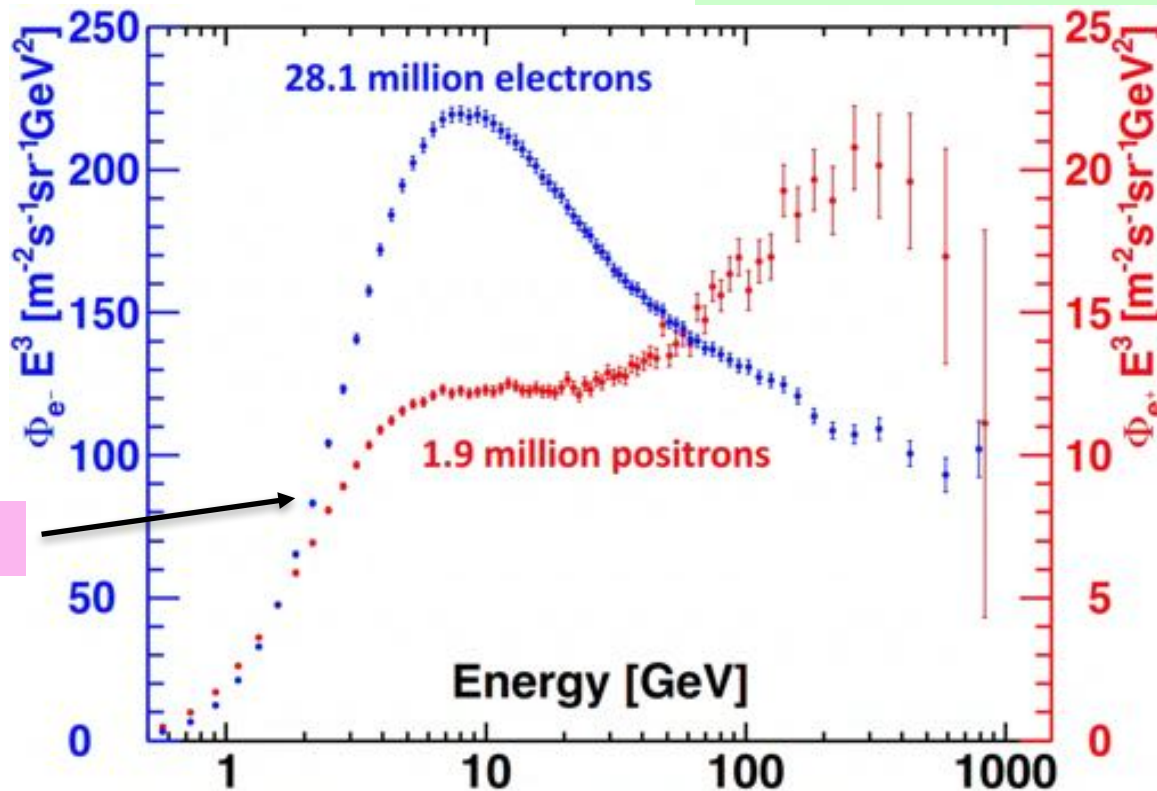
- Positrons may have a primary contribution
  - Primary: EM cascade in pulsar magnetic field or through pion production in shock acceleration (pulsar, SNR), or DM

But electron and positron may have different contributing sources  $\Rightarrow$  directly look at the individual fluxes

# Positron and electron individual fluxes

- AMS data both electron and positron do not follow simple power law
  - Source(s) contribution, or new propagation effect?

S. Ting, CERN colloquium, May 24, 2018

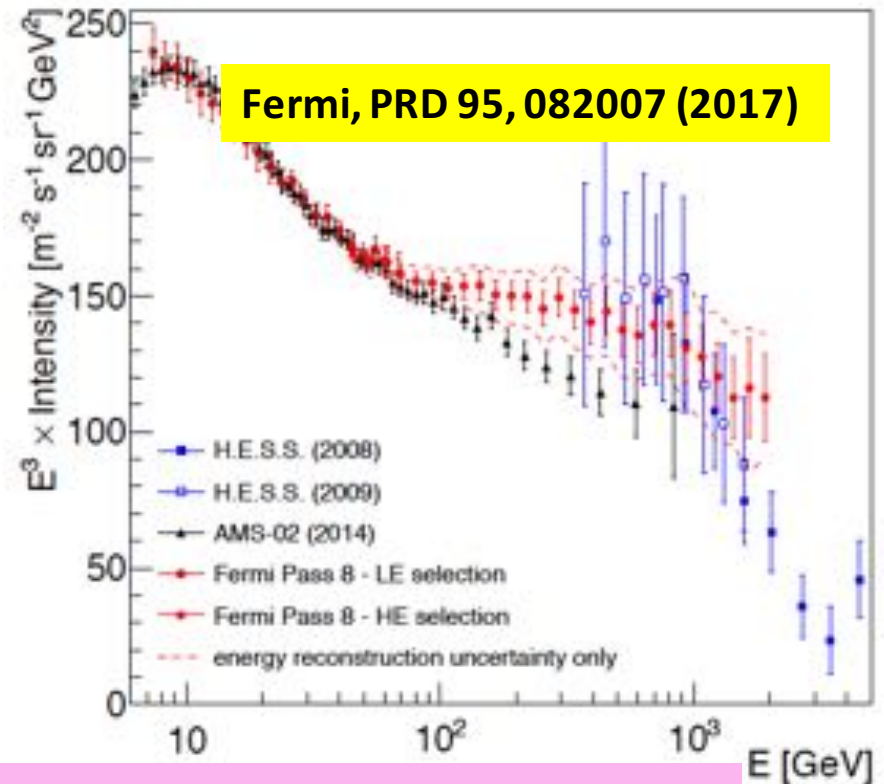
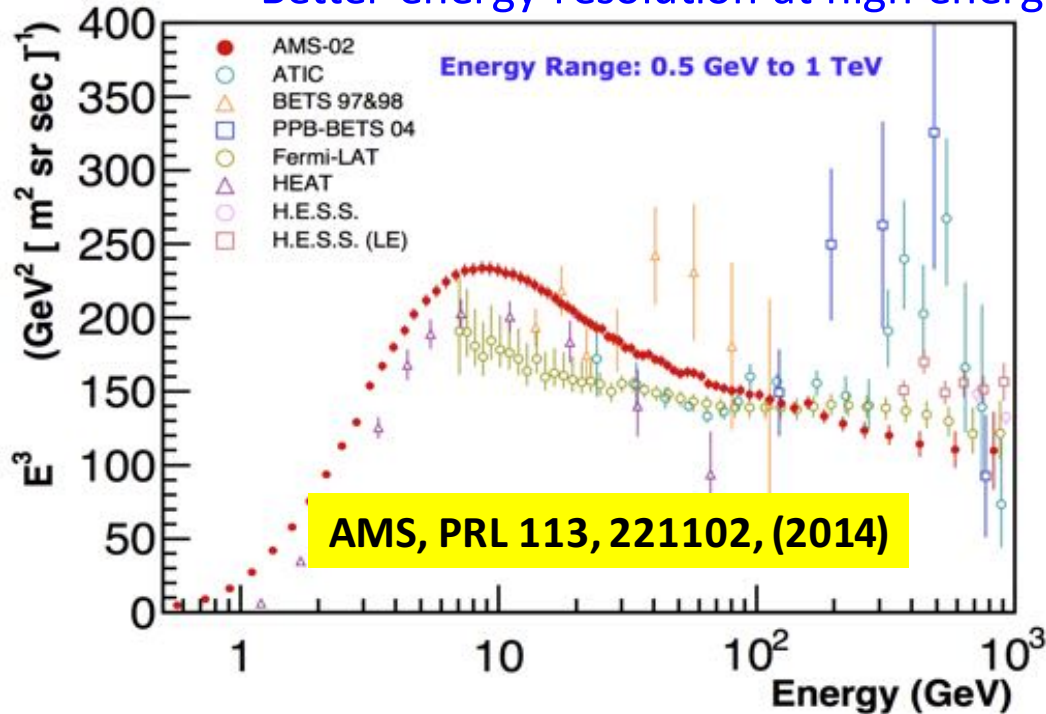


Need more data to measure the cut-off of the positron source contribution  
⇒ understand the nature of the source (DM? pulsar? Propagation?)

# Electron + positron (CRE) flux

- AMS-02 published CRE spectrum up to 1 TeV, Fermi up to 2 TeV
- CRE flux can also be measured by thick calorimetric detectors (DAMPE, CALET)

– Better energy resolution at high energy



Hardening  $\sim 30$  GeV seen by AMS and Fermi

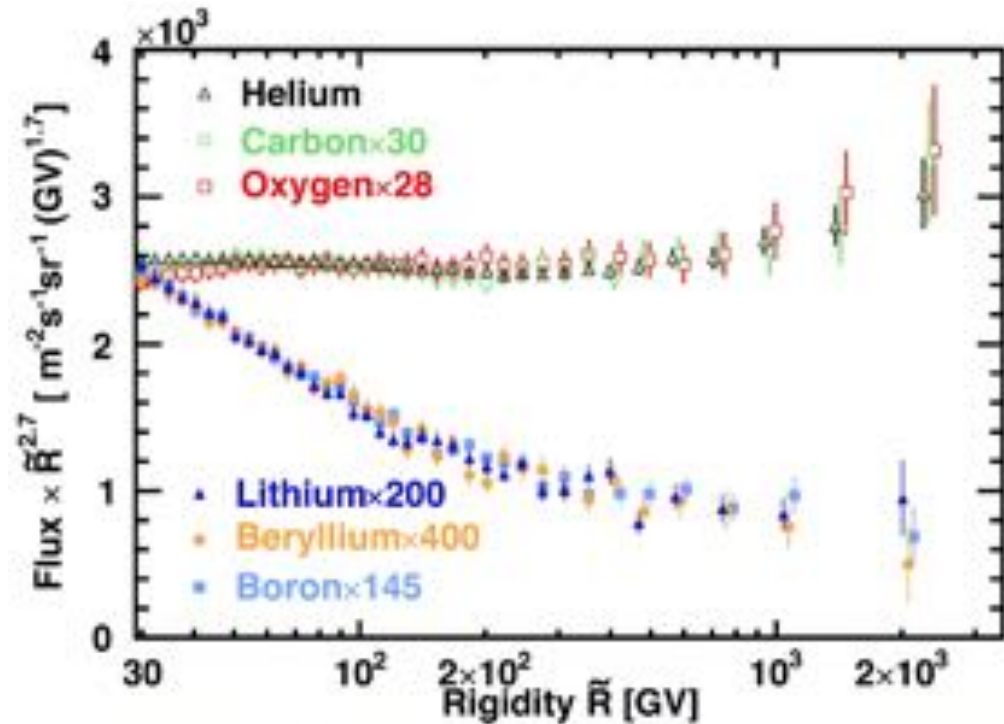
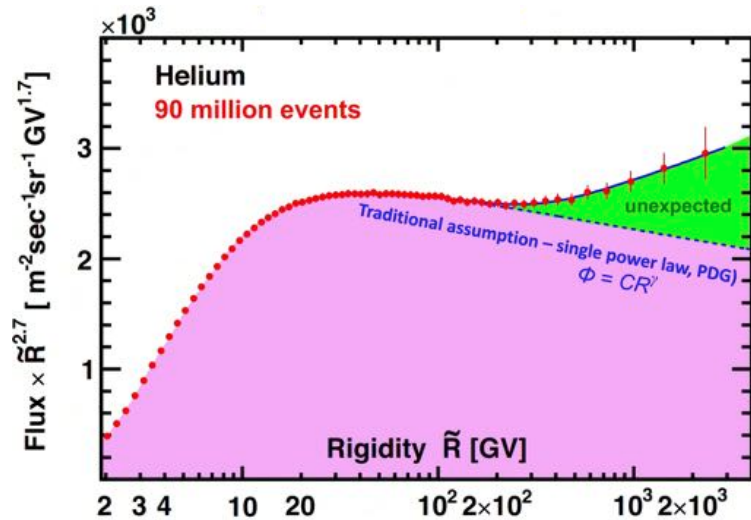
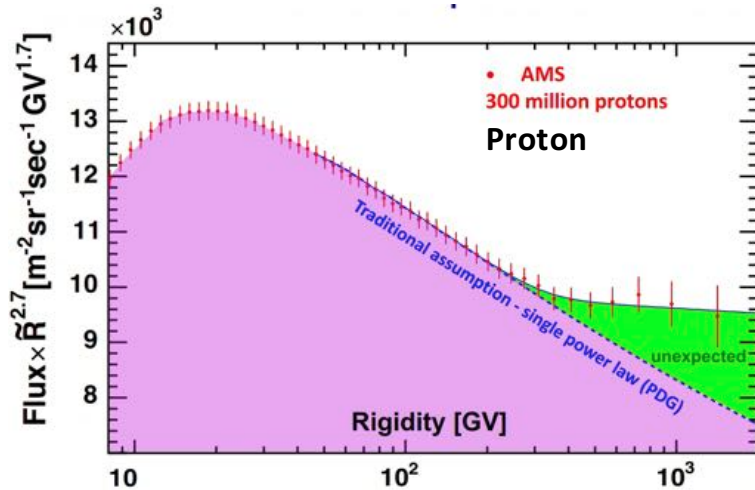
Intriguing “features” around 1 TeV

But: Fermi large systematic error due to thin calorimeter, HESS large systematic error due to shower modeling in atmosphere and energy scale (15%, not shown in figure above)

Xin **DAMPE will produce high statistics and precise measurement at multi-TeV region**

# Proton and light nuclei rigidity spectra, up to $\sim$ TV

S. Ting, CERN colloquium, May 24, 2018



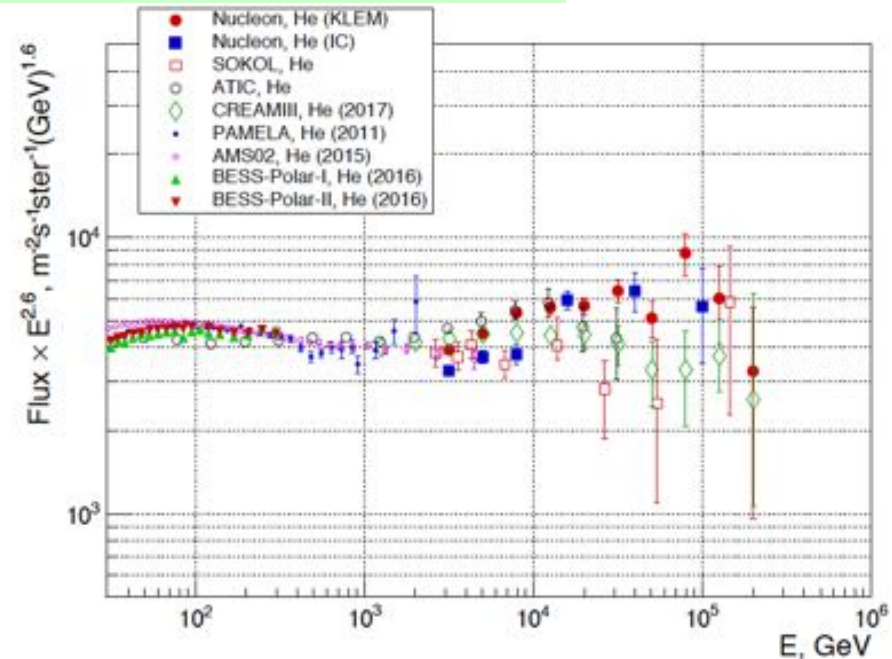
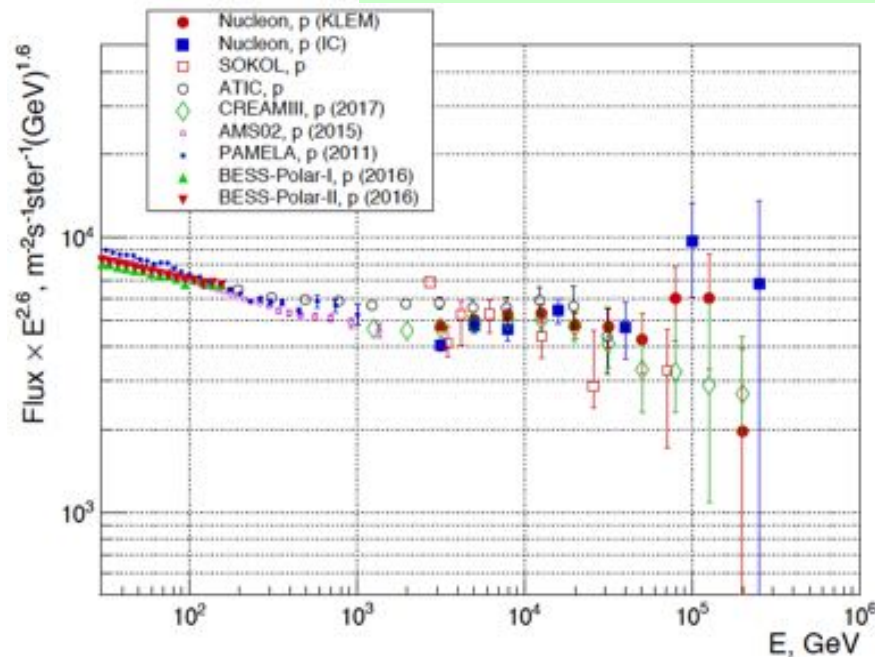
There is a general single power law breakdown around 200 GV!

Acceleration? Propagation? Mixed?

# Proton and Helium high energy spectra, 1 - 100 TeV

- 1– 100 TeV range : explored by CREAM, ATIC, NUCLEON

Cream-III, ApJ 893, 5 (2017), NUCLEON, JCAP 07, 020 (2017)



Another spectral hardening  $> 1$  TeV? and a softening  $> 10$  TeV?

New measurements to come from DAMPE, CALET and ISS-CREAM

- Near future: up to PeV to connect to ground-based EAS measurements
  - **HERD**: onboard China's Space Station (CSS), ~2025

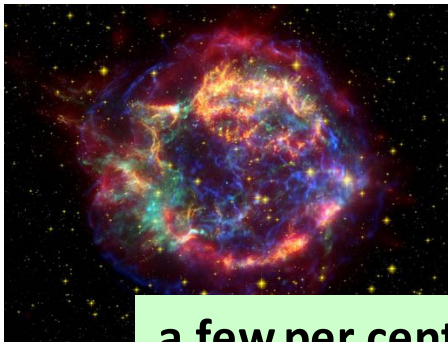
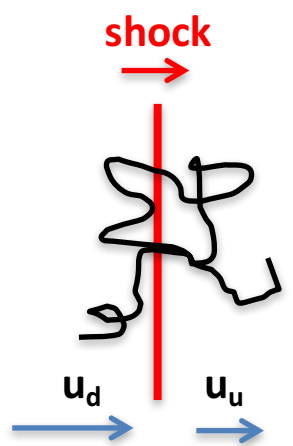
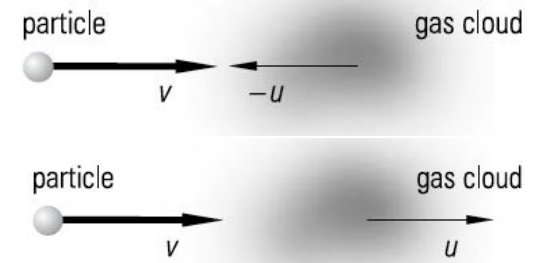
# Why power law?

- A power law can result from a process with **energy independent acceleration rate** and **energy independent escape probability**
  - Energy gained after each acceleration :  $\langle \Delta E / E \rangle = \alpha$
  - Escape probability between each acceleration :  $P_{esc}$ 
    - Acceleration probability :  $1 - P_{esc}$
- In **steady state**, the number of particles with energy above  $E_n = E_0(1 + \alpha)^n$ :
  - $N(E > E_n) = N(n \text{ accelerations}) + N(n + 1 \text{ accelerations}) + \dots$ 

$$= N_0 \sum_{m=n}^{\infty} (1 - P_{esc})^m = \frac{N_0}{P_{esc}} (1 - P_{esc})^n$$
  - Those escaped (observed):  $N_{esc}(E > E_n) = P_{esc} N(E > E_n) = N_0 (1 - P_{esc})^n$ 
    - Replace n with  $n = \frac{\log(E_n/E_0)}{\log(1+\alpha)}$
  - $N_{esc}(E > E_n) = const. \times E_n^{-\gamma}$ ,  $\gamma = -\frac{\log(1-P_{esc})}{\log(1+\alpha)}$
- The differential spectrum is then  $\frac{dN}{dE} = const. \times E^{-\gamma-1}$

# Fermi Acceleration and SNR

- Fermi (1949)** : Cosmic rays are originated and accelerated primarily in the interstellar space of the Galaxy by **collisions against moving magnetic fields**
  - Fermi mechanism (of 2<sup>nd</sup> order): head-on (gain) more likely than tail-end (loss)  $\Rightarrow$  on average  $\langle \Delta E/E \rangle \propto \beta_{\text{cloud}}^2$   $\beta_{\text{cloud}} \sim 10^{-4}$ 
    - Not efficient enough**: Takes too long to accelerate
    - Need sufficient injection (initial) energy
    - Predicts power law**, but not universal
- (1977-78)** Similar mechanism, but more efficient, with shocks in space plasmas
  - Fermi mechanism of 1<sup>st</sup> order : particle crossing back and forth of the shock front always gain energy  $\Rightarrow \langle \Delta E/E \rangle \propto \Delta \beta_{\text{shock}}$   $\beta_{\text{shock}} \sim 10^{-2}$ 
    - Efficient:  $\sim 1000$  years to reach  $10^{14}$  eV (0.1 PeV)
    - Universal power law, independent of particle energy!
  - Supernova Remnants (SNRs):** plausible source for cosmic rays up to  $\sim 10^{15}$  eV
    - Can explain the bulk of CR energy density ( $\sim 1 \text{ eV/cm}^3$ ) if few % of the kinetic energy released goes into the acceleration of protons and nuclei



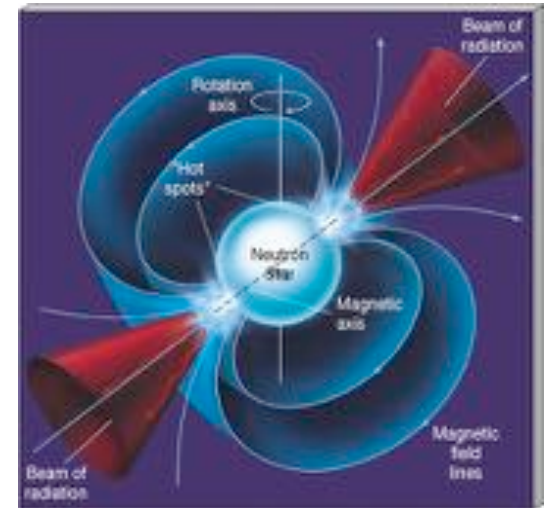
a few per century



# Pulsars, Binaries and AGNs

- Pulsars (fast spinning, highly magnetized neutron stars resulting from SN explosions)
  - Strong electric fields generated by rotating strong magnetic fields
  - Capable of converting rotational kinetic energy into radio emission (observed),  $\gamma$ -rays (observed), cosmic rays including  **$e^+e^-$  pairs**
    - Possible origin of cosmic rays in the galactic to extragalactic transition region ( $10^{15} - 10^{19}$  eV)
- Binaries with neutron star or pulsar
  - **Accretion process** generates high speed particles falling into the accretion disk, then accelerated in rotating magnetic fields
    - Acceleration to  $10^{19}$  eV possible
- **Accretion disks of compact objects are commonly associated with highly collimated relativistic jets**
  - Fermi acceleration in jets (turbulences) associated with Active Galactic Nuclei (AGN) could be the origin of extragalactic cosmic rays

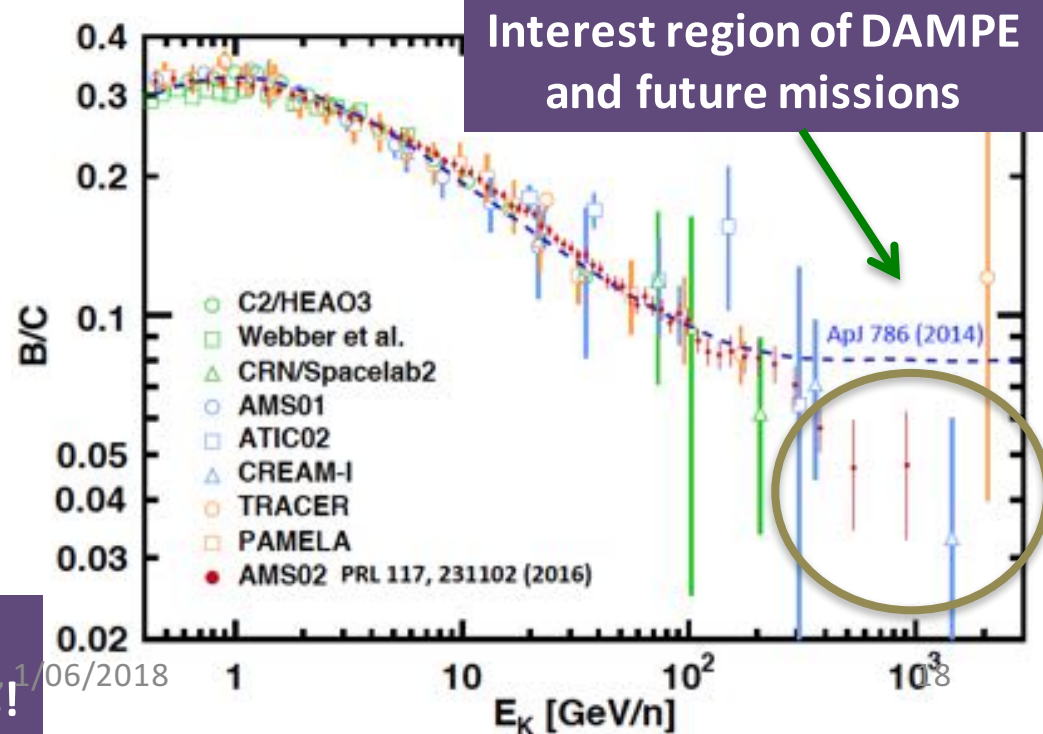
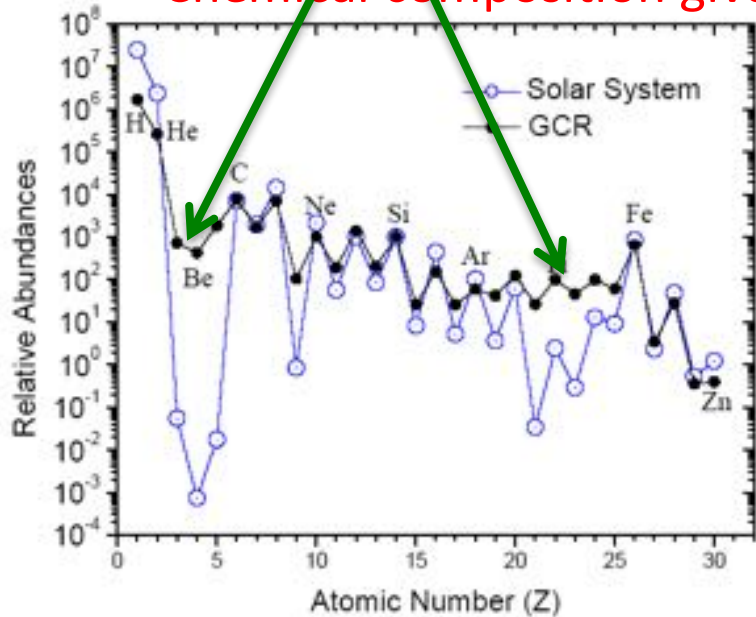
$$\nabla \times \vec{E} = \frac{\partial \vec{B}}{\partial t}$$



# Cosmic Ray Propagation in ISM

- Cosmic rays diffuse through the **interstellar medium** (ISM)
  - Random scattering with discontinuities of the interstellar magnetic fields
    - Direction becomes isotropic; Spectrum is modified:  $E^{-\gamma} \rightarrow E^{-\gamma-\delta}$
  - Interaction with ambient material in ISM (~90% H, 10% He)
    - **Production of secondary cosmic ray particles**
    - Some are mainly secondary: Li, Be, B, sub-Fe group, ...

• **Chemical composition give unique information on sources and propagation**

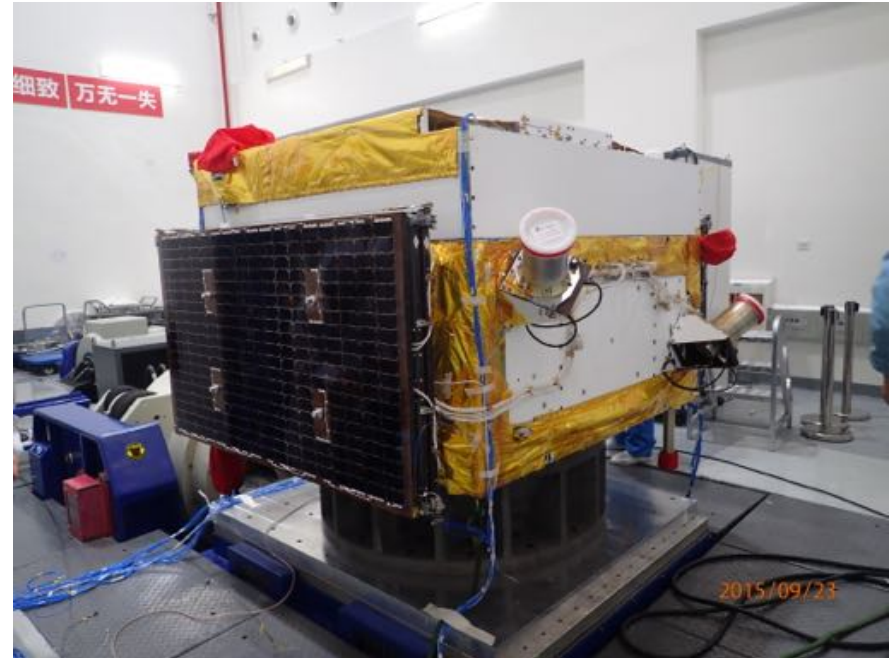


Secondary-to-primary ratios e.g. B/C, are useful to determine propagation parameters!

# The DAMPE Satellite



EQM, Oct. 2014, CERN



Integrated satellite, Sept. 2015, Shanghai

Weight : 1450/1850 kg (payload/satellite)

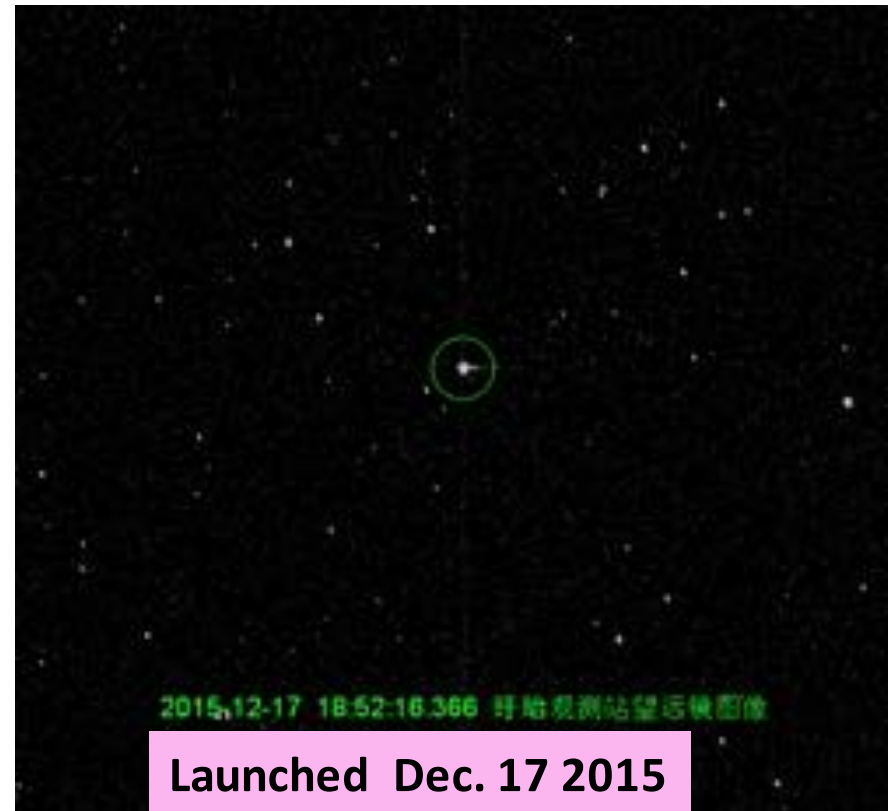
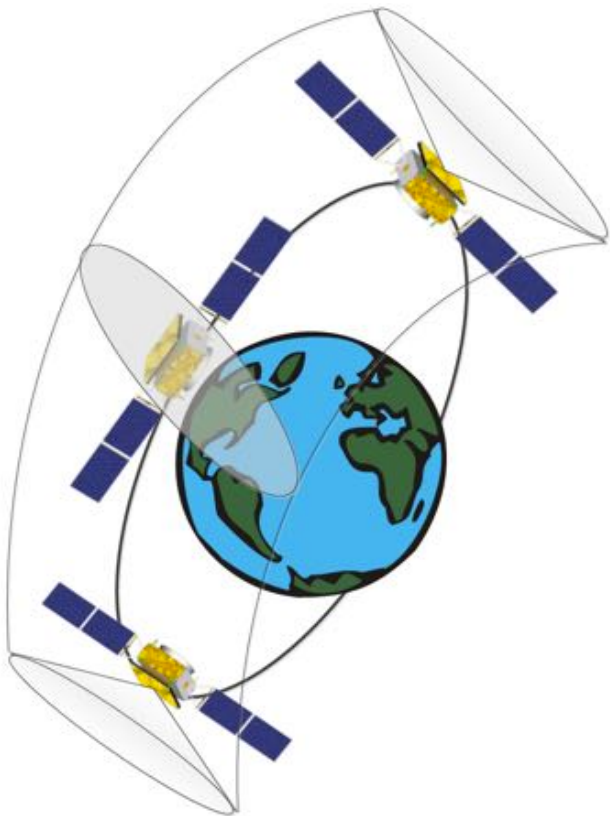
Power: 300/500 W (payload/satellite)

Readout channels: 75,916 (STK 73,728)

Size: 1.2m x 1.2 m x 1.0 m

# The Orbit

- Altitude: 500 km
- Inclination:  $97.4065^\circ$
- Period: 95 minutes
- Orbit: sun-synchronous



- Dec. 20: all detectors powered on, except the HV for PMTs
- Dec. 24: HV on!
- Dec. 30: stable trigger condition
- Very smooth operation since!

# The Collaboration

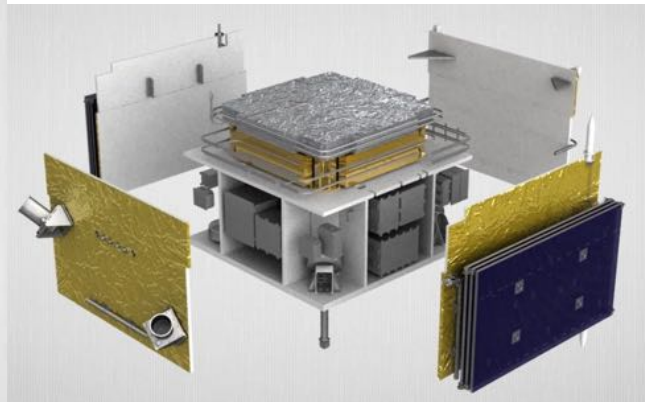
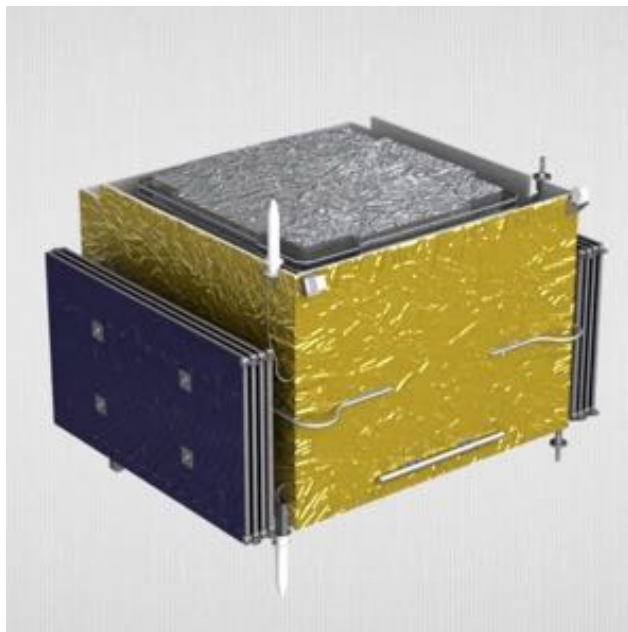
- China
  - Purple Mountain Observatory, CAS, Nanjing
  - University of Science and Technology of China, Hefei
  - Institute of High Energy Physics, CAS, Beijing
  - Institute of Modern Physics, CAS, Lanzhou
  - National Space Science Center, CAS, Beijing
- Switzerland
  - University of Geneva, Switzerland
- Italy
  - INFN Perugia and University of Perugia
  - INFN Bari and University of Bari
  - INFN Lecce and University of Salento



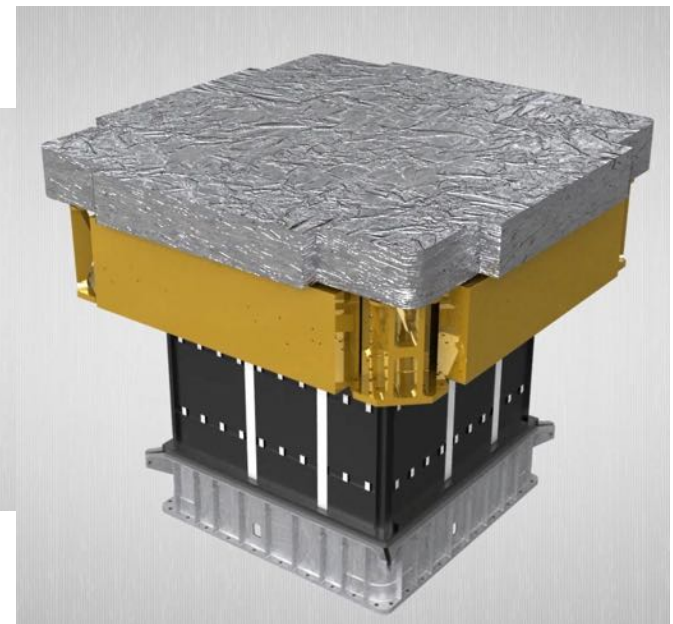
# Scientific objectives of DAMPE

- Precision TeV measurements in space
  - Measure the high energy cosmic electron and gamma spectra
  - Study of cosmic ray spectrum and composition
  - High energy gamma ray astronomy

Detection of 1 GeV - 10 TeV  $e/\gamma$ , 100 GeV - 100 TeV cosmic rays with excellent energy resolution, direction reconstruction ( $\gamma$ ) and charge measurement



LAL, 1/06/2018

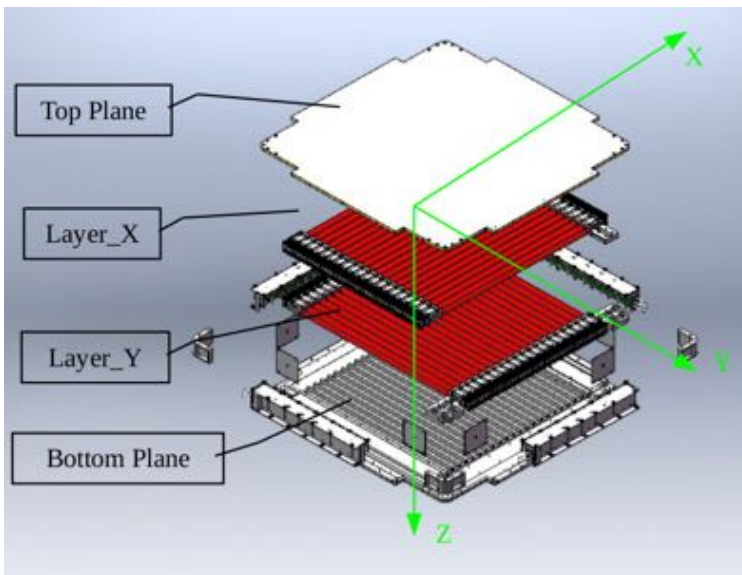
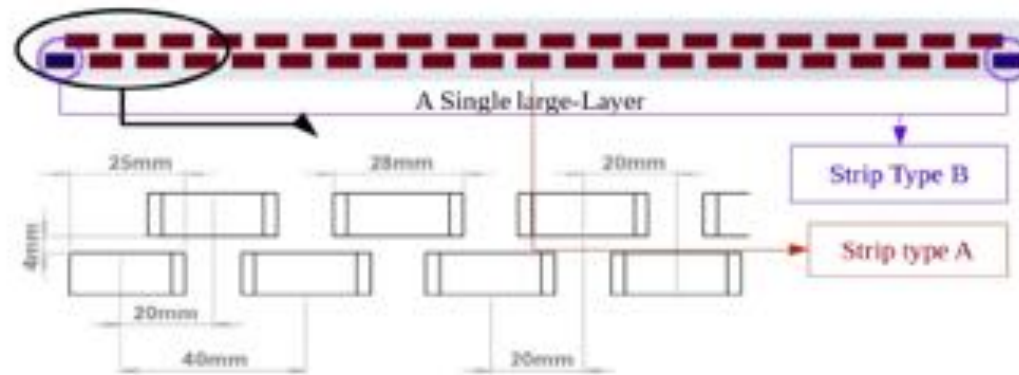


# Plastic Scintillator Detector (PSD)



2 layers (x, y) of strips 1 cm thick, 2.8 cm wide and 88.4 cm long  
Sensitive area 82.5 cm x 82.5 cm, **no dead zone**

- Strip staggered by 0.8 cm



Readout both ends with PMT, each uses two dynode signals (factor  $\sim 40$ ) to extend the dynamic range to cover  $Z = 1, 26$

# Silicon-Tungsten Tracker (STK)

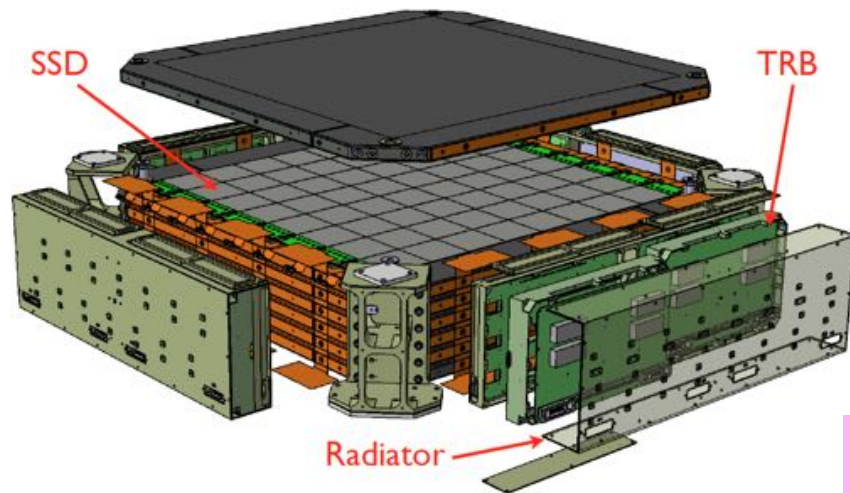


- Outer envelop 1.12m x 1.12m x 25.2 cm
- Detection area 76 x 76 cm<sup>2</sup>
- Total weight: 154.8 Kg
- Total power consumption: ~85W





# The STK structure

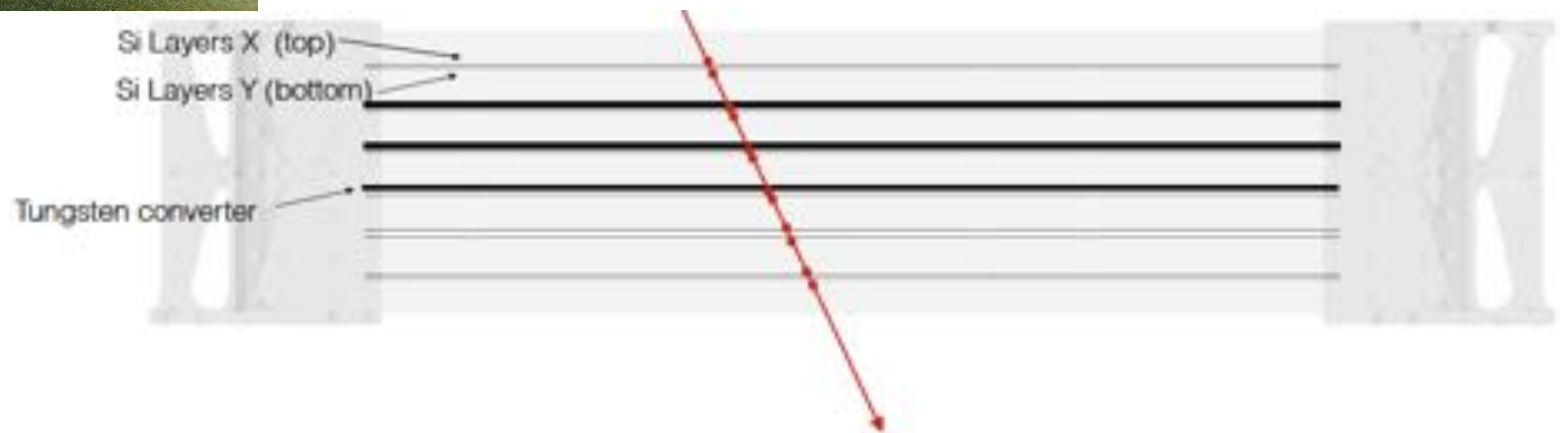
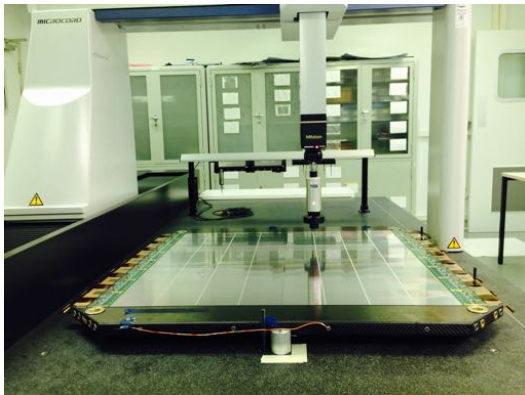
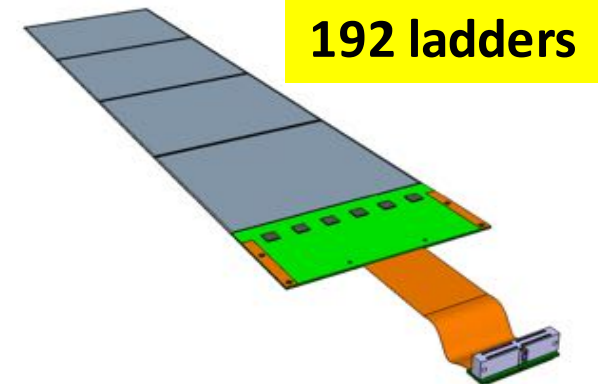


- 12 layers (6x, 6y) of single-sided Si strip detector mounted on **7 support trays**
- **Tungsten plates (1mm thick)** integrated in trays 2, 3, 4 (from the top)
  - Total  $0.85 X_0$  for photon conversion

768 silicon sensors  
 $95 \times 95 \times 0.32 \text{ mm}^3$

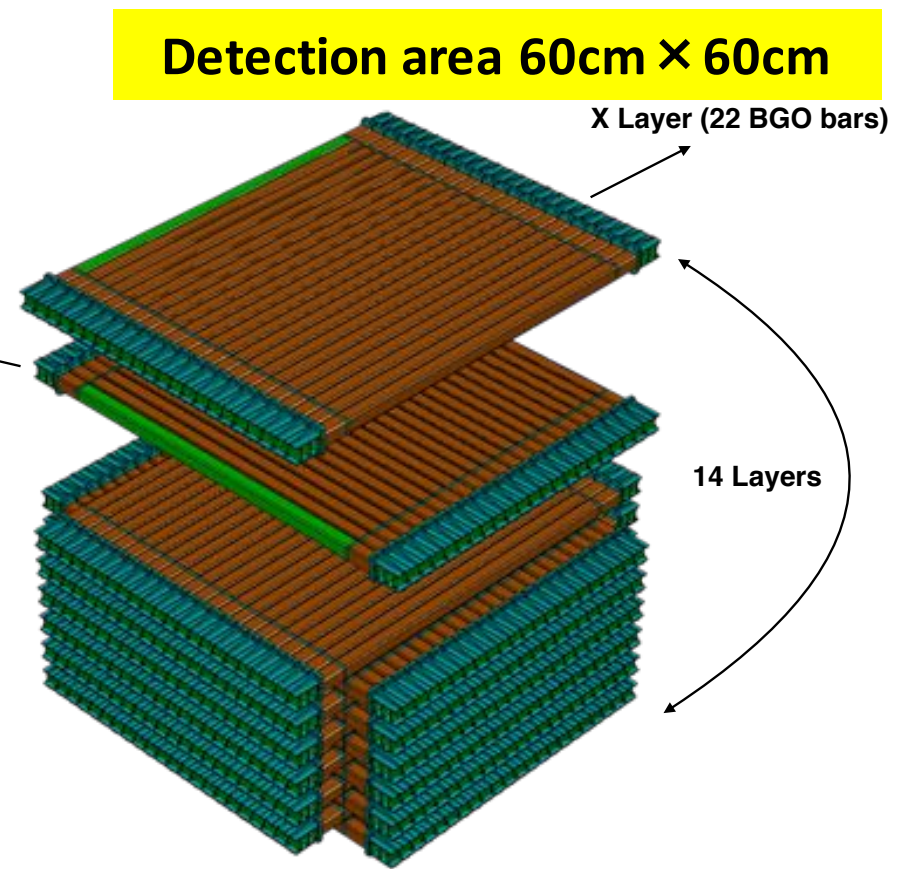
1,152 ASICs

73,728 channels



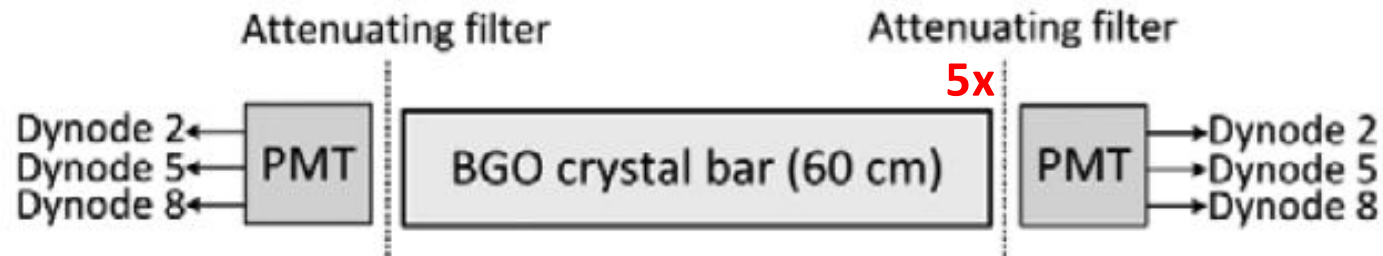
# BGO Calorimeter (BGO)

- 14-layer BGO hodoscope, 7 x-layers + 7 y-layers
  - BGO bar 2.5 cm × 2.5 cm × 60 cm, readout both ends with PMT
    - Use 3 dynode (2, 5, 8) signals to extend the dynamic range
  - Charge readout/Trigger: VATA160 with dynamic range up to 12 pC



Total thickness  $32 X_0 / 1.6 \lambda_1$

# BGO readout and trigger

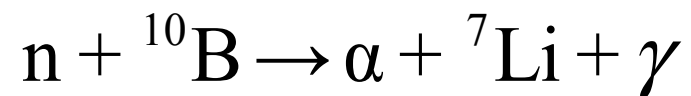
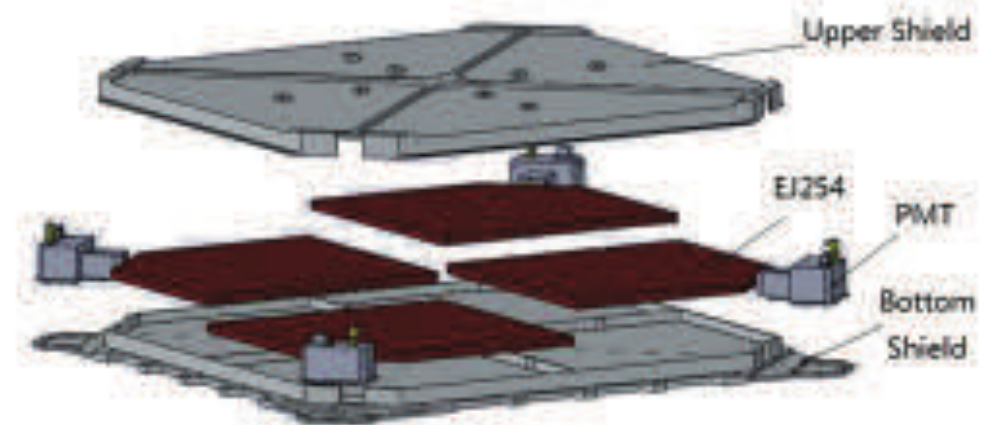


- TA (fast shaping, 22 channel OR) signals of VATA160 used for trigger
  - **Only the dynodes 5 and 8 of the top 4 and bottom 4 layers used**
  - Trigger menu: HE (not prescaled), LE, MIP-1, MIP-2, Unbiased

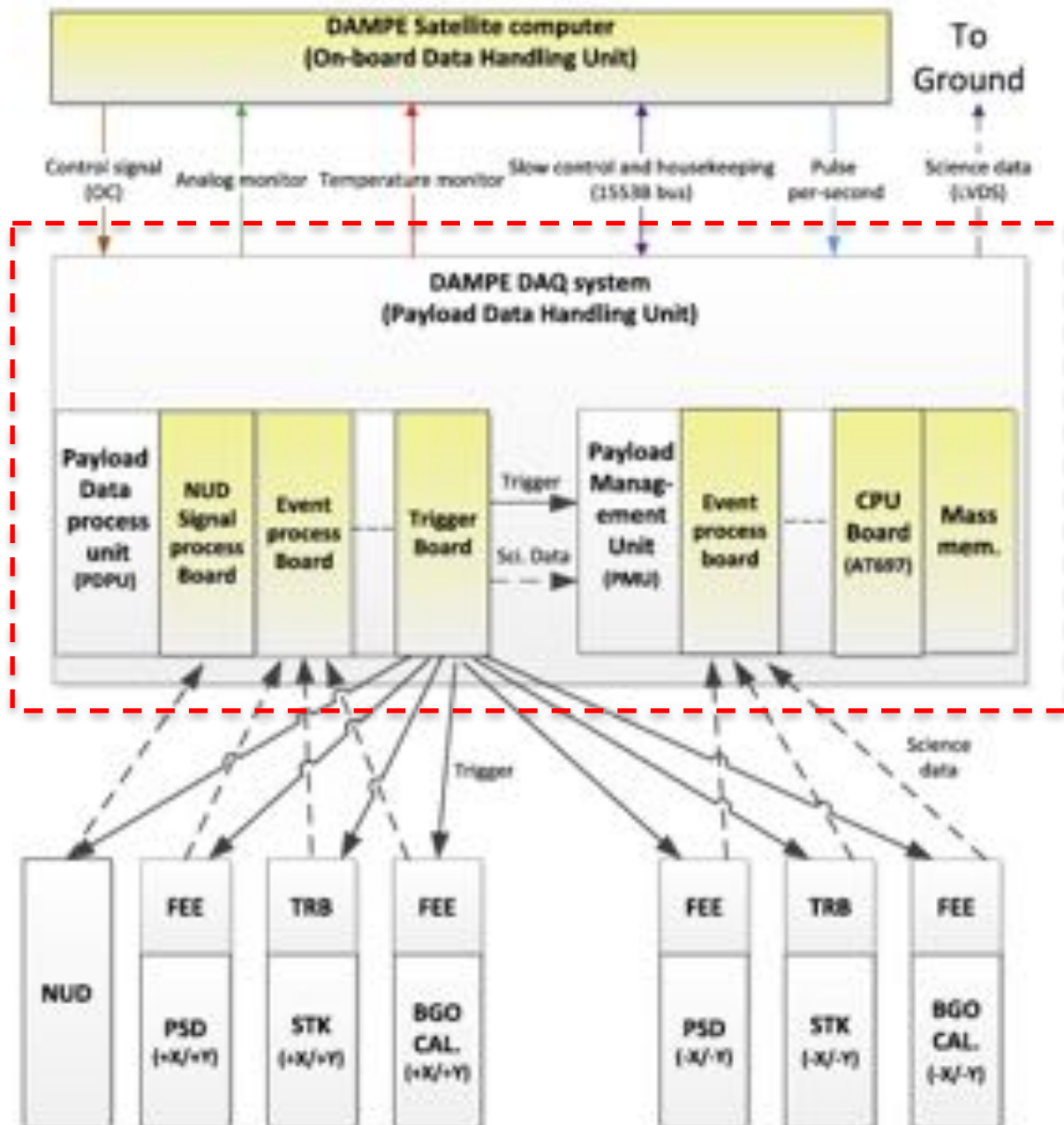
Trigger Type	Logic	Energy Threshold	Pre-scale factor
HE	L1_P_dy5	~10 MIPs	1
	& L2_P_dy5	~10 MIPs	
	& L3_P_dy5	~10 MIPs	
	& L4_N_dy8	~2 MIPs	
MIPs (Type I)	L3_P_dy8	~0.4 MIPs	4 (low latitude( $\pm 20^\circ$ ))
	& L11_P_dy8	~0.4 MIPs	Turn Off (other region)
	& L13_P_dy8	~0.4 MIPs	
MIPs (Type II)	L4_P_dy8	~0.4 MIPs	4 (low latitude( $\pm 20^\circ$ ))
	& L12_P_dy8	~0.4 MIPs	Turn Off (other region)
	& L14_P_dy8	~0.4 MIPs	
	L1_N_dy8	~0.4 MIPs	
LE	& L2_N_dy8	~0.4 MIPs	8 (low latitude( $\pm 20^\circ$ ))
	& L3_N_dy8	~2 MIPs	64 (other region)
	& L4_N_dy8	~2 MIPs	
	(L1_P_dy8 & L1_N_dy8)	~0.4 MIPs ~0.4 MIPs	
Unbiased	(L2_P_dy8 & L2_N_dy8)	~0.4 MIPs ~0.4 MIPs	512 (low latitude( $\pm 20^\circ$ ))
			2048 (other region)

# Neutron Detector (NUD)

- 4 large area boron-doped plastic scintillators ( 30 cm × 30 cm × 1 cm)
  - Detect the delayed thermal neutron capture signal to help e/h separation
  - Gating circuit to detect delayed signal with a settable delay (0-20 $\mu$ s) after the trigger from the BGO



# DAQ system



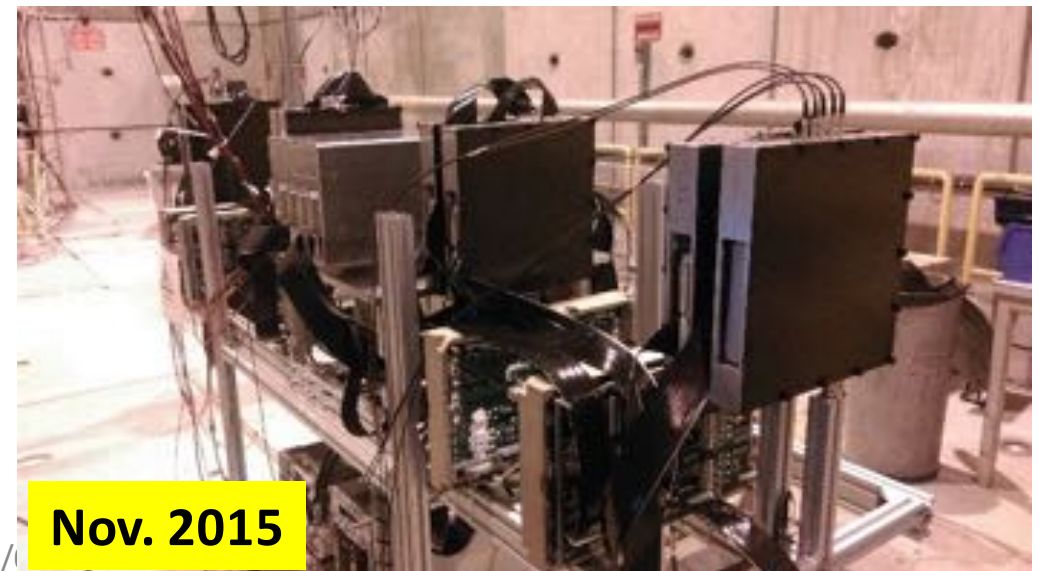
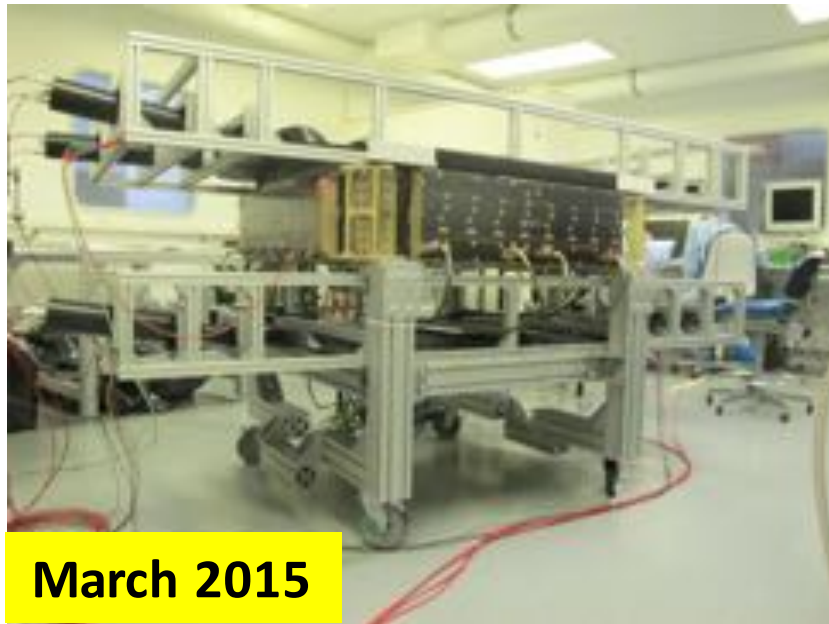
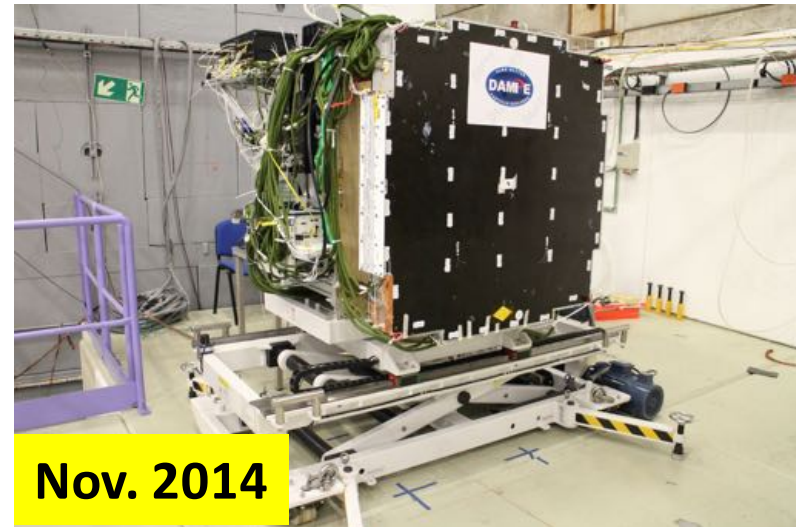
- 2 crates
- All modules with double redundancy
- 16 GB memory

Trigger latency 1  $\mu$ s

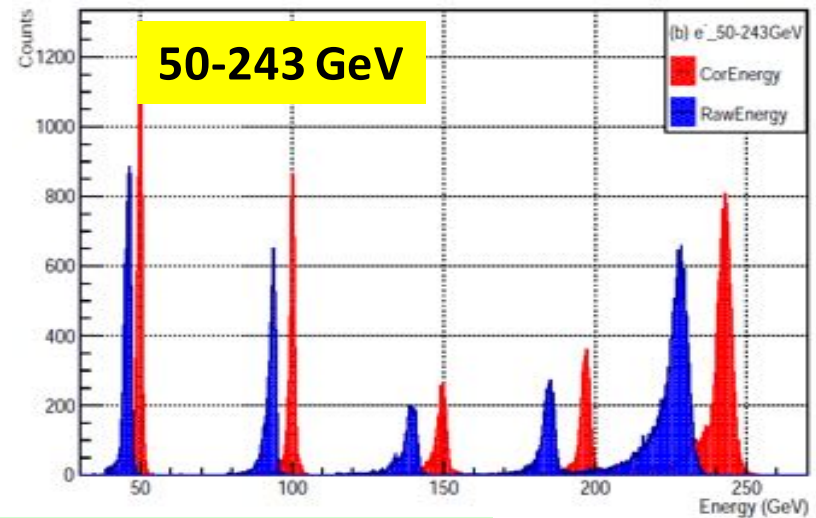
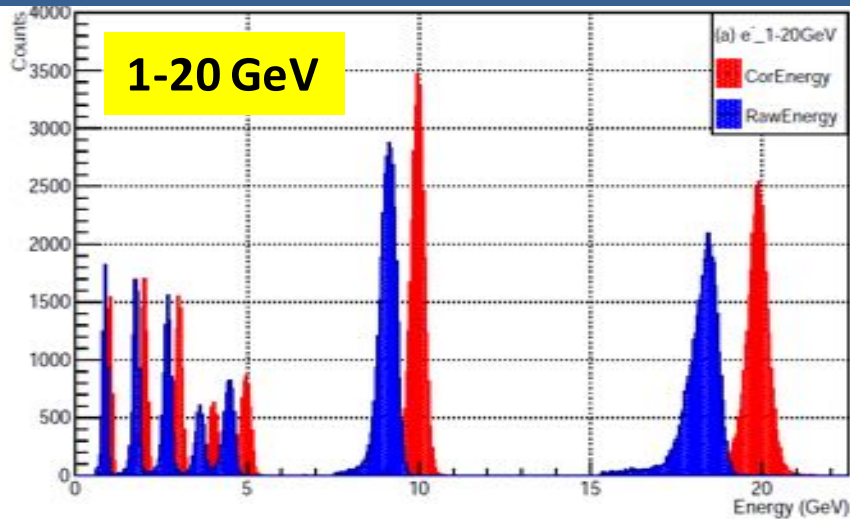
3 ms fixed DAQ dead time

# On-ground calibration

- Several weeks at CERN PS and SPS beams from Oct. 2012 – Nov. 2015 (EQM)
  - Plus many cosmic muon data (FM)

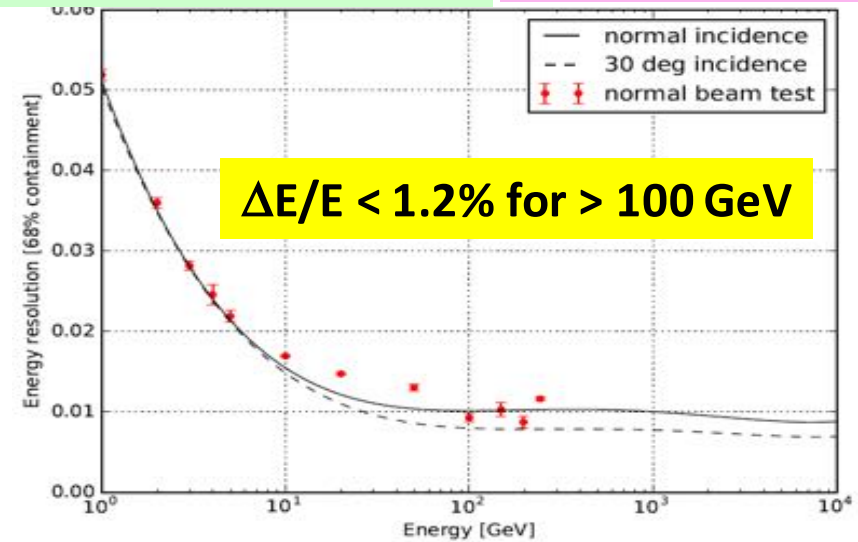
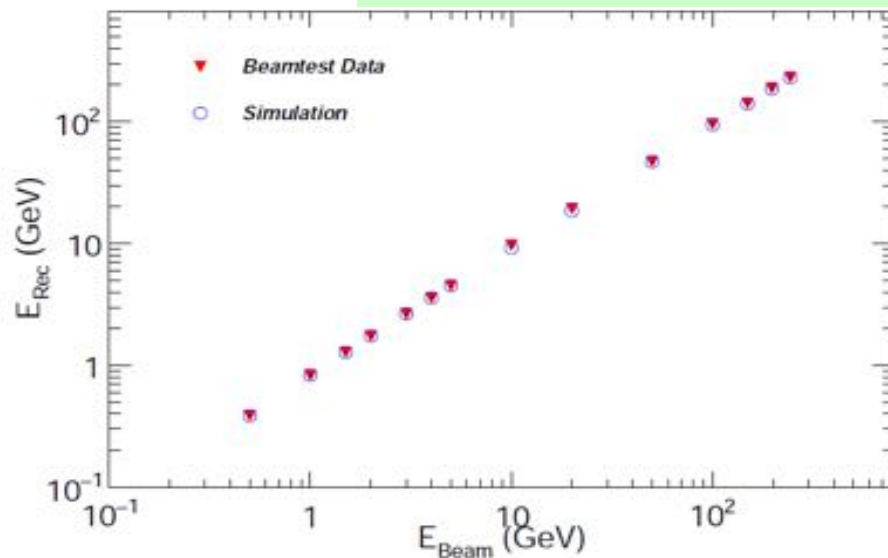


# Electron energy linearity and resolution



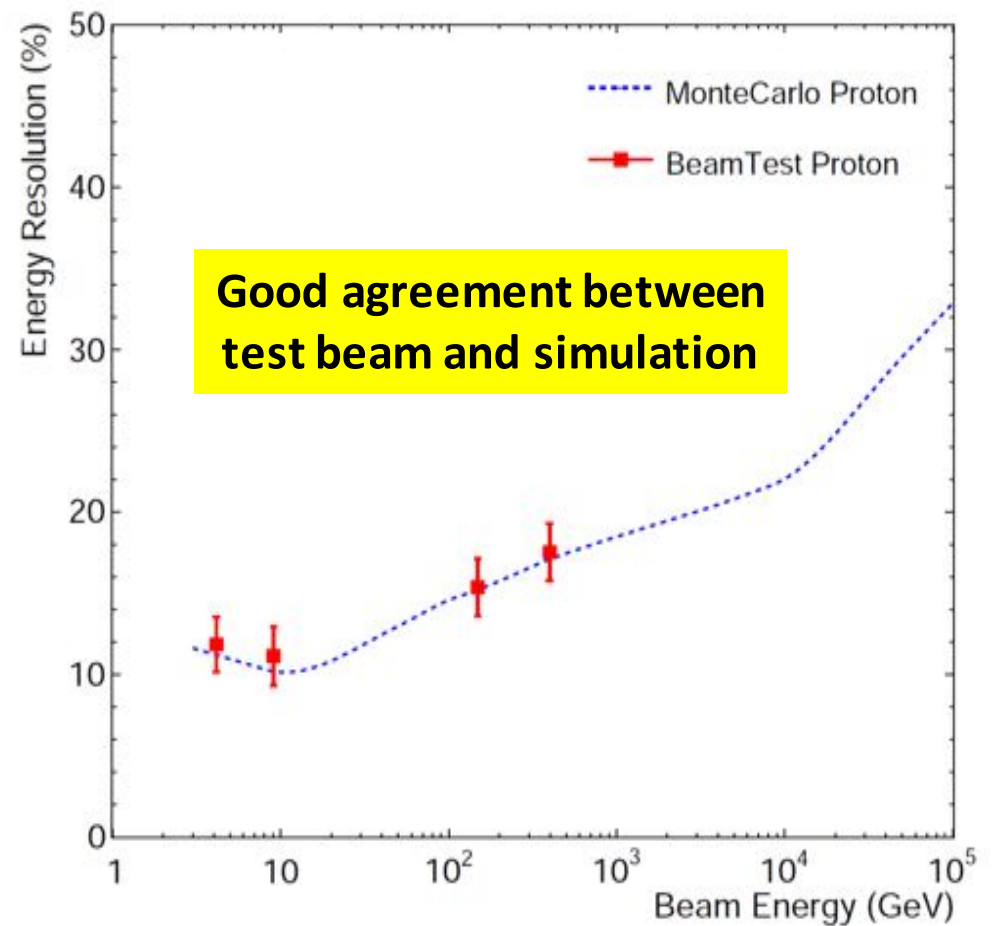
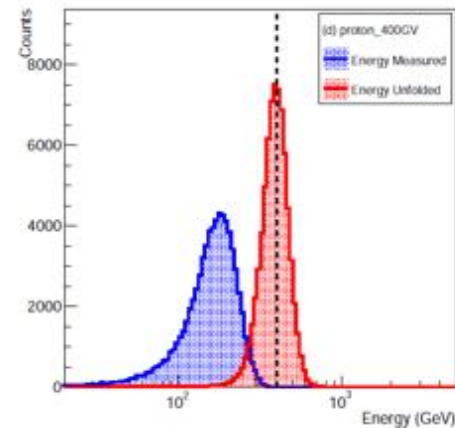
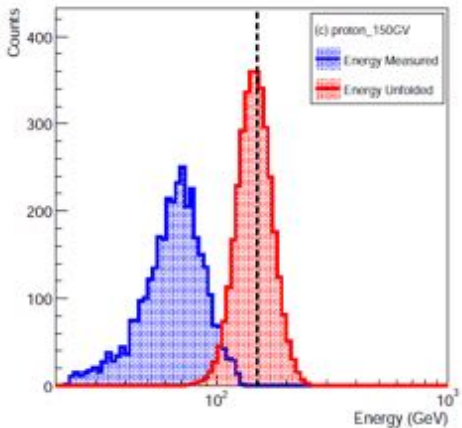
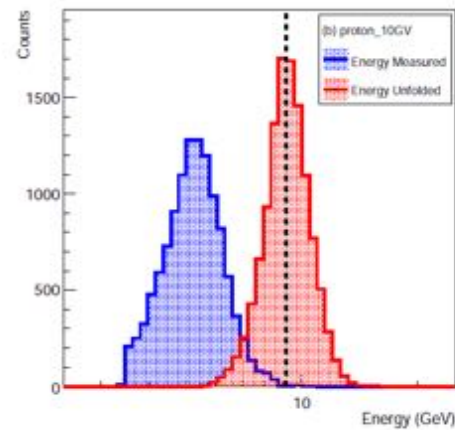
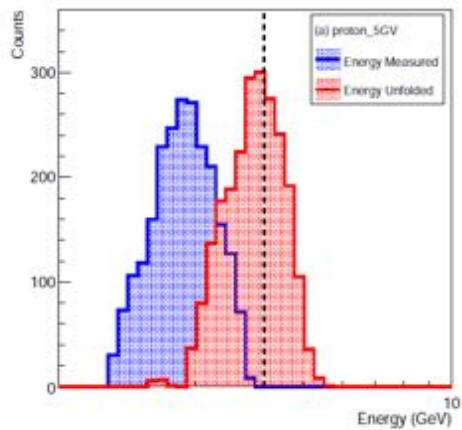
Energy correction: ~6-7% for 100 GeV – 1 TeV

NIM A 856 (2017)11



Good linearity and resolution  
Good agreement between test beam and simulation

# Proton energy resolution

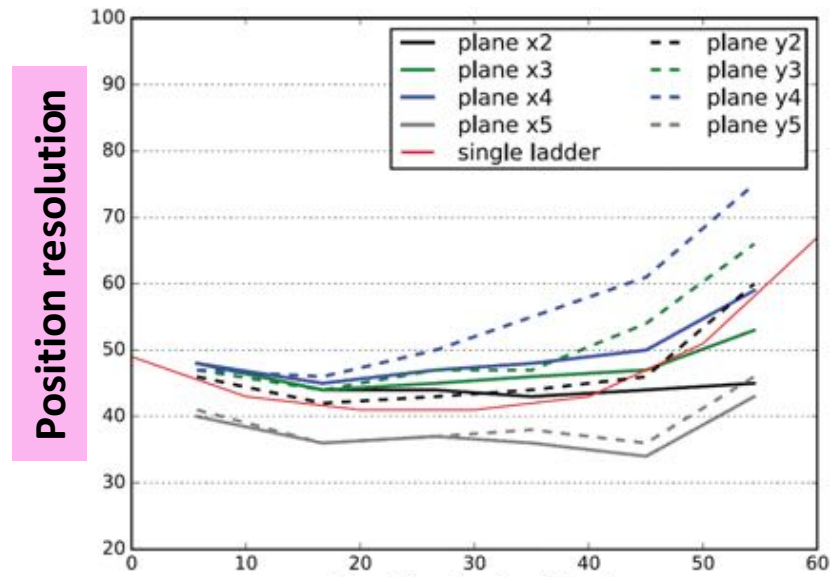
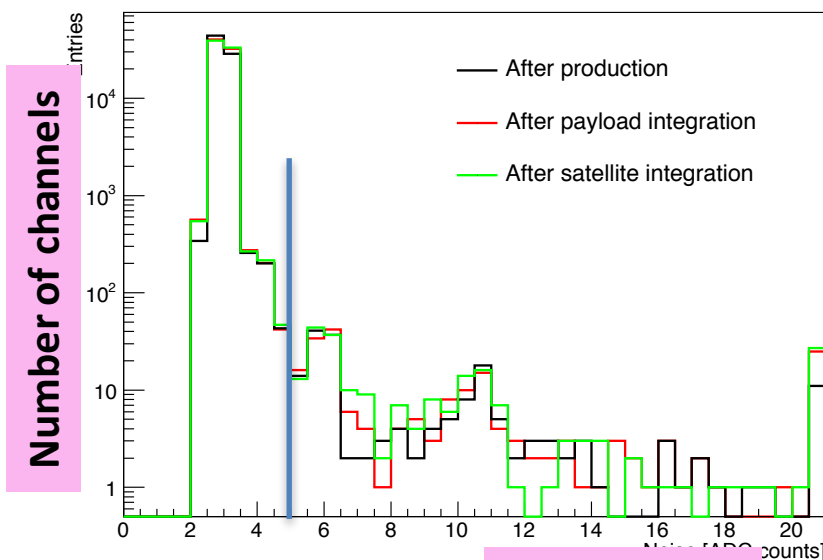


Proton energy cannot be easily corrected. Need unfolding!



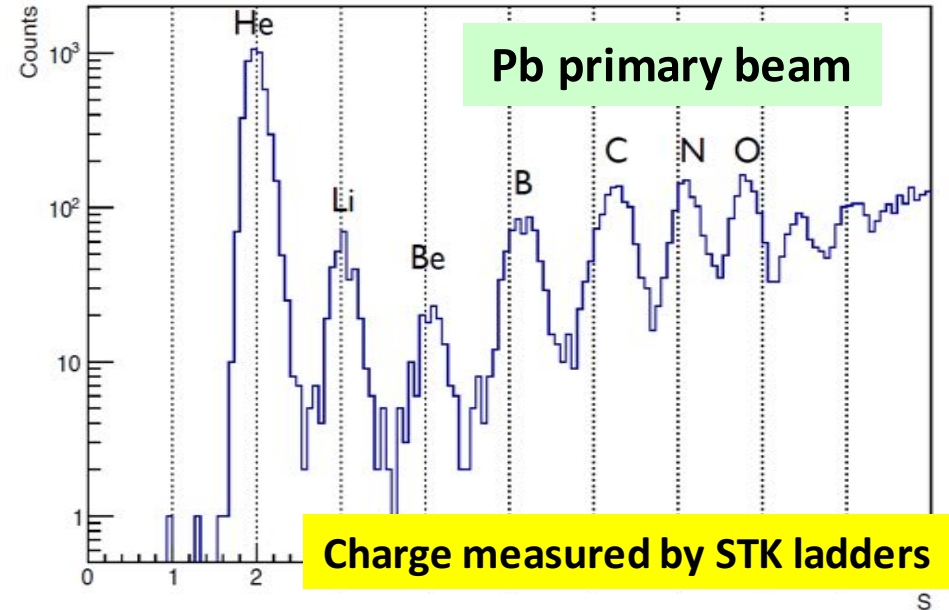
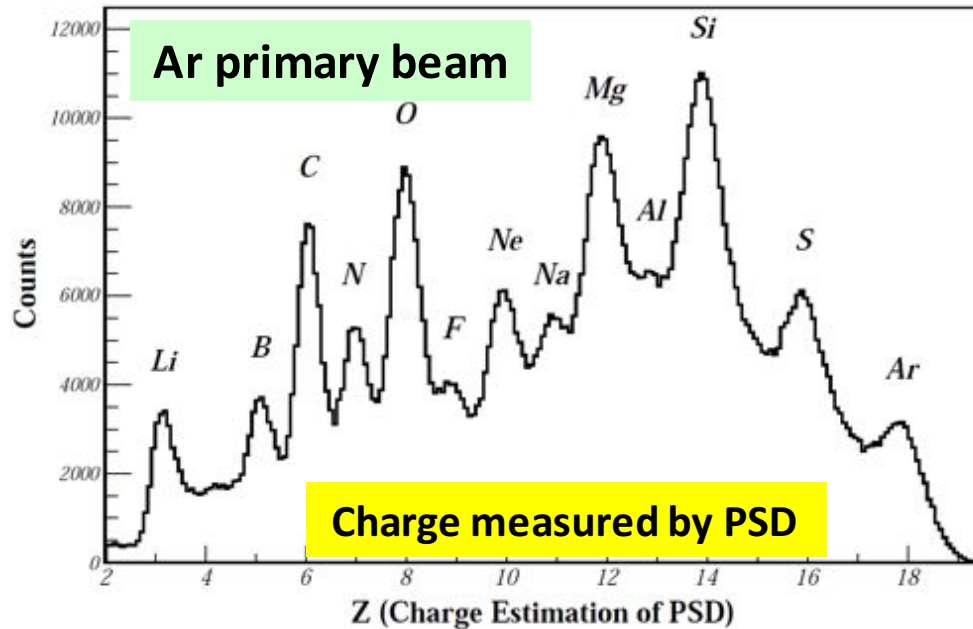
# STK on-ground calibration

- Extensively tested and calibrated with particle beams at CERN and with cosmic ray muons
- STK remained in excellent quality through ~6 months of transportation, integration, space environmental tests, ...
  - **Number of noisy channels <0.4 % before launch**
- Large amount of cosmic data collected to align the STK
  - **Excellent position resolution achieved before launch**
    - **40 – 50  $\mu\text{m}$  for vertical entry particles (requirement 75  $\mu\text{m}$ )**



# Charge measurements with beams

- Test with ion fragment beams at CERN

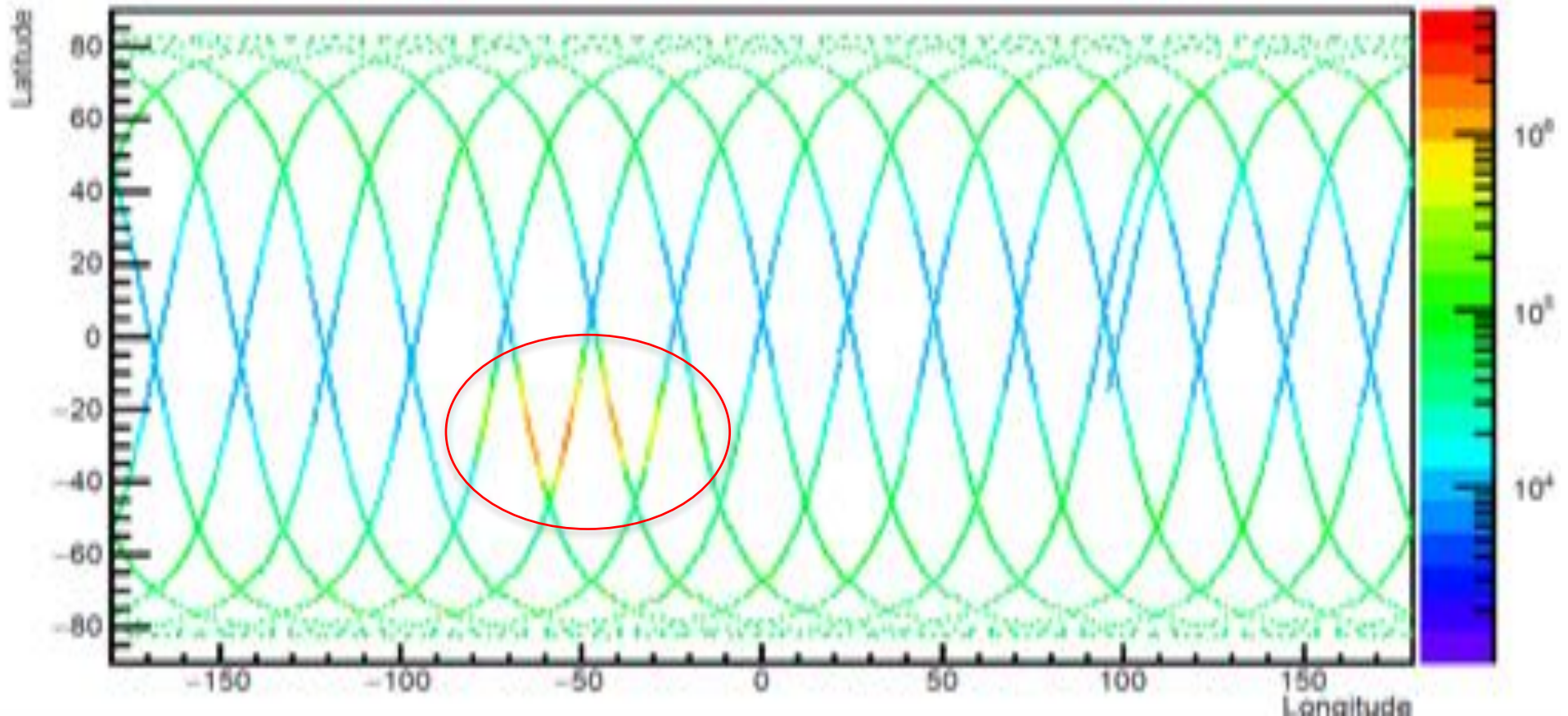


STK has better resolution at low Z, but saturate at  $Z \sim 8$



# Particle hit counts vs orbit

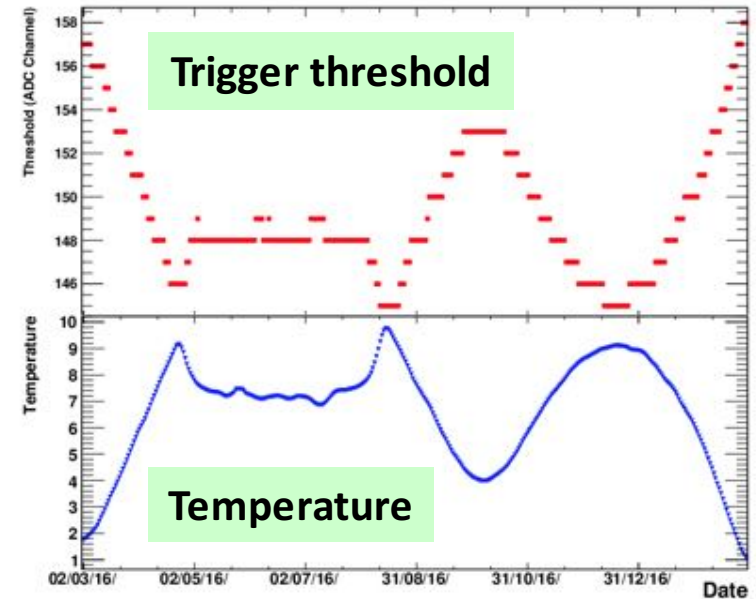
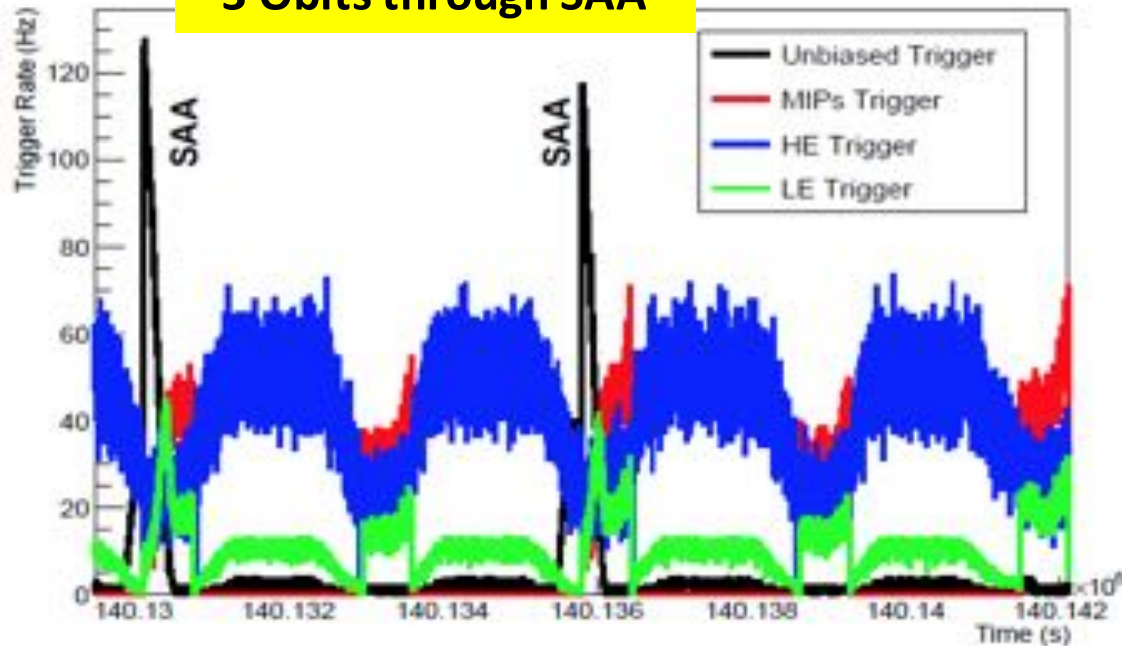
Hits of +X FEE Dynode 8 Layer 1



- 15 orbits/day
- ~50 Hz average trigger rate
  - Main high energy trigger and prescaled low energy and MIP triggers

# Trigger rate in orbit

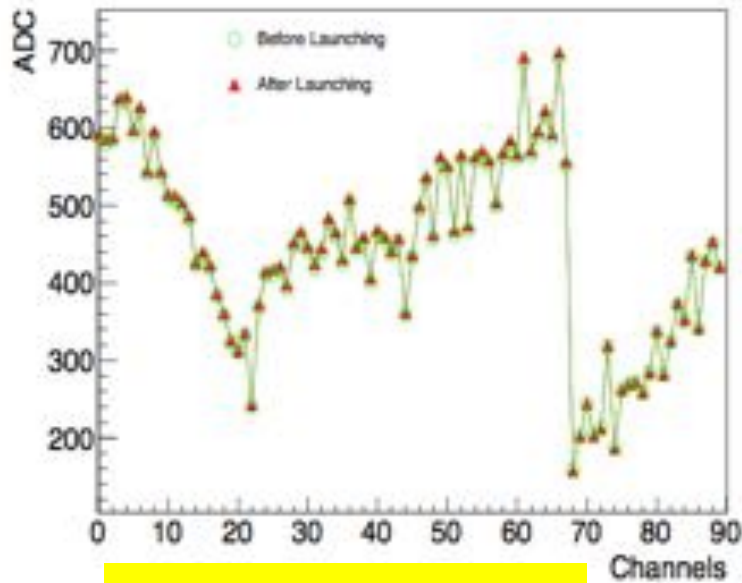
3 Orbits through SAA



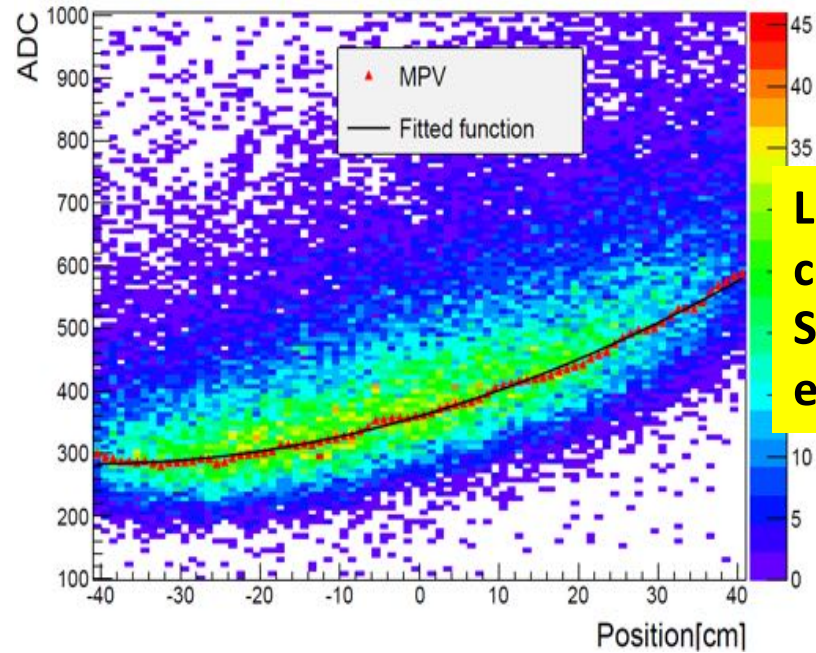
- HET trigger rate 20 – 60 Hz
  - Events in South Atlantic Anomaly (SAA) regions not used

- Small trigger threshold variation with temperature
  - ~13 ACD (0.04 MIP) in full temperature range

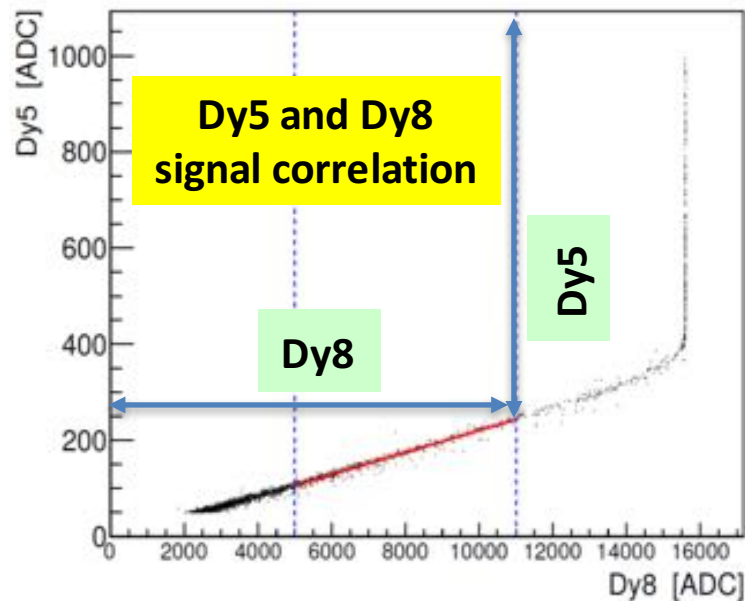
# PSD in-flight calibration



Pedestal comparison



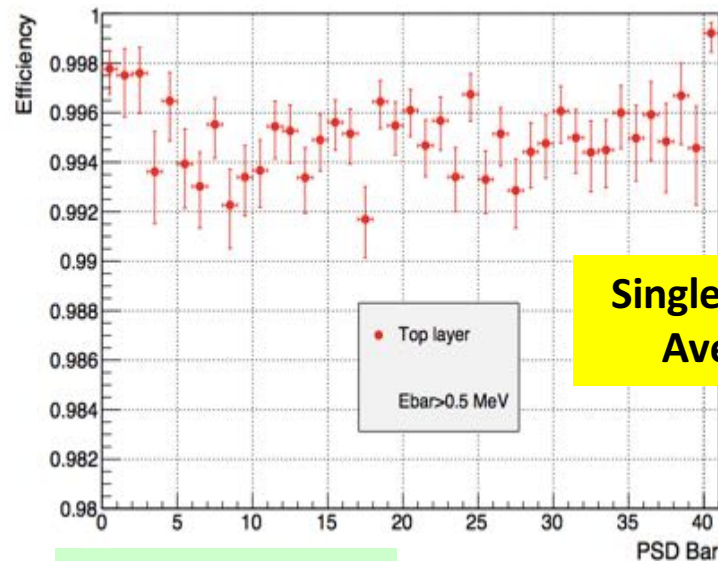
Light attenuation calibration, using STK track for extrapolation



Dy5 and Dy8 signal correlation

Dy5

Dy8

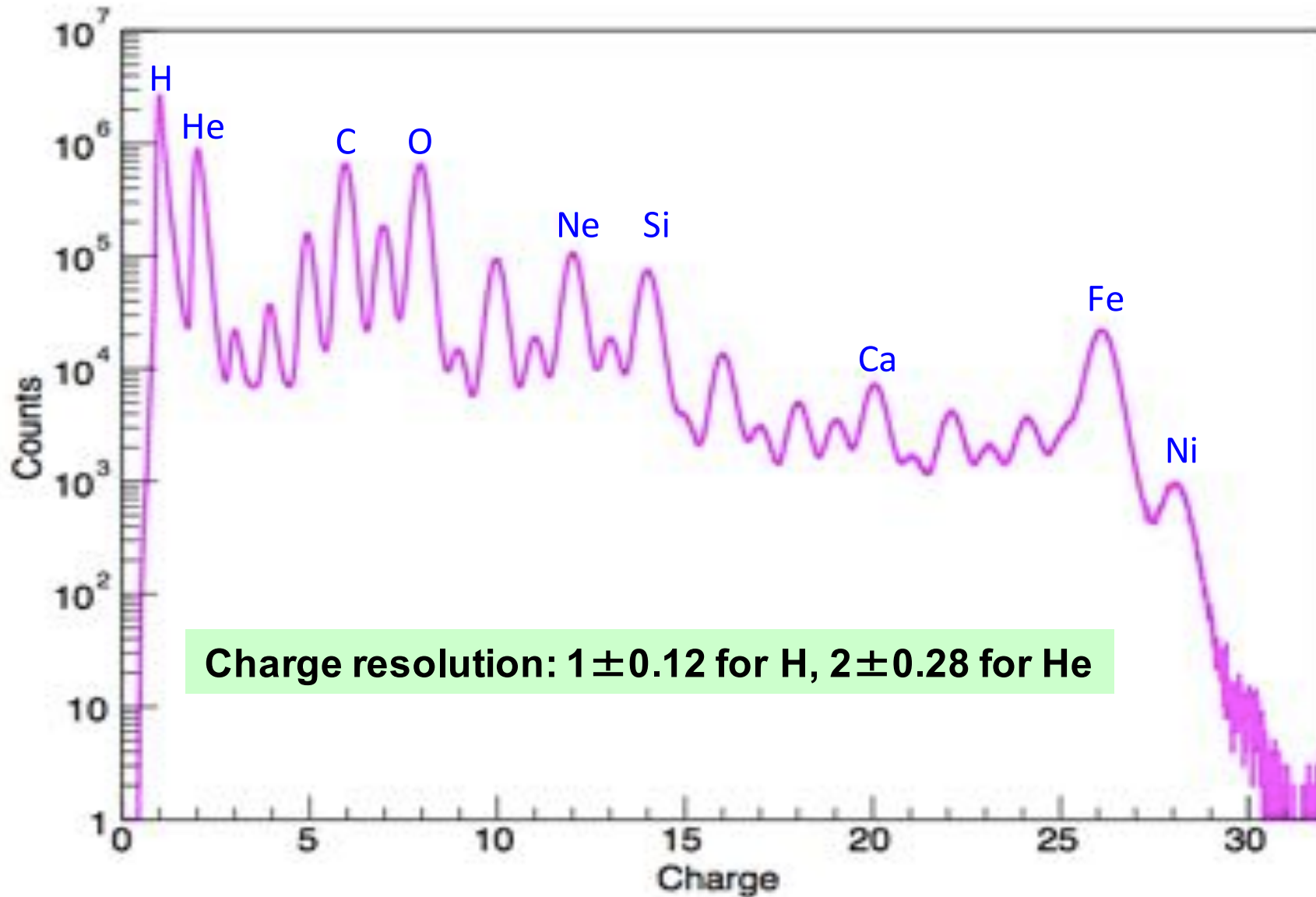


Single layer efficiency  
Average ~99.5%

PSD bar number

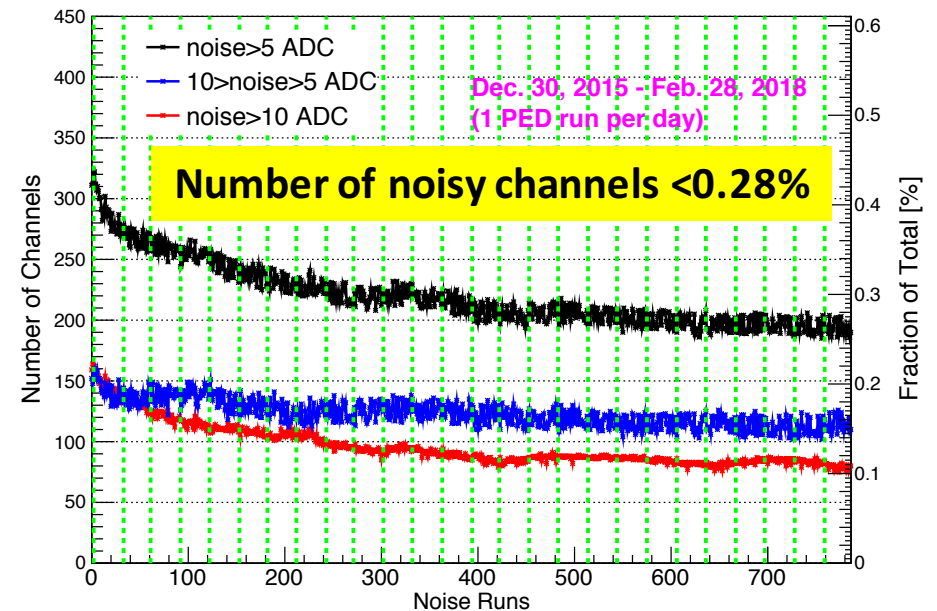
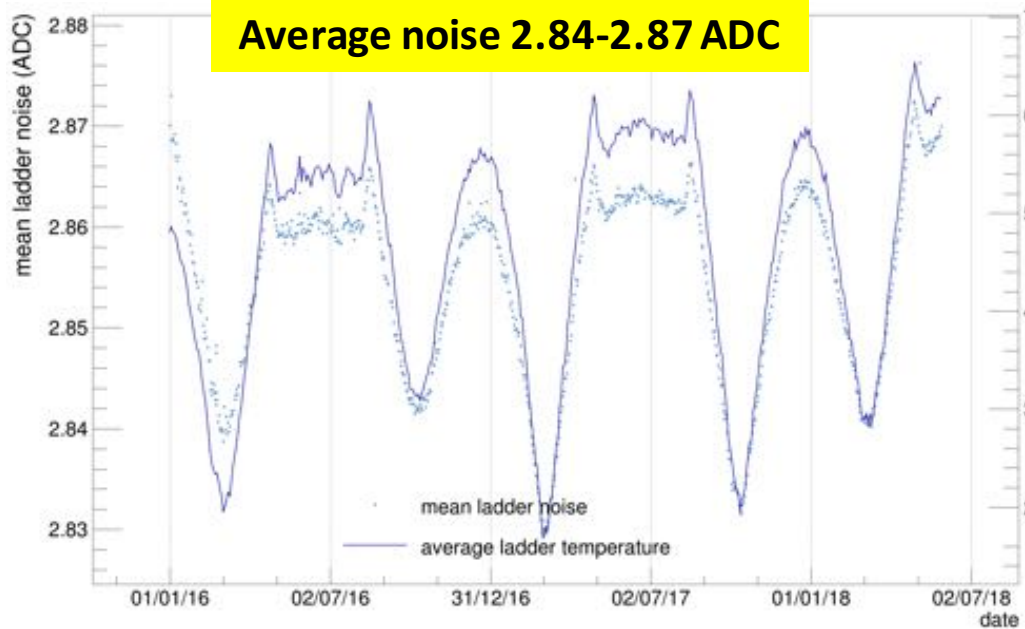
Proc. Sci. (ICRC2017) 168 (2017)

# PSD charge measurement



Charge resolution:  $1 \pm 0.12$  for H,  $2 \pm 0.28$  for He

# STK Noise very stable since launch



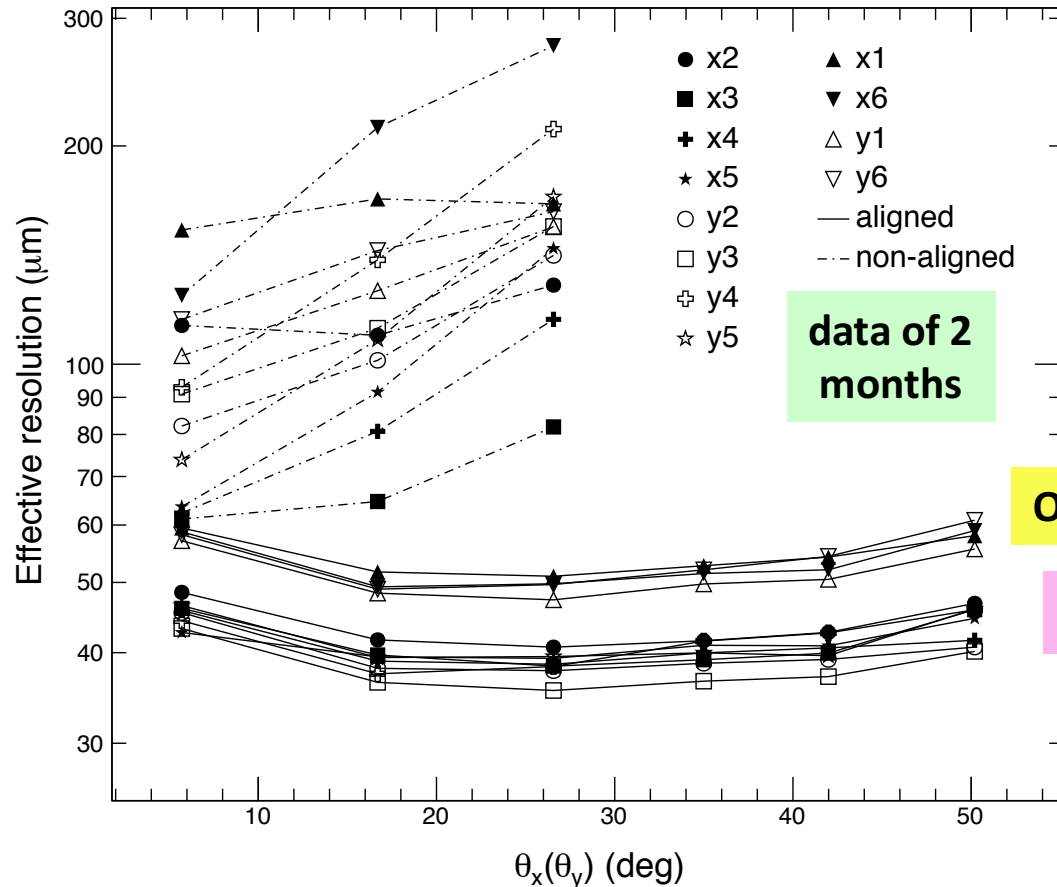
- Bulk of noise correlated with temperature
  - Very small temperature coefficient
    - $\sim 0.01$  ADC per  $2^\circ\text{C}$ , stability  $\pm 1.4\%$
- Simplification for operation
  - data compression thresholds updated only once on Feb. 22, 2016 using average noise of Feb. 13-17, 2017

- Detector started in good shape, Steadily improved in the first 2 year due to stabilization effect

Range of variation (0.3 ADC) more precise than the on-board pedestal calculation (2 ADC)!

# STK in-flight alignment

- Good thermal stability guaranteed a good short term mechanical stability



Re-align every 2 weeks to correct for long term shift

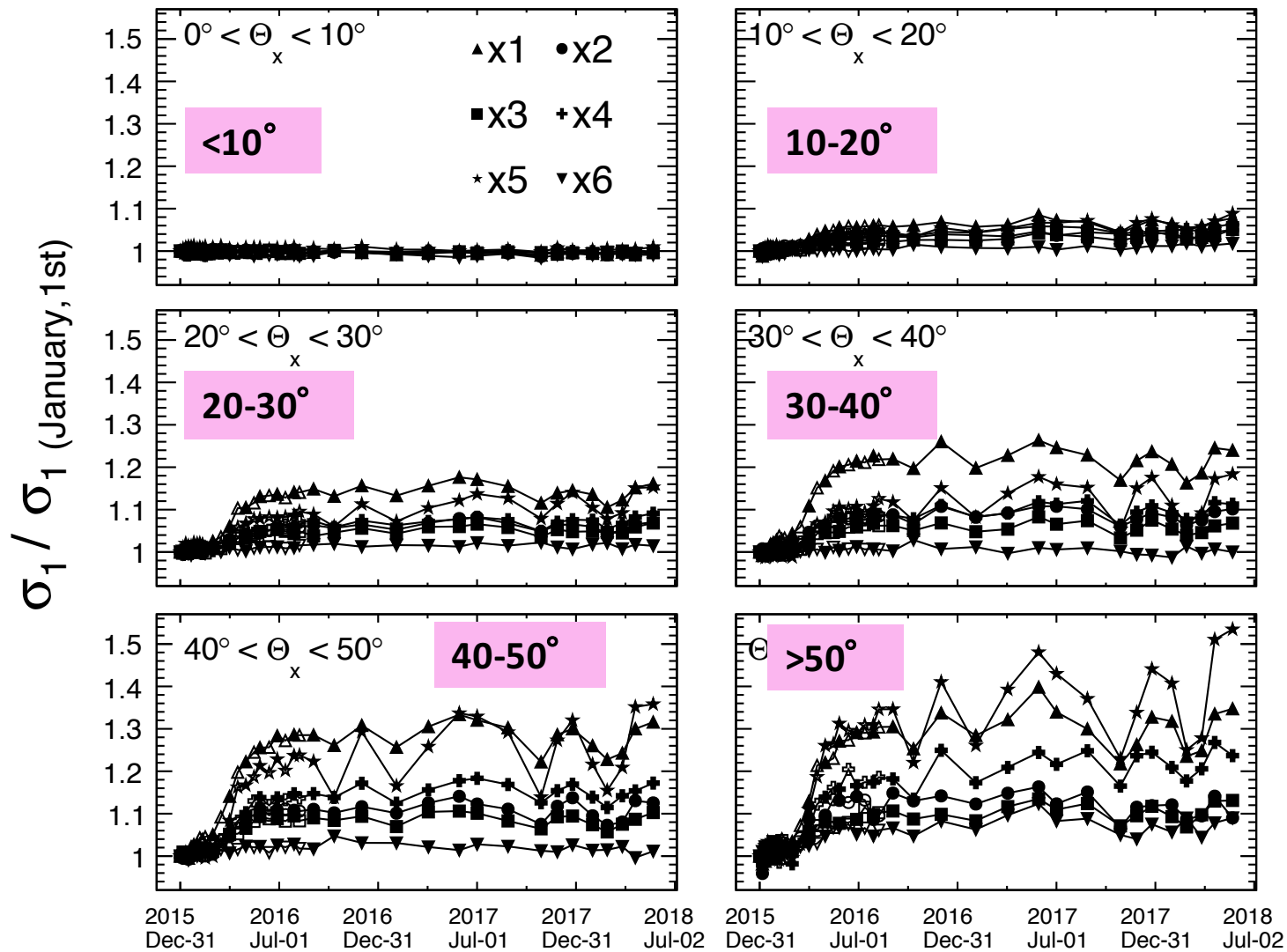
Outside layers with larger extrapolation errors

Intrinsic position resolution 40 -50  $\mu\text{m}$

Unbiased hit residual of 12 layers before/after (re)alignment, as function of incidence angle



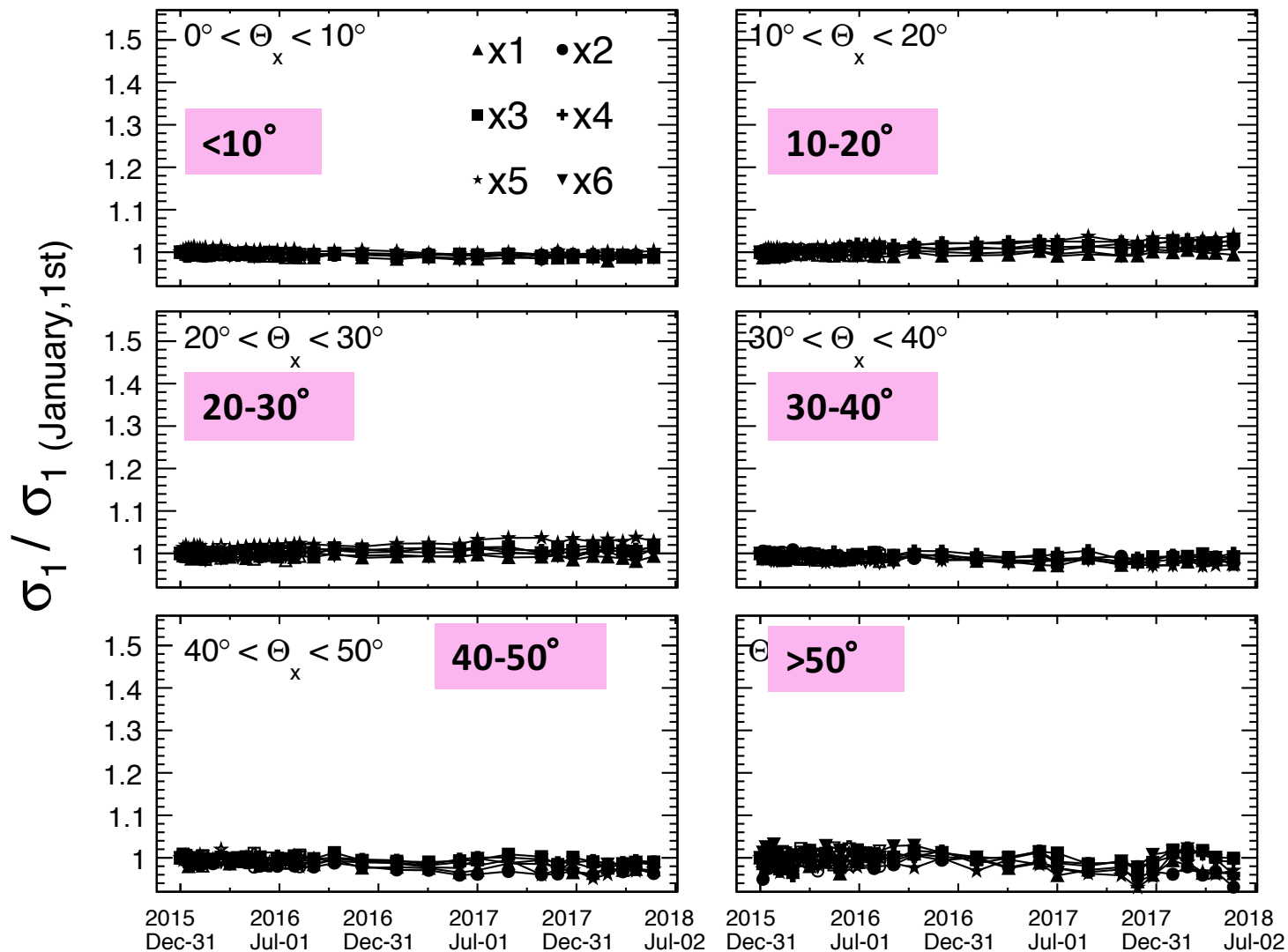
# Residual ratio evolution: initial alignment



Launch to  
May 2018

Use alignment of Jan. 2016: tray movement in Z direction affects resolution of large angle tracks

# Residual with alignment: launch to May 2018

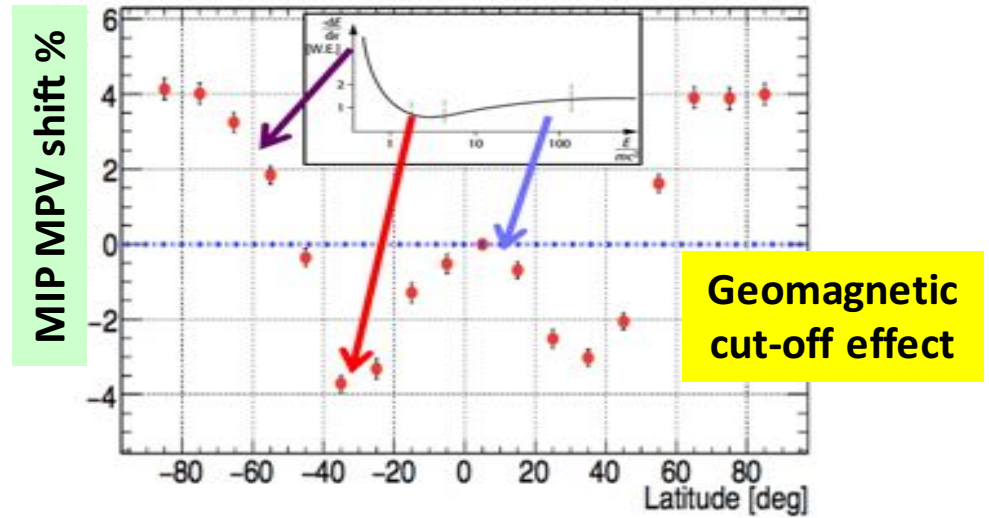
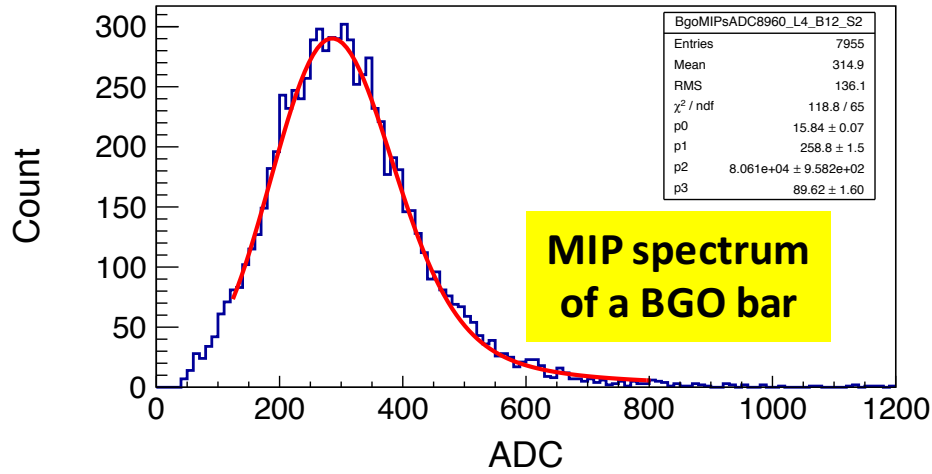


Launch to May 2018

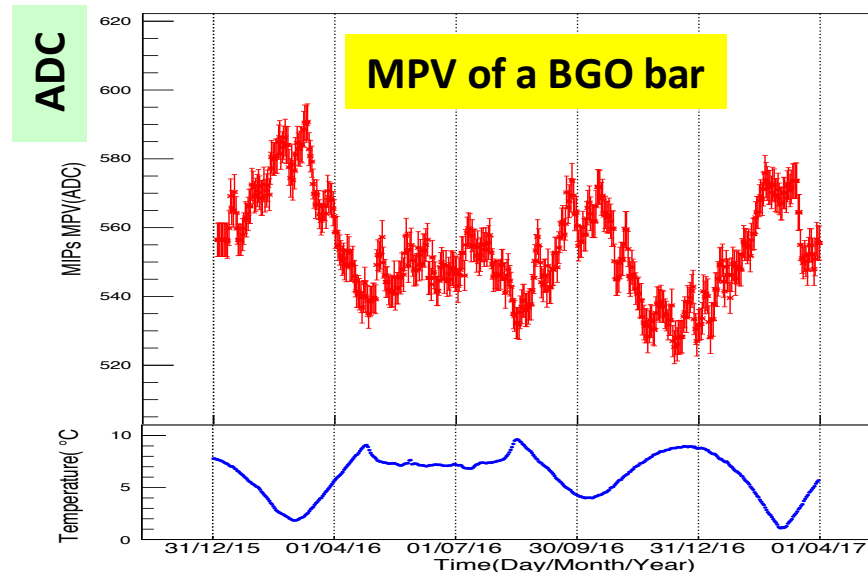
Bi-weekly update of alignment is sufficient, stability ~2%

# BGO in-flight MIP calibration

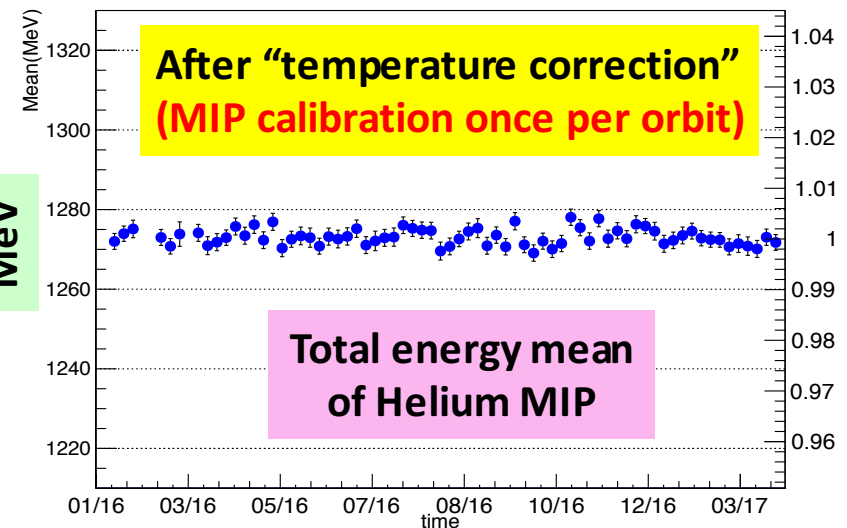
- “MIP” calibration: ADC  $\rightarrow$  MeV and equalization, **use events near the equator,  $\pm 20^\circ$**



Stability of Helium MIPs



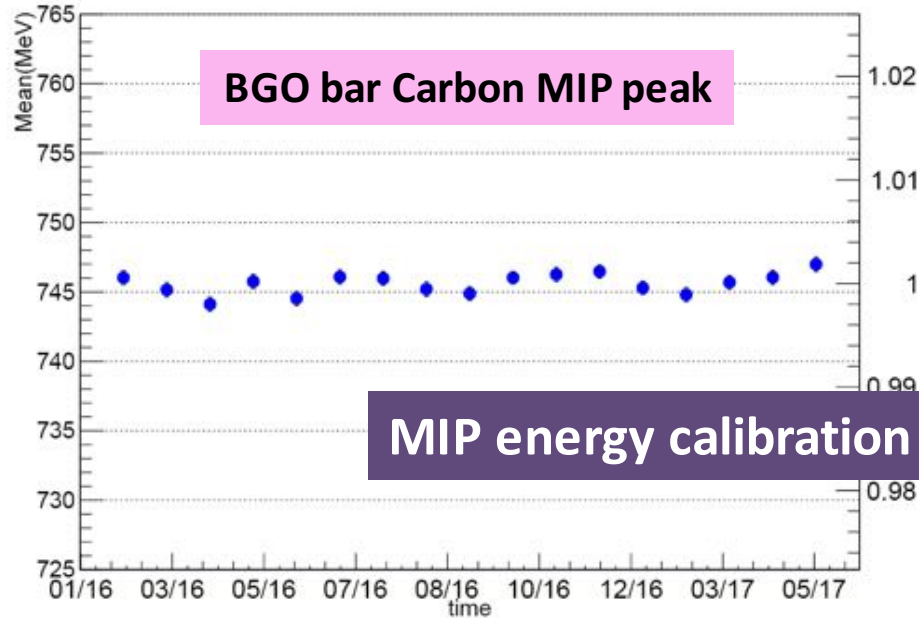
Proton “MIP” MPV vs temperature (time)



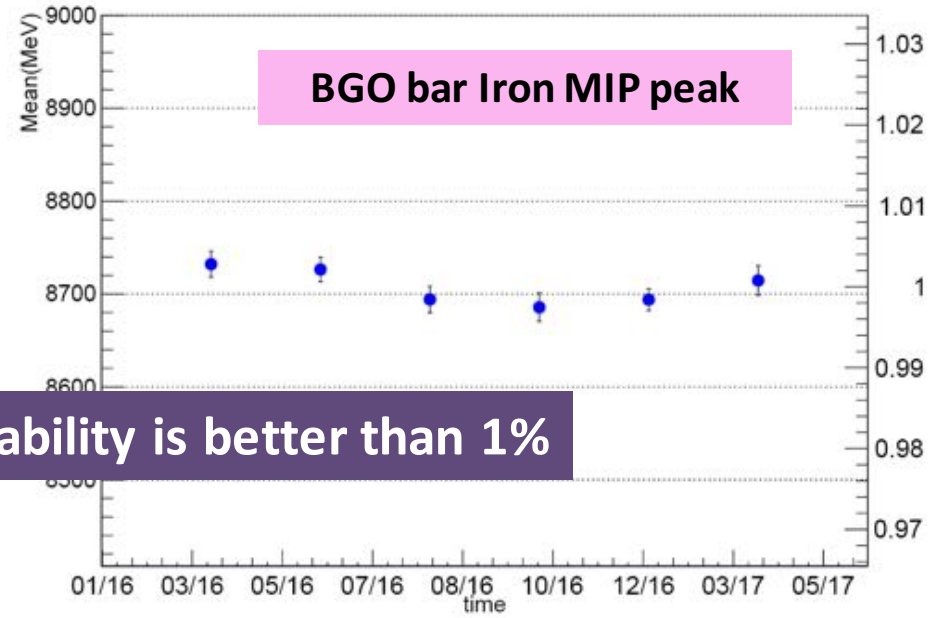
Helium “MIP” mean vs time, stable <1%

# MIP energy calibration stability

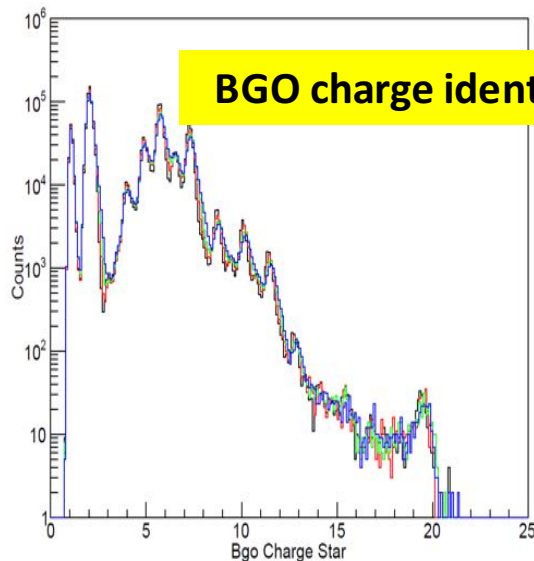
Stability of Carbon MIPs



Stability of Fe MIPs



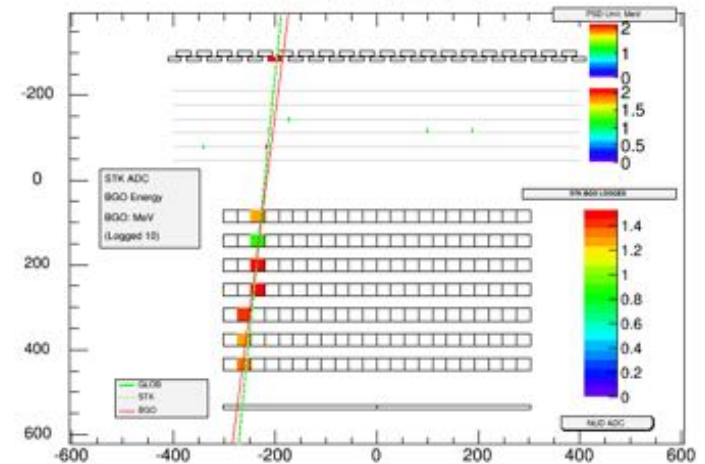
MIP energy calibration stability is better than 1%



Xin Wu

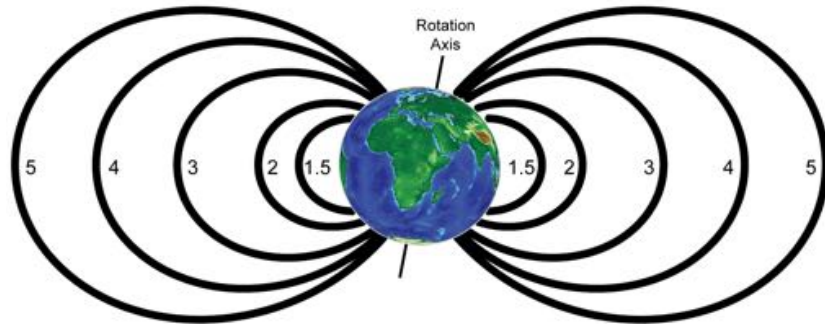
LAL, 1/06/2018

XOZ (Reversed Z)



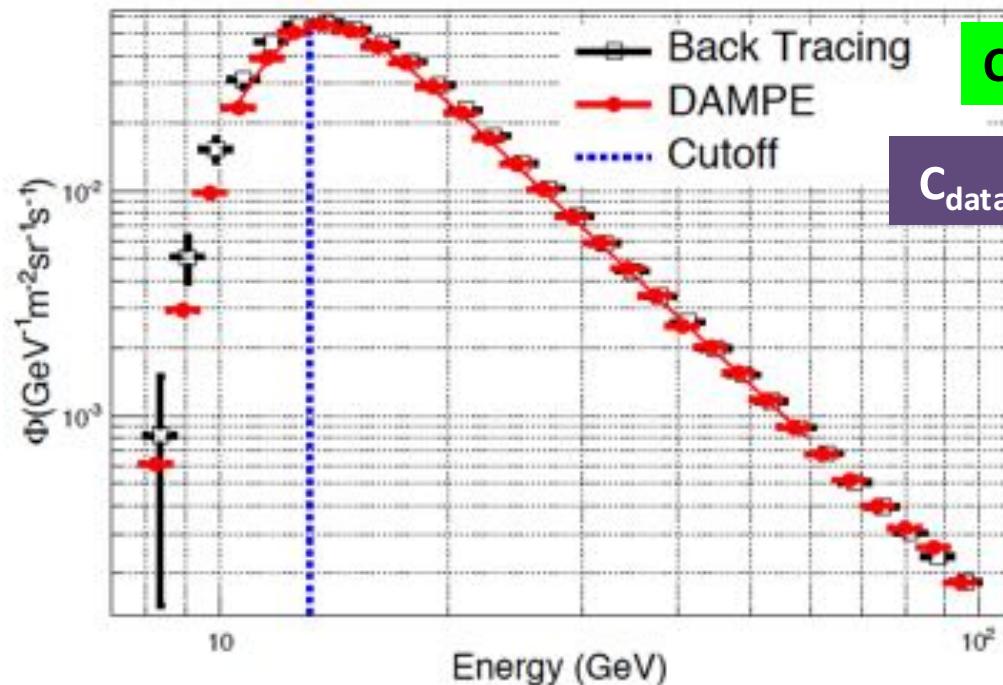
# Absolute energy scale validation

- Overall energy scale can be checked with geomagnetic cut-off effects
  - Charge particles detected in a geomagnetic zone have specific cut-off in the flux (deflection by the magnetic shield)



McIlwain L shells

- Use L in 1 – 1.14, cut-off ~ 13 GeV
- Measured cut-off compared to MC simulation with IGRF-12 model and back-tracing code (**International Geomagnetic Reference Field**)



Cut-off : 13.20 GeV (data) vs. 13.04 GeV (IGRF)

$$C_{\text{data}}/C_{\text{pred}} = 1.0125 \pm 0.0174(\text{stat.}) \pm 0.0134(\text{sys.})$$

Absolute energy scale

- ~1.25% above expectation
- ~2% at  $1\sigma$  level

**Not correction applied, use as systematics**

# The electron ( $e^+e^-$ ) flux measurement

Four ingredients:

1. Reconstructed energy spectrum 
$$\frac{dN_i/dE_{reco}}{\epsilon_i \cdot W_i} = \frac{N_i - B_i}{\epsilon_i \cdot W_i} \text{ GeV}^{-1}$$

- $N_i$ : number of events observed after **fiducial** and **selection** cuts
- $B_i$ : number of estimated background
- $\epsilon_i$ : **efficiency** of all selection cuts applied after the fiducial cut
- $W_i$ : bin width in GeV (corrected reconstructed energy)

2. Unfolding to true energy spectrum

- Detailed studies showed smearing effect is negligible with corrected energy ( $\Delta E/E < 1.5\%$  above 20 GeV):

$$\frac{dN_i/dE_{true}}{\epsilon_i \cdot W_i} \approx \frac{dN_i/dE_{reco}}{\epsilon_i \cdot W_i}$$

3. **Acceptance** and live time correction

$$\Phi_i(E_{true}) = \frac{dN_i/dE_{true}}{A_i T} = \frac{N_i - B_i}{\epsilon_i A_i W_i T} \text{ GeV}^{-1} \text{ cm}^{-2} \text{ sr}^{-1} \text{ s}^{-1}$$

- $A_i$ : acceptance of the “fiducial” cut in  $\text{cm}^2 \text{sr}$
- $T$ : live time corresponding to the dataset (30.12.15-08.06.17, 2.8 billions events)

4. Error evaluation

- Statistical error of  $N_i$  and systematic (+statistical) errors of  $B_i$ ,  $A_i$ ,  $\epsilon_i$ ,  $T$

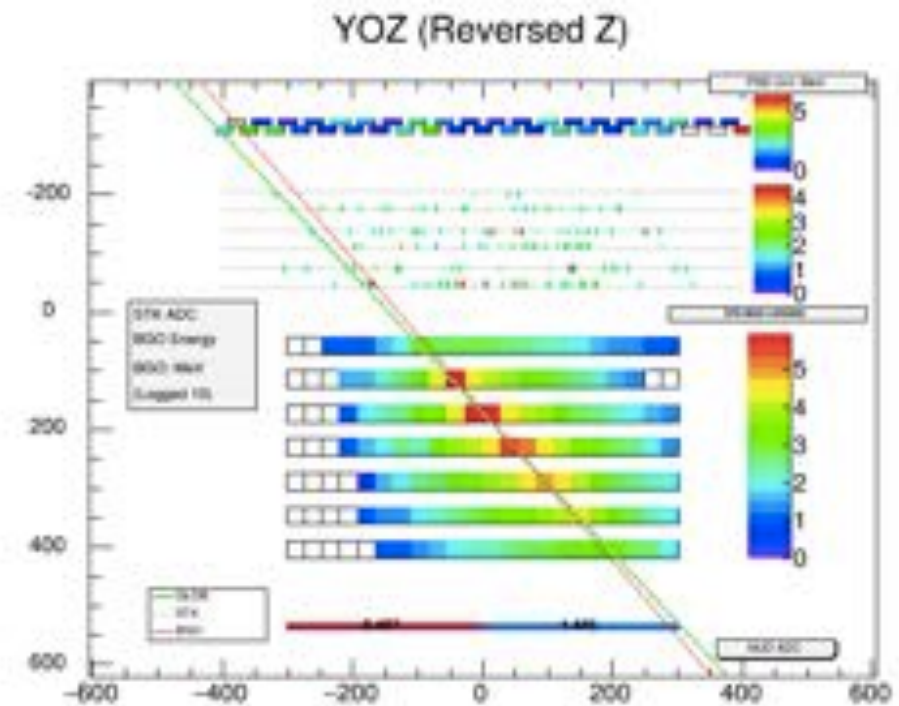
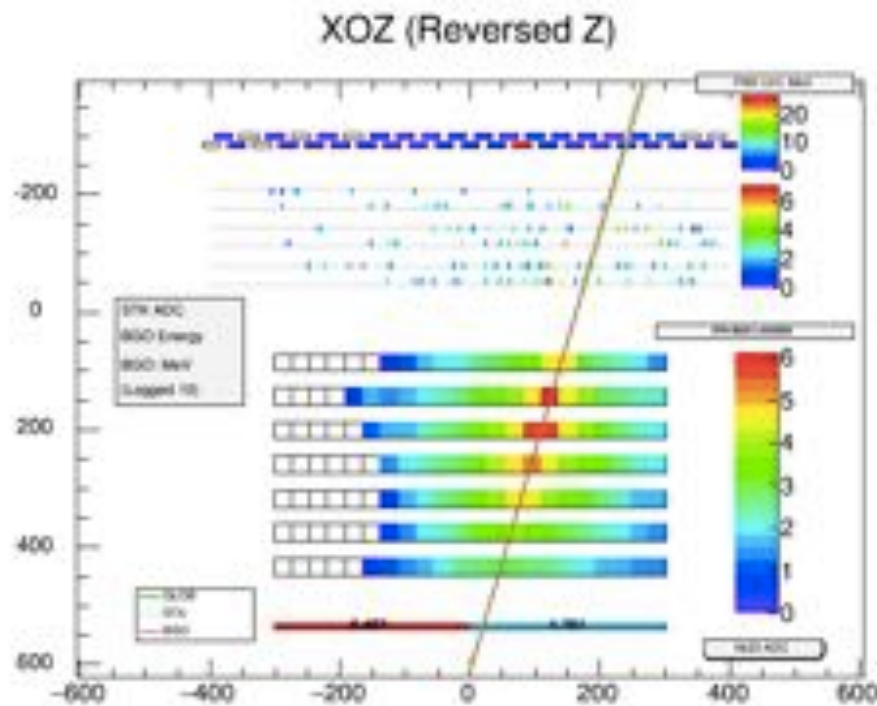
# Cross checks with independent analyses

- 3 independent analyses have been performed, using different PID (e-p separation) methods
  - Shower shape ( $\zeta$  method): combine lateral and longitudinal shower shape variables to one parameter  $\zeta$
  - Principal component analysis
  - boosted decision tree
- Three methods gave very consistent (within the statistical uncertainties) results of the final electron flux

The analysis of the  $\zeta$  method is presented here

# The global shower shape variable $\zeta$

- Electrons have narrower and short showers
  - Lateral shower shape
    - $\text{sumRms}$  = sum of the shower width of all 14 BGO layers
  - Longitudinal shower shape
    - $\mathcal{F}_{\text{last}}$  = ratio of layer energy to total BGO energy of the last layer that has energy

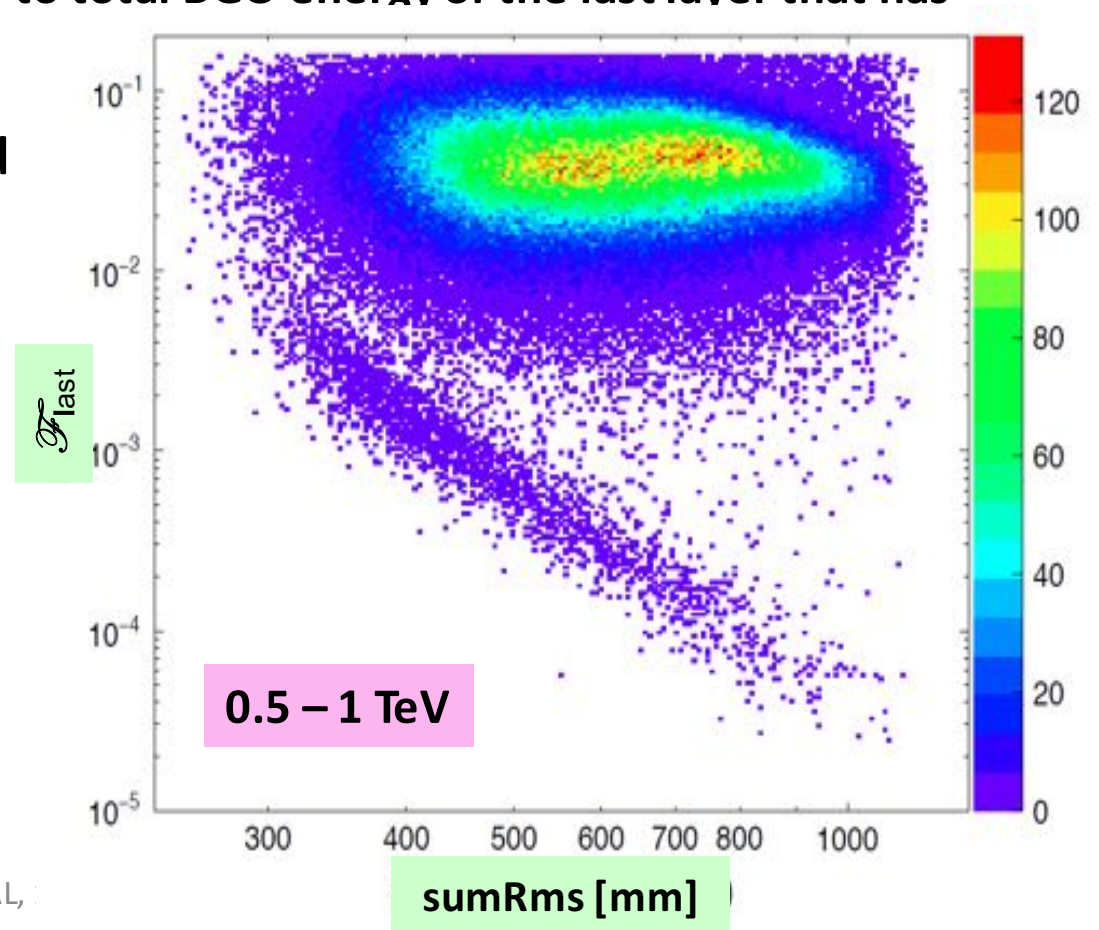
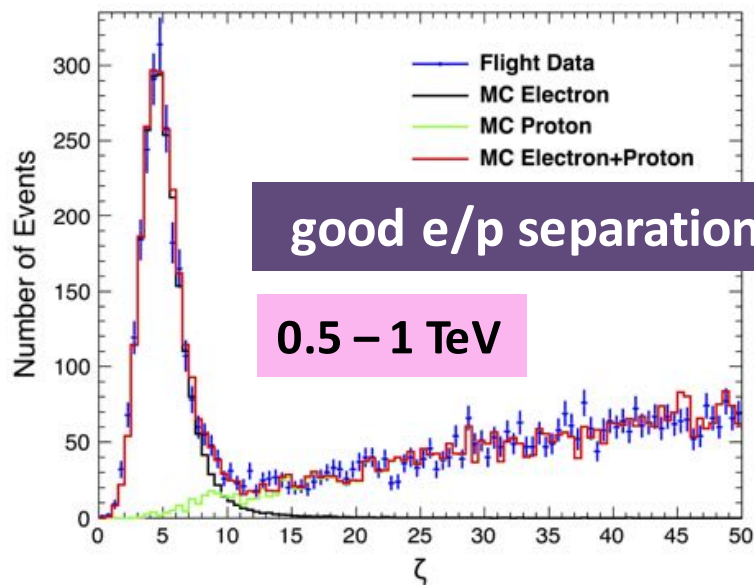




# The global shower shape variable $\zeta$

- Electrons have narrower and short showers
  - Lateral shower shape
    - **sumRms** = sum of the shower width of all 14 BGO layers
  - Longitudinal shower shape
    - $\mathcal{F}_{\text{last}}$  = ratio of layer energy to total BGO energy of the last layer that has energy
- **sumRms** and  $\mathcal{F}_{\text{last}}$  are combined to a global shower variable

$$\zeta = \mathcal{F}_{\text{last}} \times (\text{sumRms})^4 / (8 \times 10^6)$$



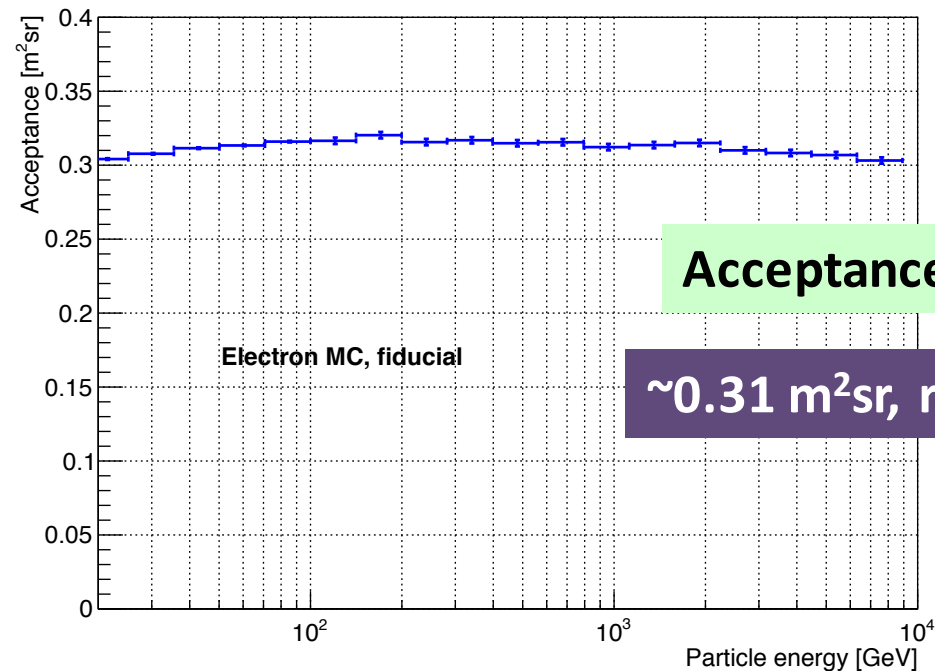
# The cut flow

- **Fiducial cuts**
  - Define acceptance
- **Trigger:** passed the High Energy Trigger (HET)
- **Selection**
  - **Pre-selection (clean up)**
    - Remove lateral entry, large shower and some heavy nuclei MIPs to facilitate background extrapolation later
  - **Heavy nuclei removal: separate cuts for 2 mutually exclusive samples: track-matched and BGO only**
    - Track-matched: removing heavy nuclei with PSD and STK charge
    - BGO-only: removing heavy nuclei with top 2 BGO layers
  - **Signal extraction using the  $\zeta$  variable**

# Fiducial cuts

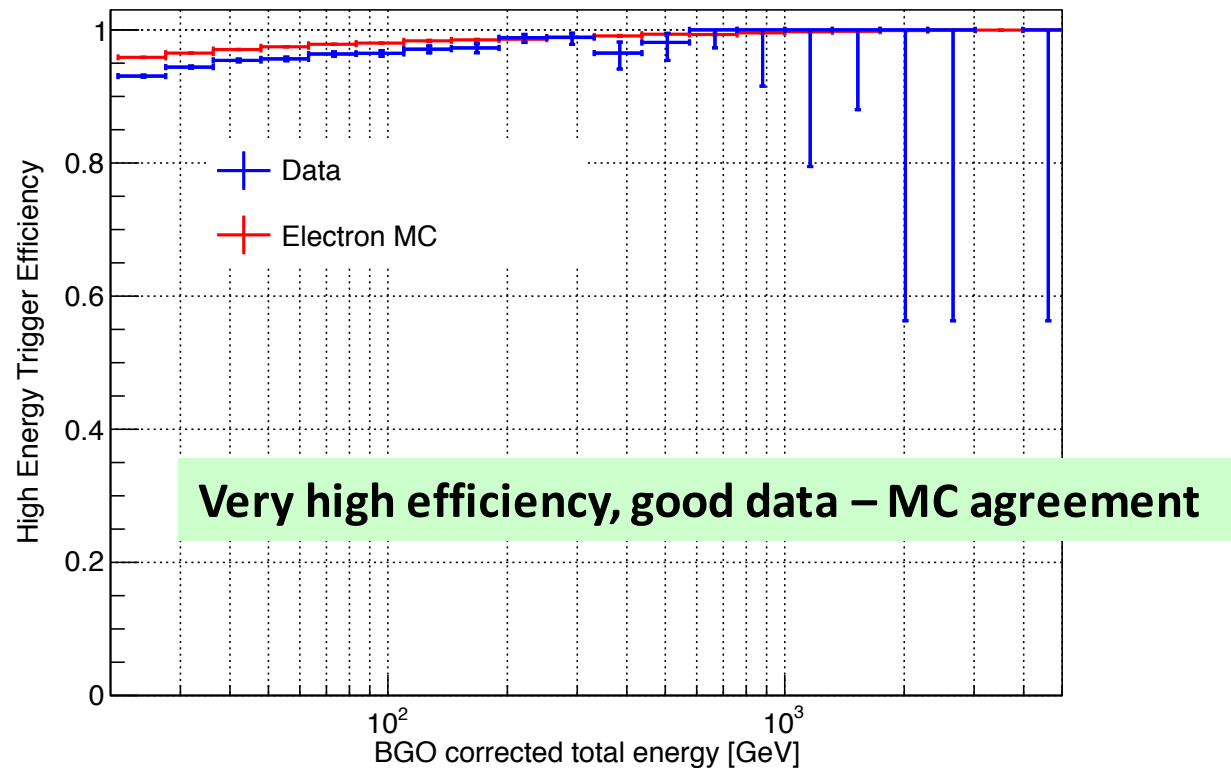
- **3 cuts to ensure:**
  - The particle energy is well contained in the BGO
  - The particle is entering from the top of the detector
- **Fiducial cut 1**
  - BGO full-span: shower direction extrapolates to within 28 cm from the center at the top and the bottom surfaces of the BGO in both X and Y
    - BGO bar length is 60 cm
- **Fiducial cut 2**
  - Remove events in which the BGO bar with maximum energy in second, third and fourth layer is on the outside (bar 0 or 21)
- **Fiducial cut 3**
  - Remove events with max. layer energy/total energy deposited  $> 35\%$

# Acceptance



- **Systematics are evaluated by checking the data-MC consistency in cut variables**
  - Residual differences used to estimate systematic uncertainties
- **Total error 2.2%, flat in energy. Main contribution from the BGO full-span cut (2%)**
  - **BGO full-span cut systematics: the precisely reconstructed electron track can be used to evaluate the extrapolation resolution of the shower direction**
  - Data-MC difference in extrapolation resolution  $\sim 2$  mm  $\rightarrow$  2% acceptance change

# Trigger Efficiency



- Trigger efficiency is evaluated from the pre-scaled Low Energy trigger
  - Unbiased for the High Energy Trigger, validated with MC
  - Cross checked with the (heavily) pre-scaled Unbiased Trigger
- The overall agreement is excellent. Difference at low energy comes mainly from proton contamination which has lower trigger efficiency
- MC efficiency used for flux calculation, half of the difference as systematics  
→ **1.5% at 25 GeV and 1% at 2 TeV**

# Preselection

- **Very loose clean-up cuts**
  - 2 cuts to reduce large hadron shower and lateral entry events + 1 cut to remove heavy nuclei MIPs
- **maxRms < 100 mm**
  - maxRms: the maximum width of all layers with energy > 1% of the total energy
- **Number of hits in the last layer (nBarLayer13)**
  - $n\text{BarLayer13} < 8 \log(\text{totalE}) - 5$ 
    - nBarLayer13 = number of bars with energy > 10 MeV in the last BGO layer
- **Low energy cleaning cut** (for events with raw energy < 250 GeV only)
  - Angular dependent lower cut on sumRms

**Preselection cuts are highly efficient for signal (>99.9%), and have negligible (<0.03%) systematics uncertainties**

# Heavy nuclei removal

- Heavy nuclei contamination is negligible in the signal region in data because of their large shower shape
- But heavy nuclei should be removed in the background region of data
  - **Bkg region is used to normalize the  $\zeta$  template from proton MC**
- Different cuts are used for events with and without a track match
  - **Track-matched: removing heavy nuclei with PSD and STK charge**
    - PSD bar is identified by extrapolating the STK track to the PSD
  - **BGO-only: removing heavy nuclei with top 2 BGO layers**

**Cuts are defined to be highly efficient for signal (>99%), and have negligible (<0.3%) systematics uncertainties**

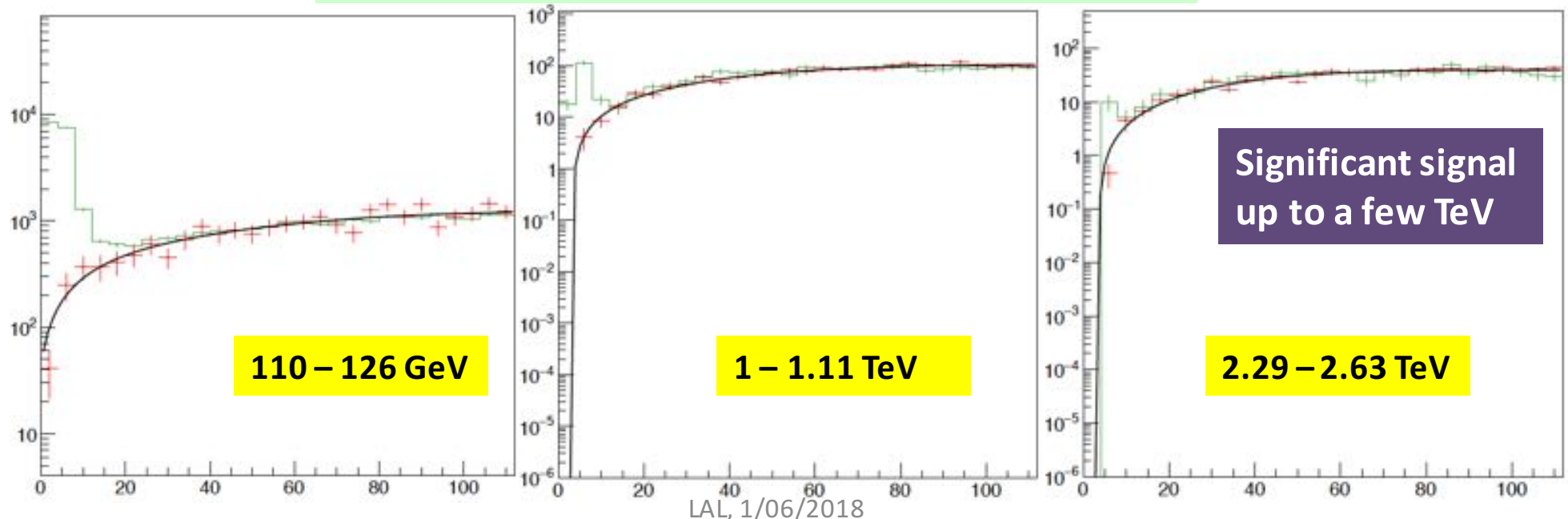
- Systematics are evaluated by data-MC comparison of cut variables
  - **Tracking efficiency has good data-MC agreement (see next page)**
    - No systematic assigned since events failed track selection go to the "BGO only" category

# Signal extraction using the $\zeta$ variable

- **Strategy**

- Extract smooth  $\zeta$  templates of each energy bin from proton MC, using interpolation across energy bins to reduce fluctuation, and then fit
- In each energy bin of data
  - Fit the proton  $\zeta$  template to data in the background region ( $20 < \zeta < 100$ )
  - Subtract the number of bkg. in the signal region ( $\zeta < 8.5$ ) predicted by the fitted template to obtain the signal:  $S_i = N_i - B_i$

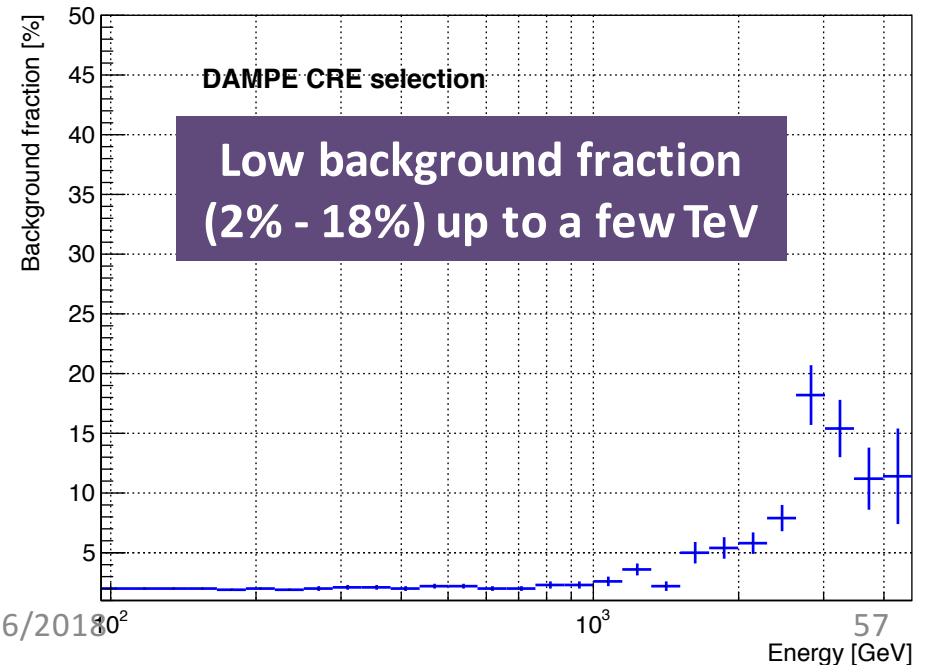
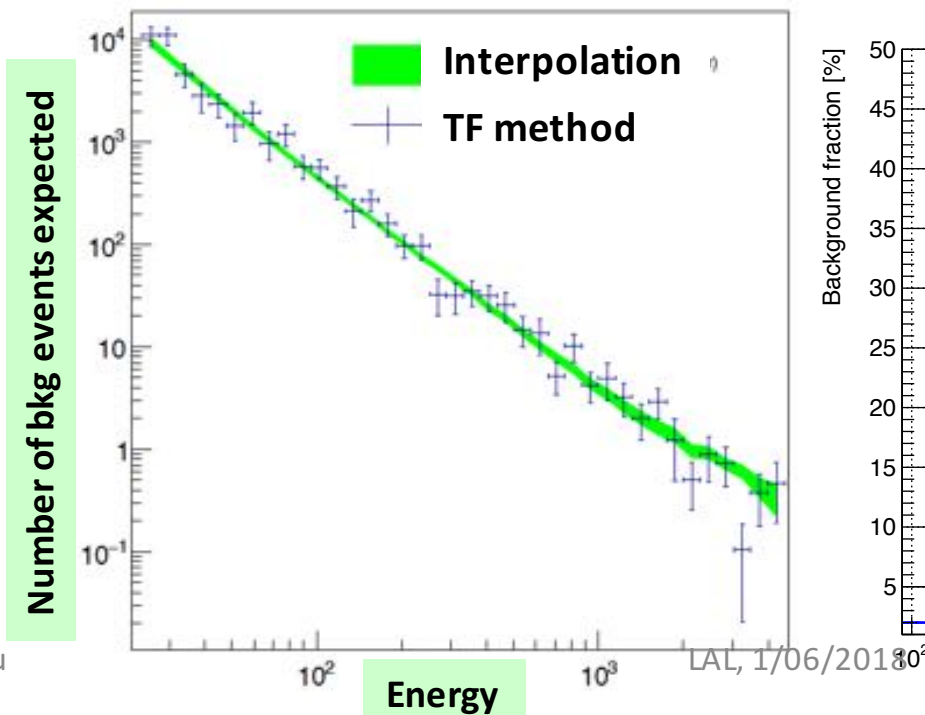
bin\_0000109.65-000 **3 examples. Total 38 bins from 24 GeV to 4.57 TeV** 002290.87-0002630.27\_GeV





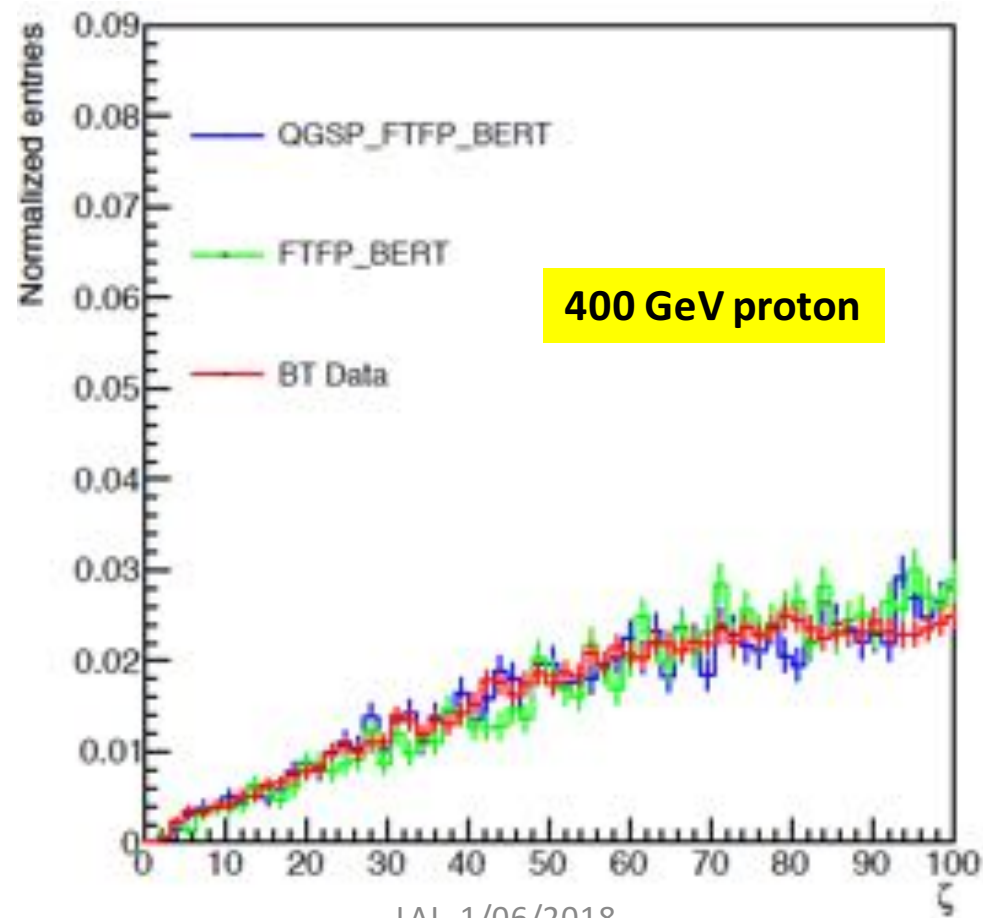
# Systematics of background estimate

- Sources of systematics considered
  - Choice of interpolation fitting function
  - MC Statistical uncertainty in interpolation fit
  - Choice of binning of  $\zeta$  for interpolation across energy bins
  - Choice of control region
  - Data statistical uncertainty in the control region fit
- Cross checked with the method using a simple MC transfer factor (TF) to scale events from background region to signal region



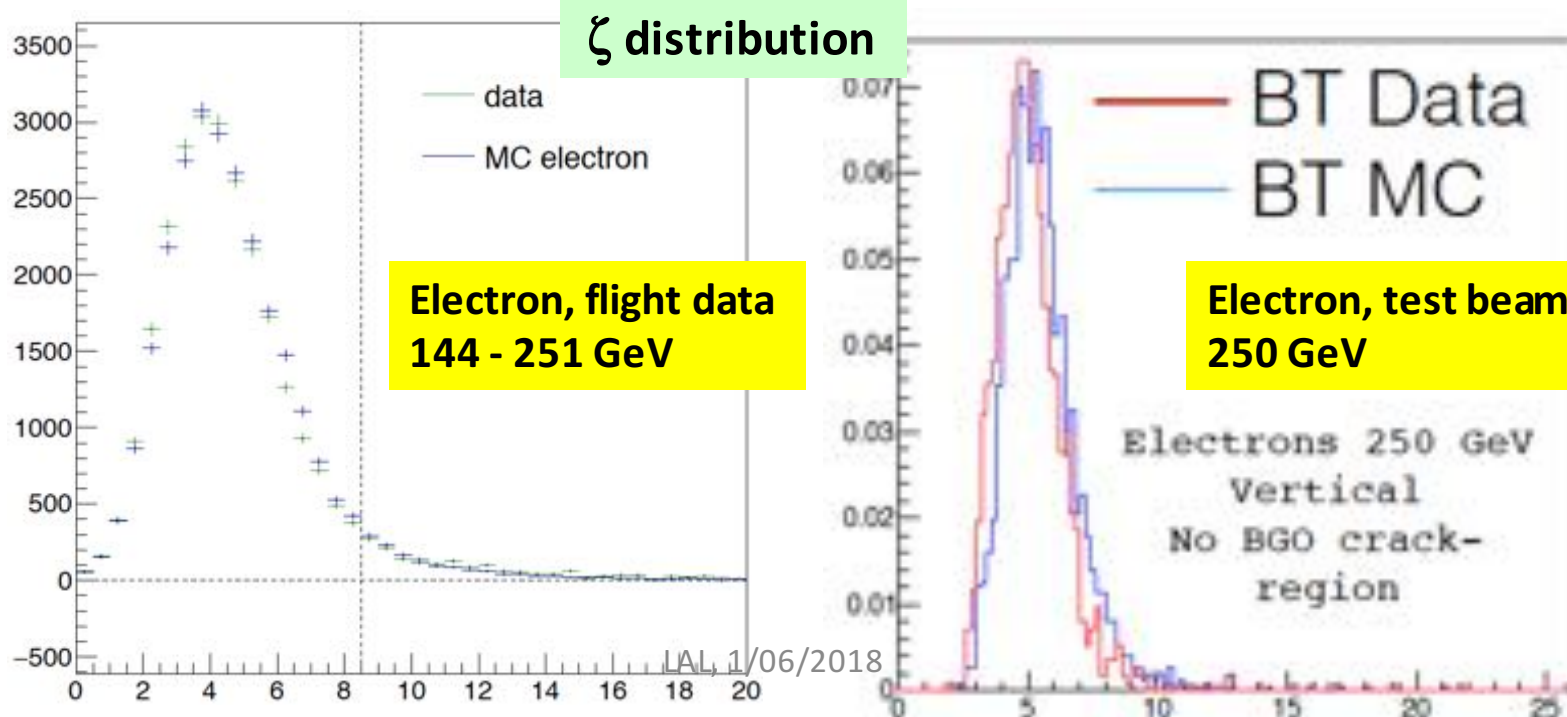
# Validation of the proton $\zeta$ distribution

- Validation with 400 GeV protons data taken at the CERN SPS
  - Two MC hadronic models are compared: QGSP and FTFP
  - Data-MC have good agreement (within statistics)
  - Two hadronic models have similar distributions



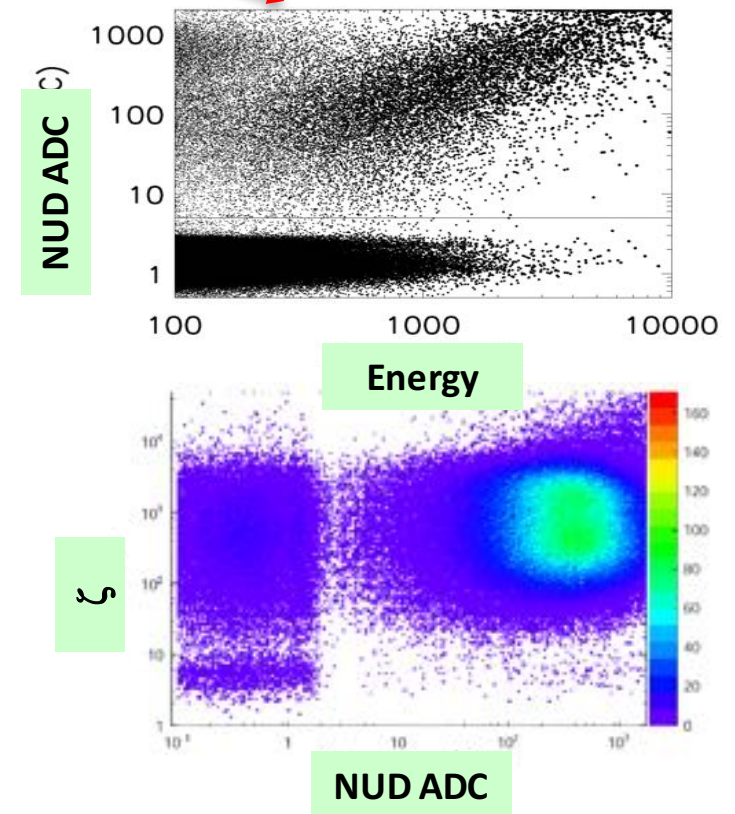
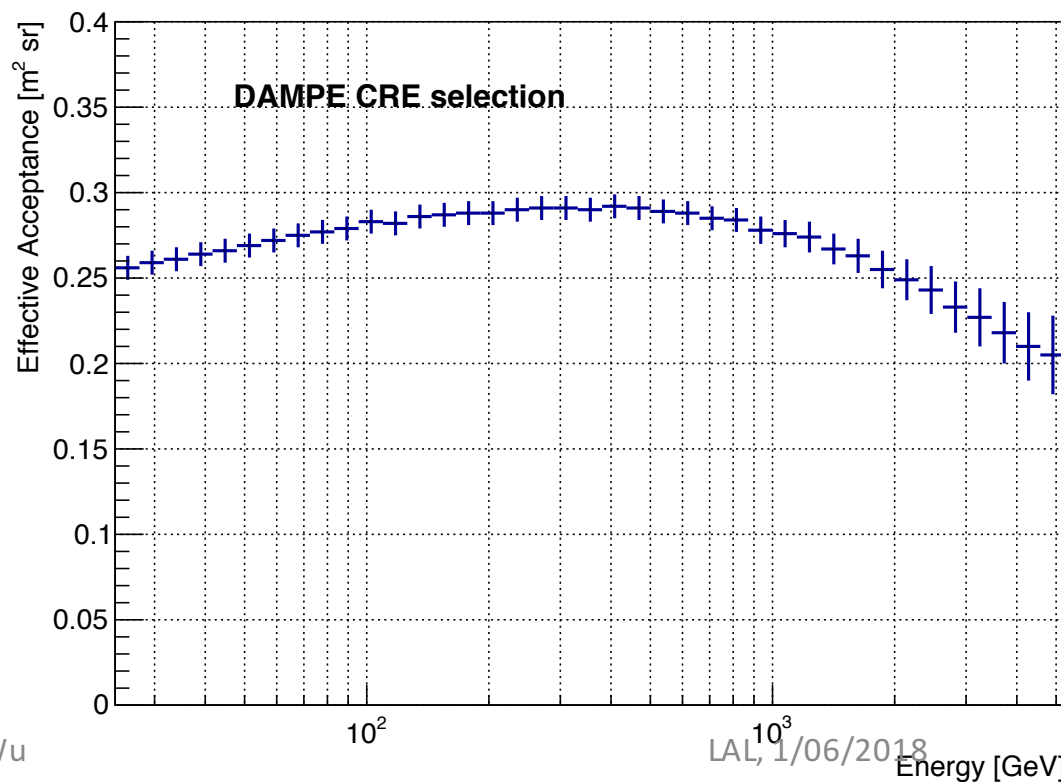
# Efficiency and systematics of the $\zeta$ cut

- Compare the  $\zeta$  distribution of electron MC to data after subtracting the proton background
  - Very good agreement in general
  - Small energy-dependent difference : -1.9% at 25 GeV to 8.4% at 2 TeV
    - Confirmed with 250 GeV electron CERN test beam data
  - **MC efficiency is corrected for this difference**
    - Half of the difference is taken as systematics



# Effective acceptance and systematics

- Since no unfolding is needed, the acceptance and efficiency can be multiplied to become the “effective acceptance”
  - Efficiency is smooth vs. energy, drop of efficiency due to tight cut
  - **Simple tight cut ( $\zeta > 8.5$ ) to select a clean sample for first publication**
    - Validated with loose (energy dependent) cut  $\rightarrow$  compatible results
  - Future: multivariate analysis (ML), Neutron detector



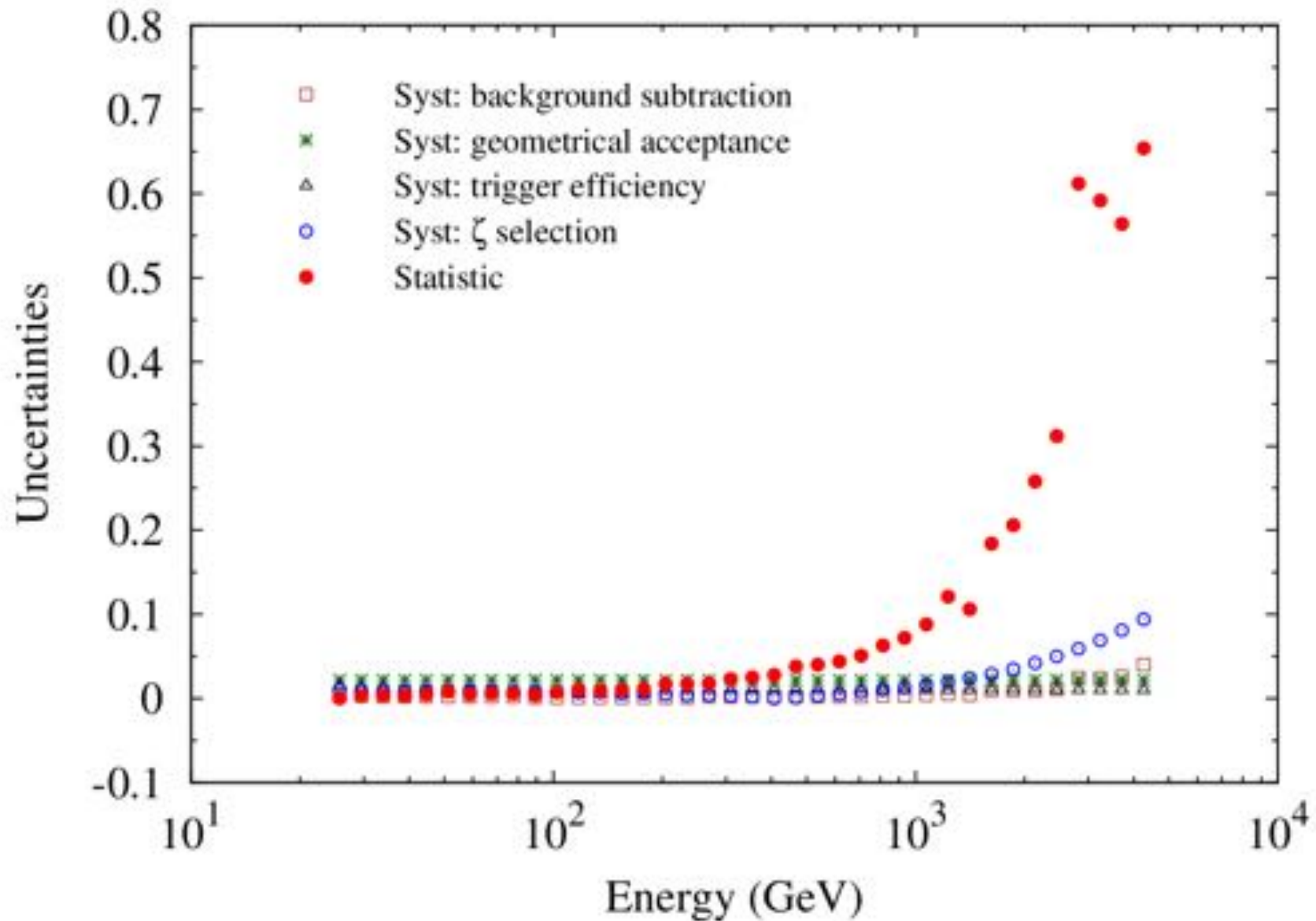
# Summary of all uncertainties

- **Acceptance: 2.2%**
  - main contributor BGO geometrical acceptance
- **Efficiency: 1.8% (25 GeV) - 9.4% (4.5 TeV)**  $\Phi_i(E_{true}) = \frac{dN_i/dE_{true}}{A_i T} = \frac{N_i - B_i}{\epsilon_i A_i W_i T}$ 
  - main contributors: trigger and  $\zeta$  cut
- **(Ni – Bi) "statistical error":**  $\Delta Ni$  is stat.,  $\Delta Bi$  is syst. and stat. (from bgk norm.)
  - 25 GeV:  $\delta(Ni - Bi) = 0.32\%$ , negligible
  - 2 TeV:  $\delta(Ni - Bi) = 25.6\%$ , dominated by  $\delta Ni = 24.2\%$  ( $N = 17$ )
- $T = 34913811.6$  sec, estimated file by file, remove DAQ d.t. (3.0725 ms) and operational down time
  - Two independent calculations agree within 0.08%
- **Total systematics on flux: < 10%**
  - 2.8% (25 GeV) to 9.6% (4.5 TeV)

**Plus  $\lesssim 2\%$  of absolute energy scale uncertainty ( $\rightarrow \sim 5\%$  shift in flux )**

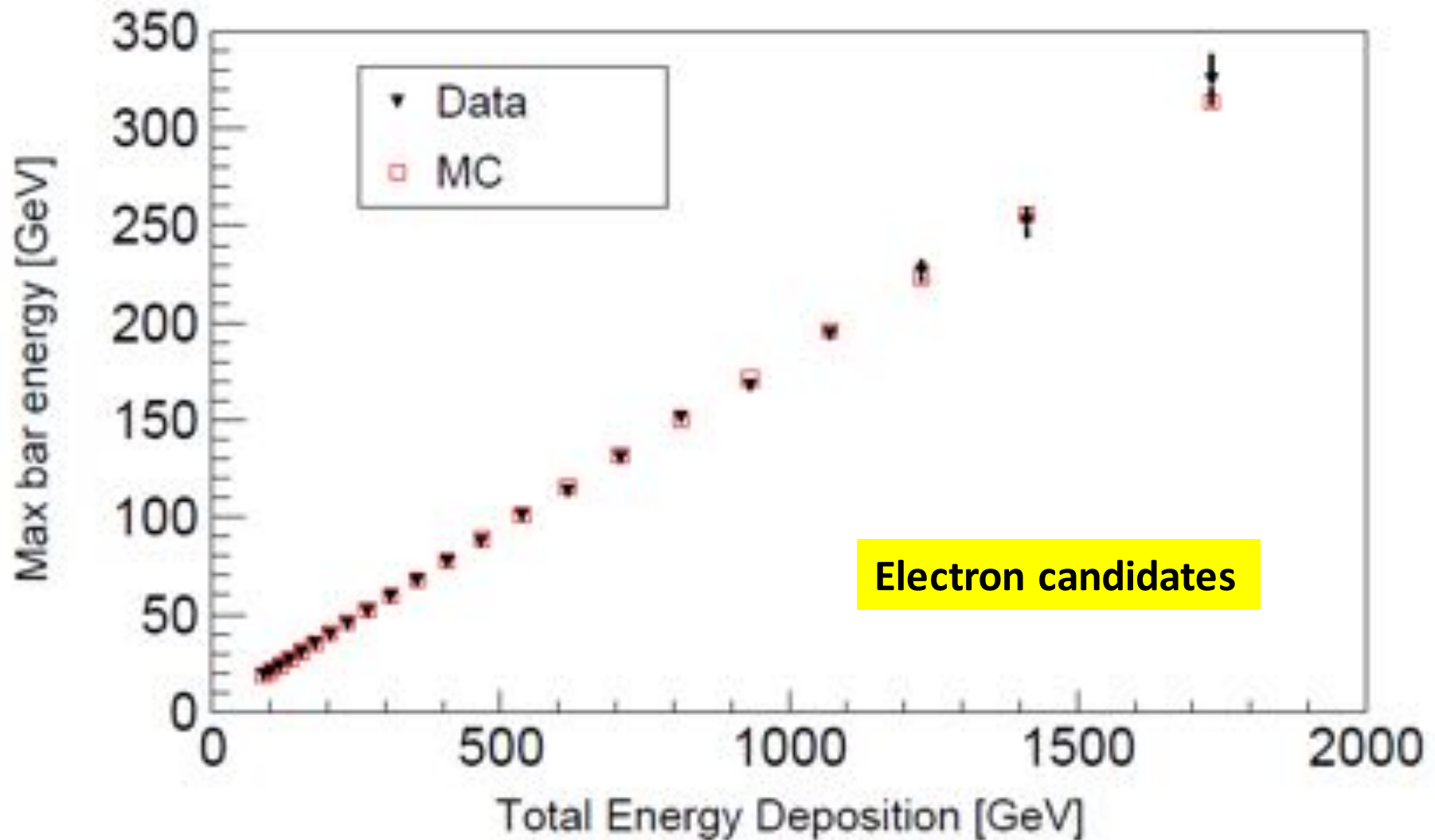
**Most precise  $\sim$ TeV measurement!**

# Systematic and statistical uncertainties



Xin V **Statistical error dominating at  $\sim$ TeV, can be improved with more data**

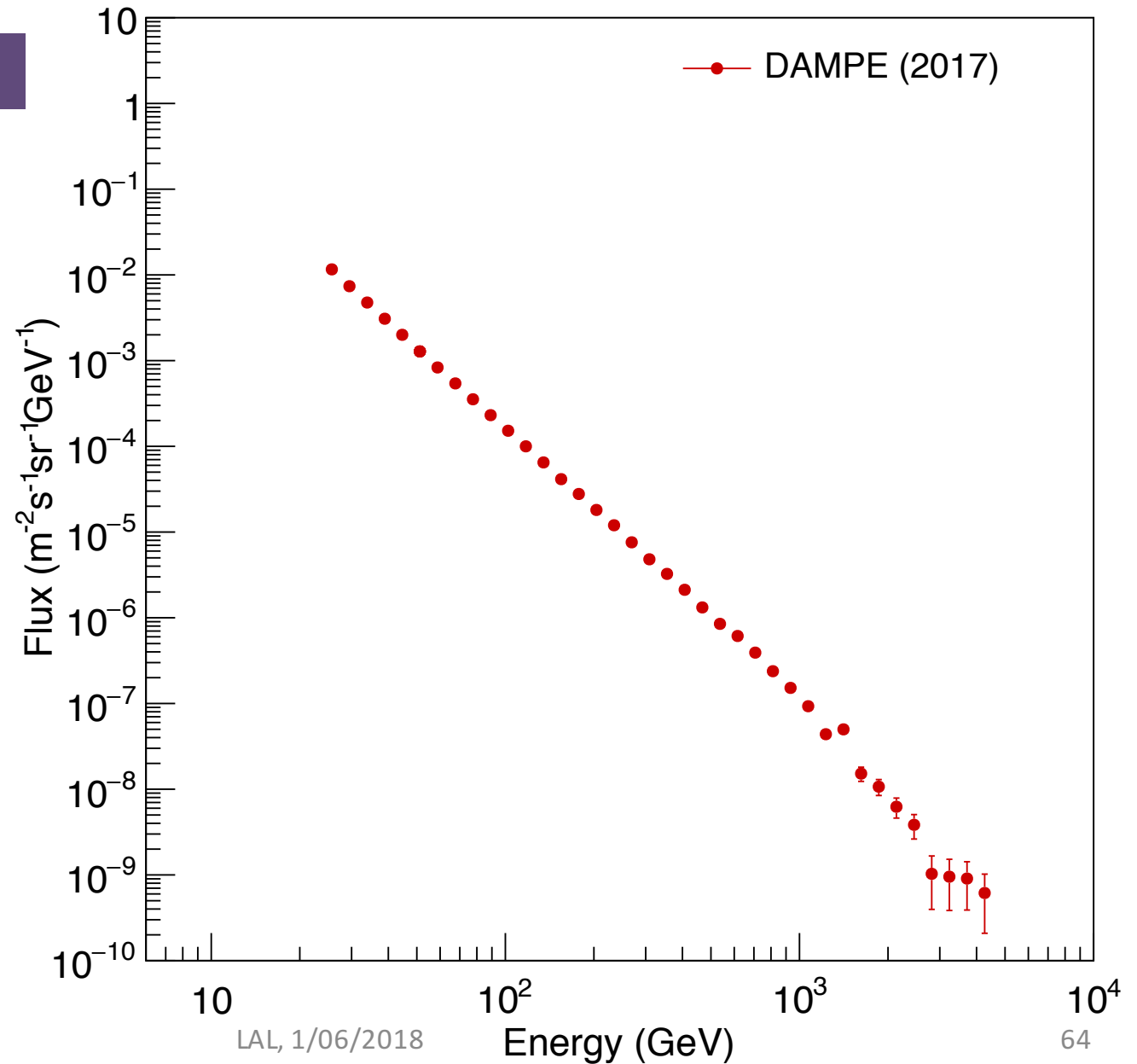
# No saturation effect



No saturation effect in BGO bars up to more than 300 GeV per bar

# DAMPE electron + positron (CRE) flux

~8 orders of magnitude!





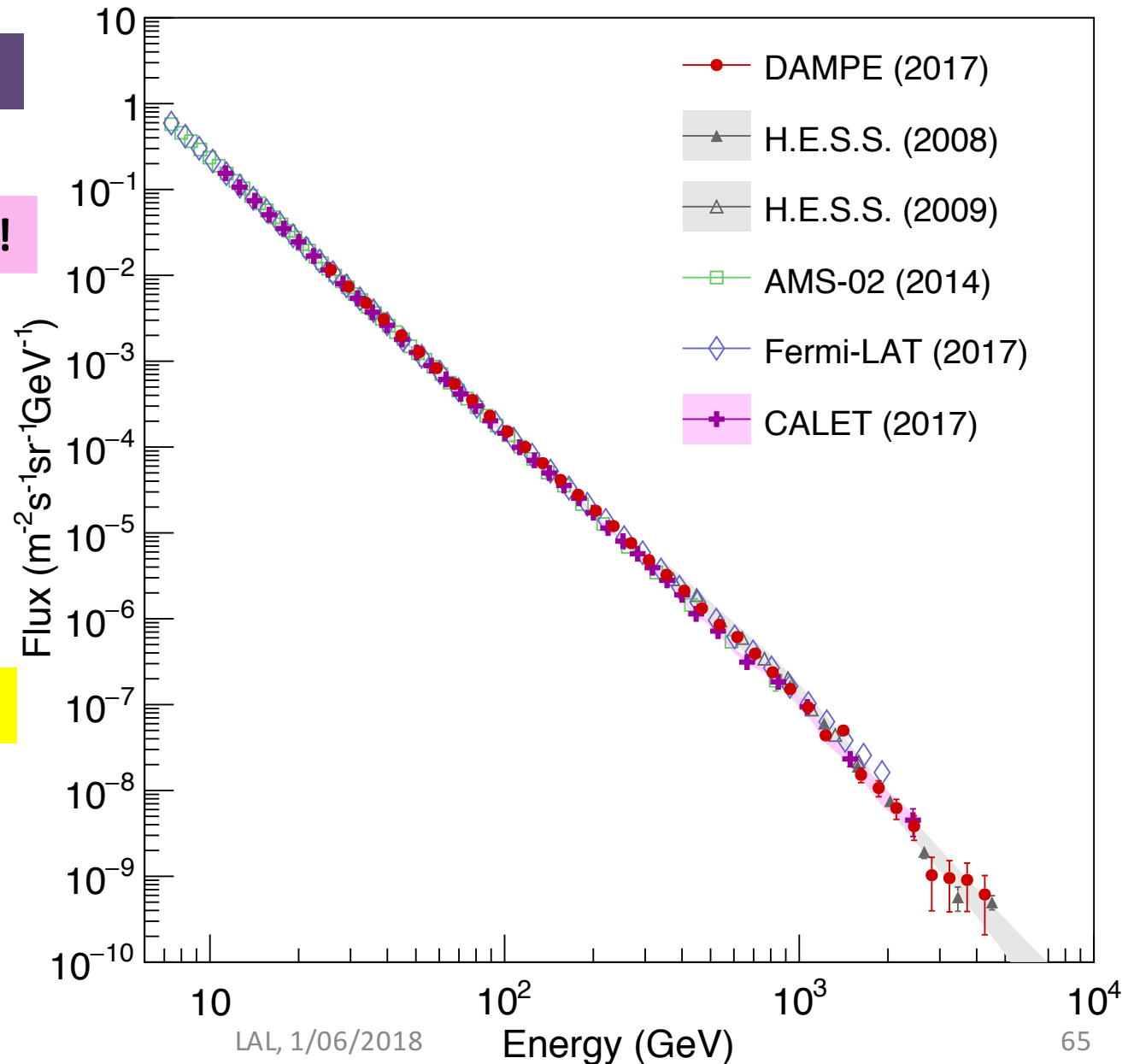
# CRE flux comparison

~8 orders of magnitude!

hard to see the features!

hard to tell differences!

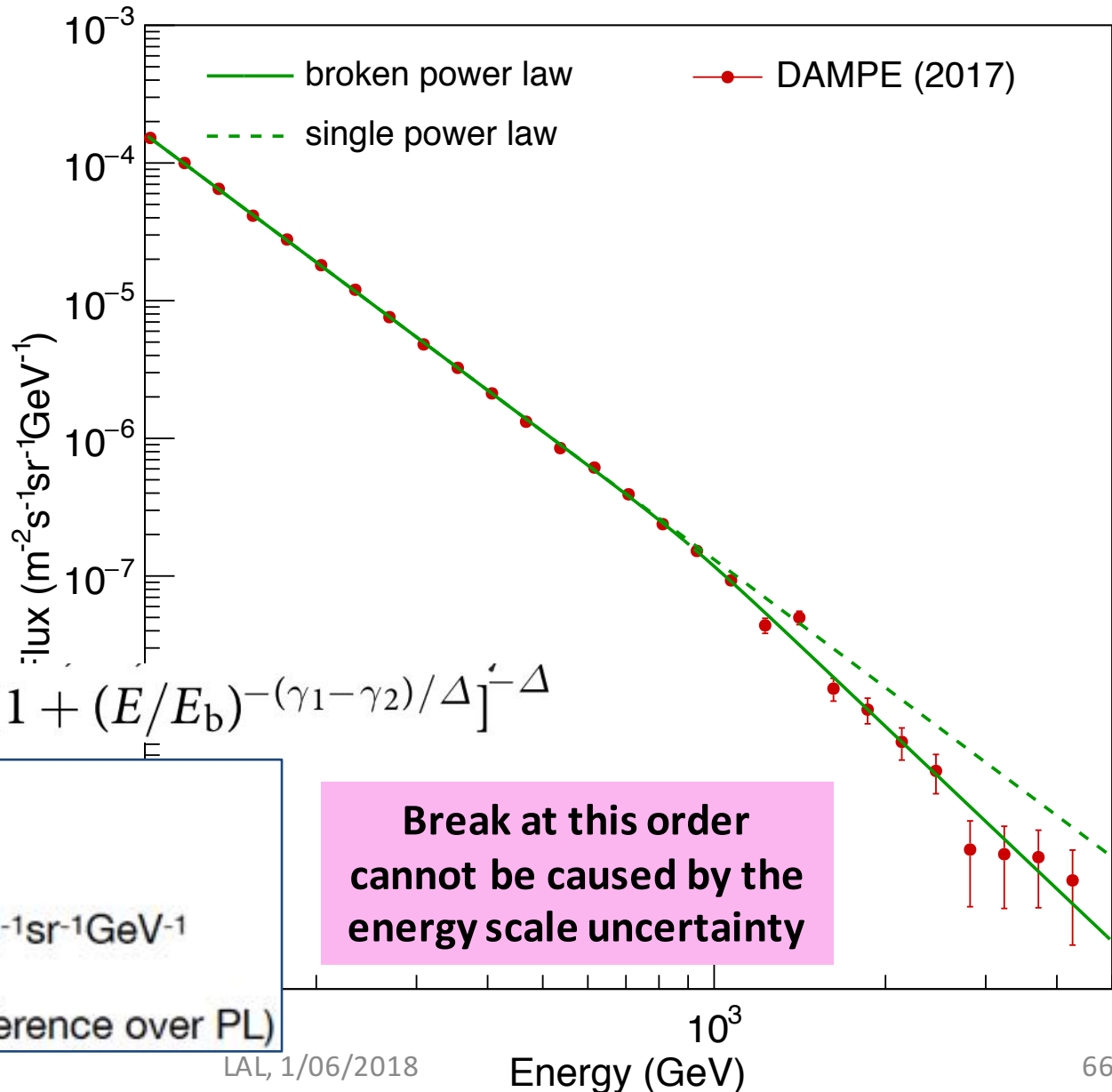
5-20% where other experiments have comparable precisions (< 1 TeV)



# Zoom in to > 100 GeV

A break around 1 TeV is clearly observed!

Fit with Smoothly Broken Power-Law



$$\Phi = \Phi_0 (E/100 \text{ GeV})^{-\gamma_1} [1 + (E/E_b)^{-(\gamma_1 - \gamma_2)/\Delta}]^{-\Delta}$$

$\gamma_1 = 3.09 \pm 0.01$   
 $\gamma_2 = 3.92 \pm 0.20$   
 $E_b = 914 \pm 98 \text{ GeV}$   
 $\Phi_0 = (1.64 \pm 0.01) \times 10^{-4} \text{ m}^{-2} \text{ s}^{-1} \text{ sr}^{-1} \text{ GeV}^{-1}$   
 $\Delta = 0.1$   
 $\chi^2/\text{NdF} = 23.3/18$  (6.6 $\sigma$  preference over PL)

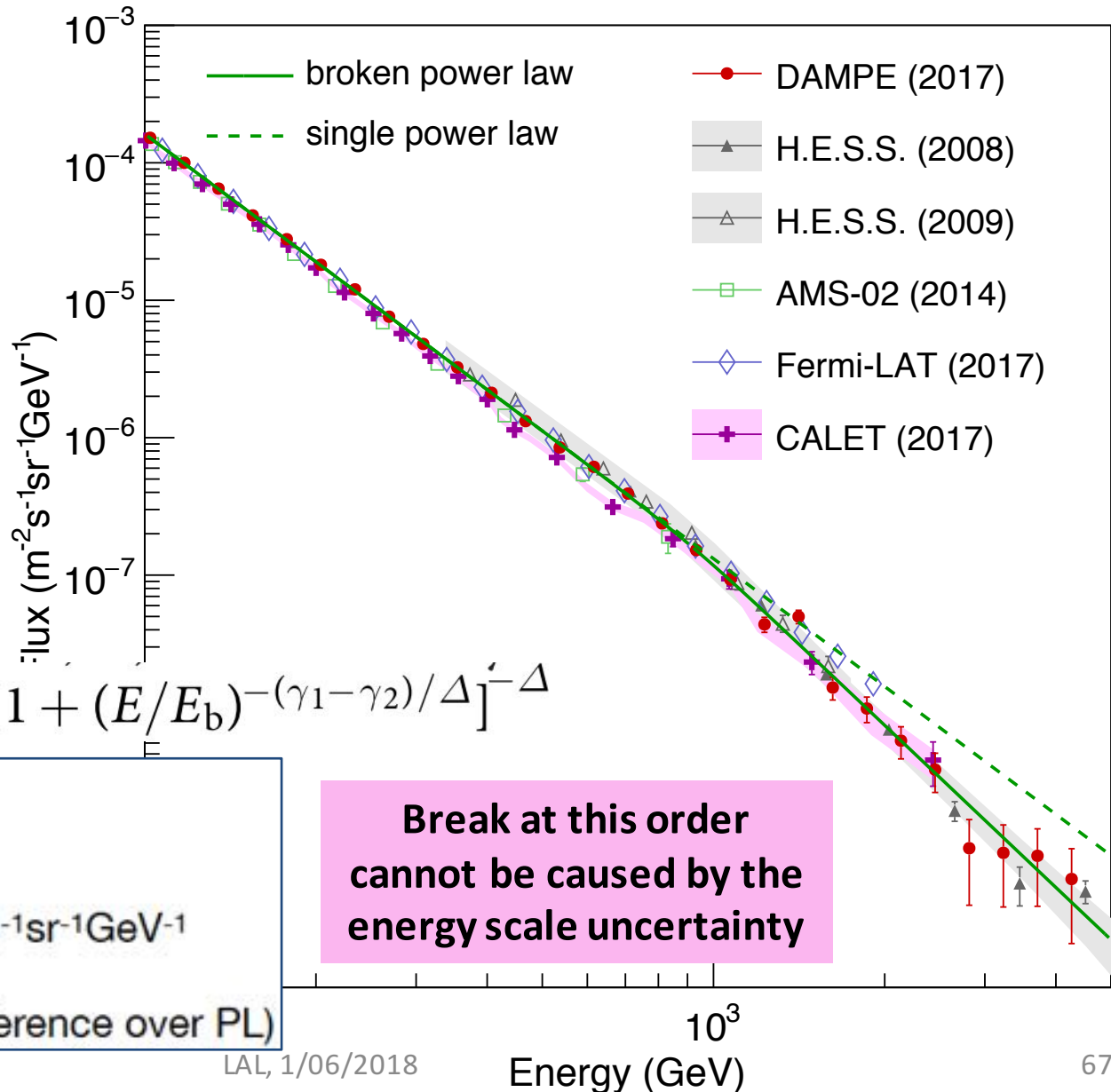
Break at this order cannot be caused by the energy scale uncertainty

# Zoom in to > 100 GeV

A feature around 1 TeV is clearly observed!

Also indicated by H.E.S.S. and CALET

Fit with Smoothly Broken Power-Law



$$\Phi = \Phi_0 (E/100 \text{ GeV})^{-\gamma_1} [1 + (E/E_b)^{-(\gamma_1 - \gamma_2)/\Delta}]^{-\Delta}$$

$\gamma_1 = 3.09 \pm 0.01$   
 $\gamma_2 = 3.92 \pm 0.20$   
 $E_b = 914 \pm 98 \text{ GeV}$   
 $\Phi_0 = (1.64 \pm 0.01) \times 10^{-4} \text{ m}^{-2} \text{ s}^{-1} \text{ sr}^{-1} \text{ GeV}^{-1}$   
 $\Delta = 0.1$   
 $\chi^2/\text{NdF} = 23.3/18$  (6.6 $\sigma$  preference over PL)

# Scaling up the flux by $E^3$

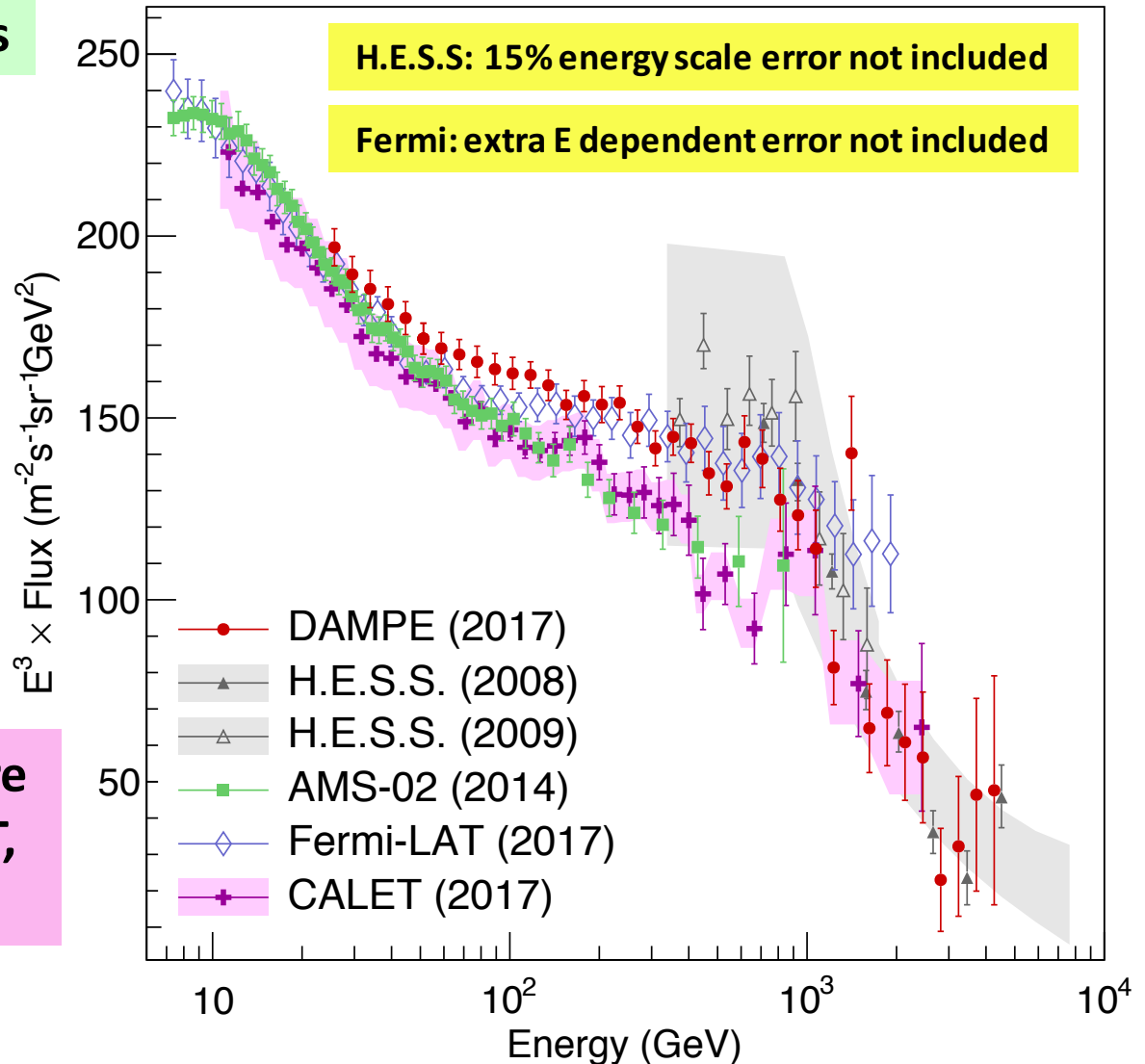
Easier to see spectral changes

But also distort the spectrum and exaggerate fluctuations!

Two features have emerged:

- a hardening at  $\sim 30\text{-}50$  GeV
- A break at  $\sim 1$  TeV

Many hypotheses  $\rightarrow$  need more data from DAMPE/AMS/CALET, and HERD!



# Scaling up the flux by $E^3$ , before DAMPE

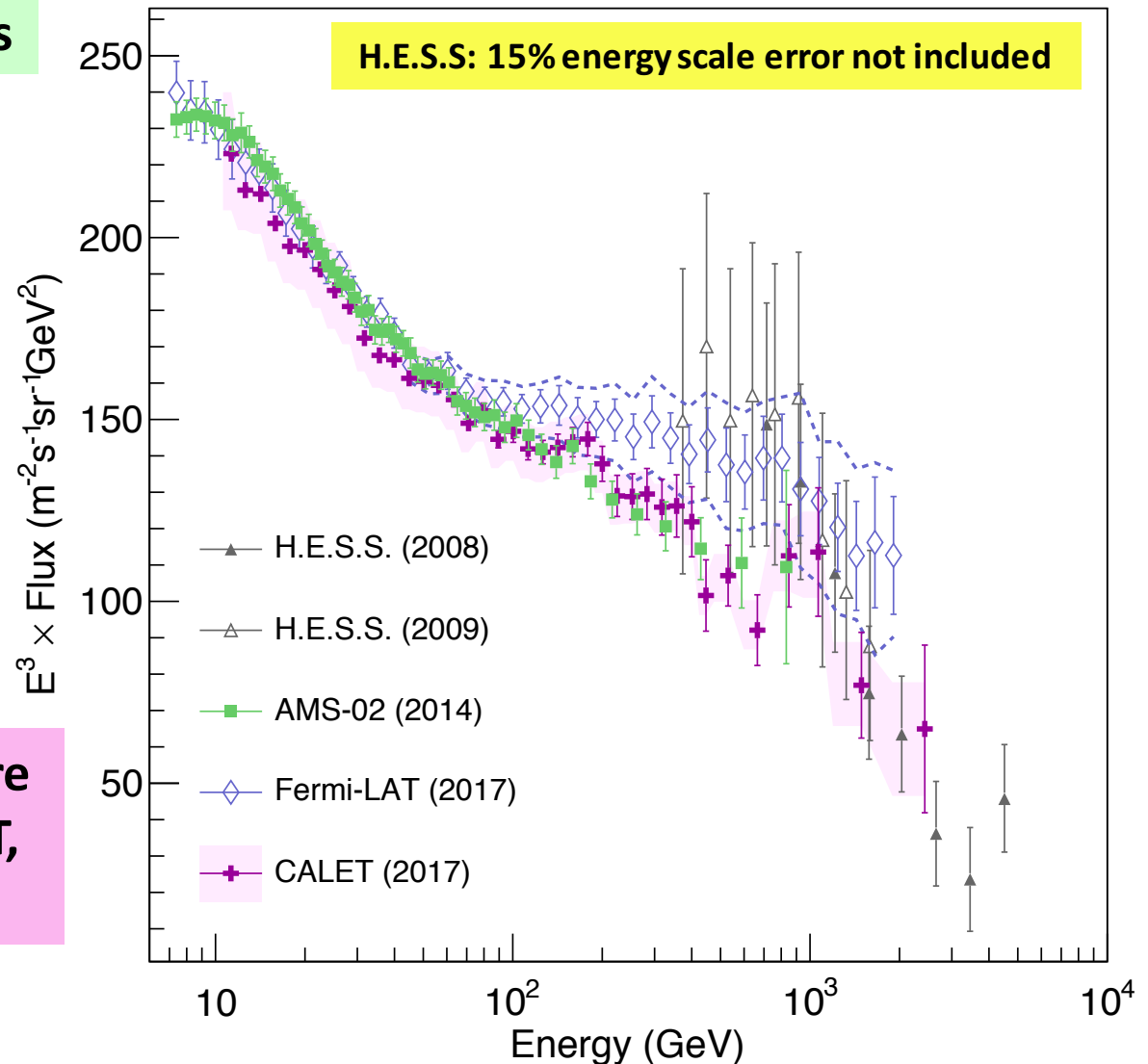
Easier to see spectral changes

But also distort the spectrum and exaggerate fluctuations!

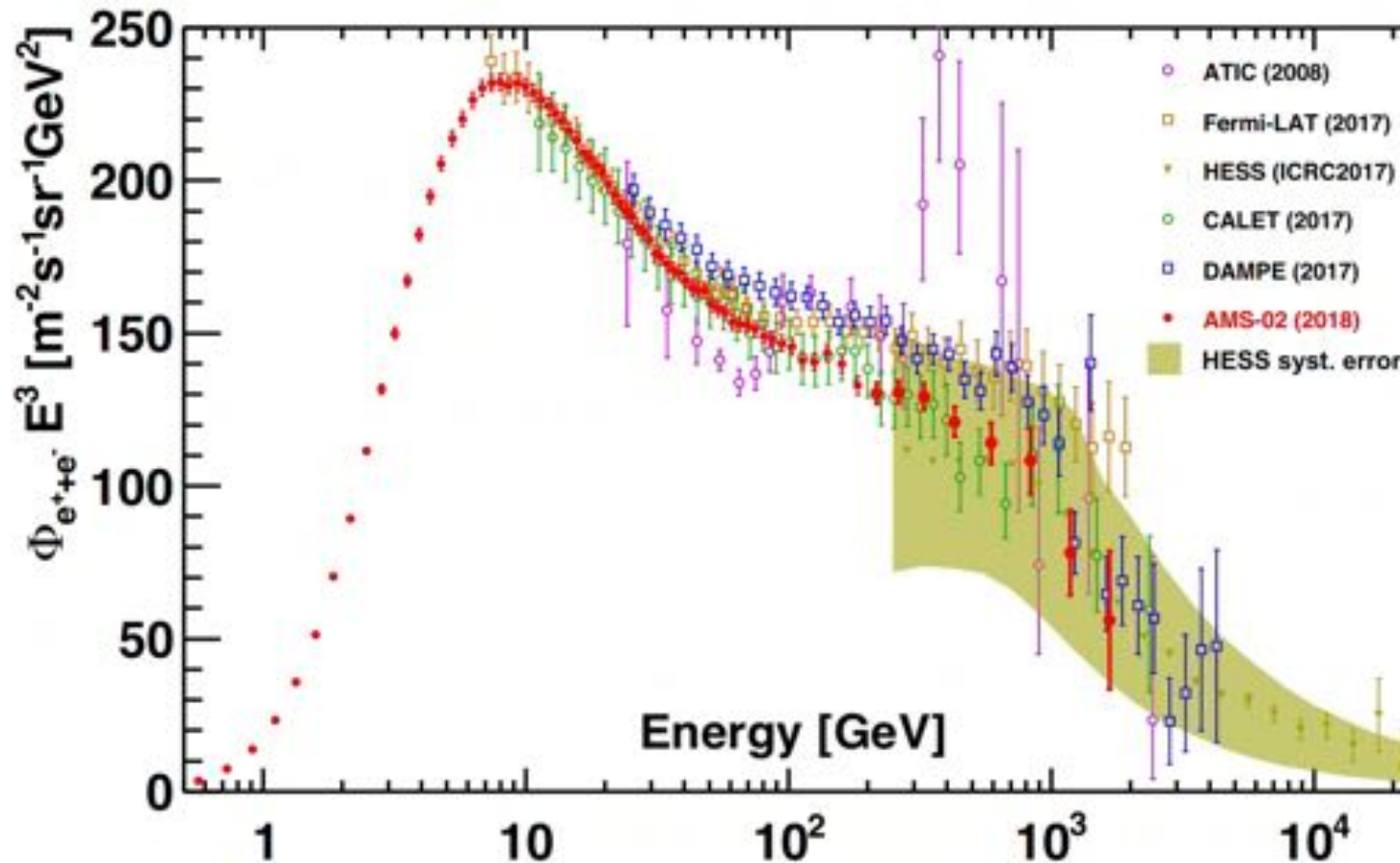
Two features have emerged:

- a hardening at  $\sim 30\text{-}50$  GeV
- A break at  $\sim 1$  TeV

Many hypotheses  $\rightarrow$  need more data from DAMPE/AMS/CALET, and HERD!

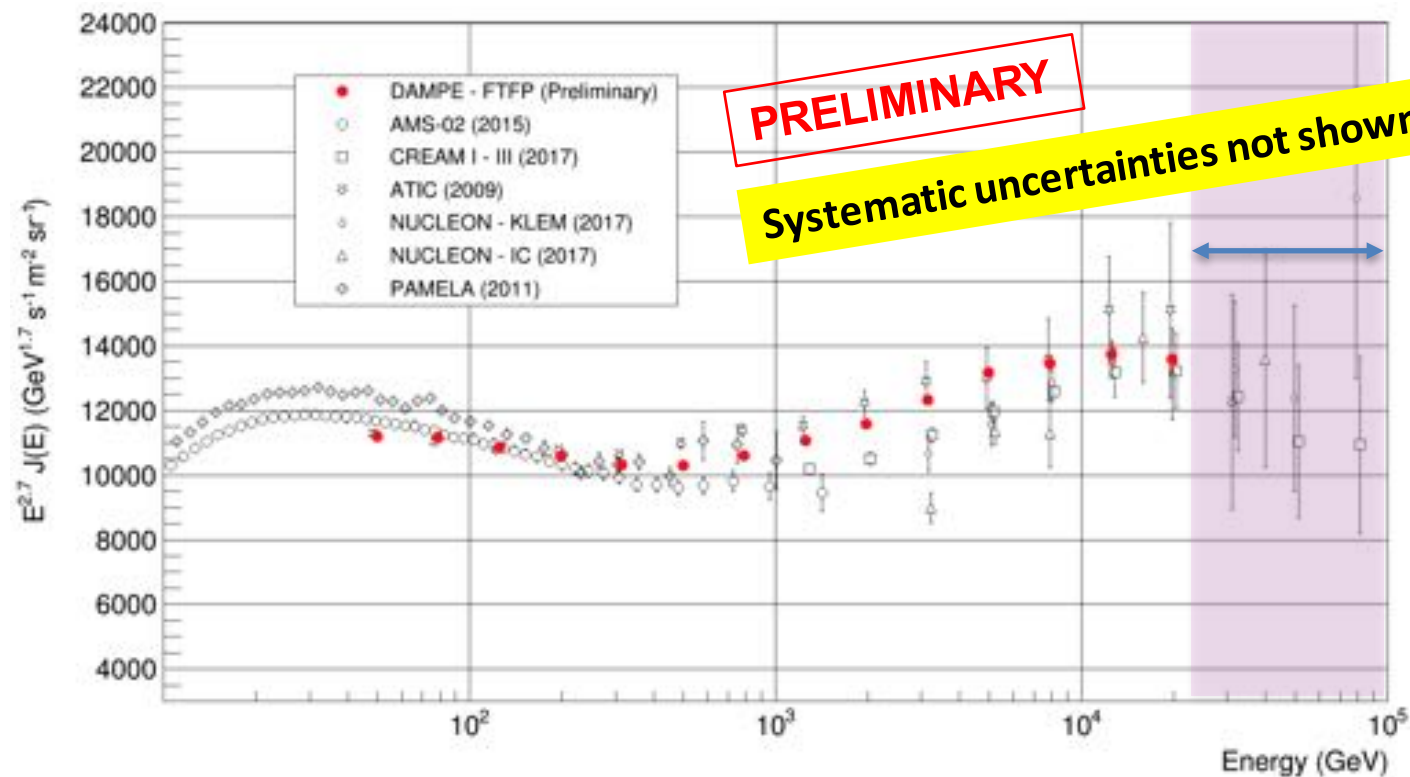


# Latest AMS result compatible with the TeV break



S. Ting, CERN colloquium, May 24, 2018

# Proton spectrum beyond 10 TeV/nucleon



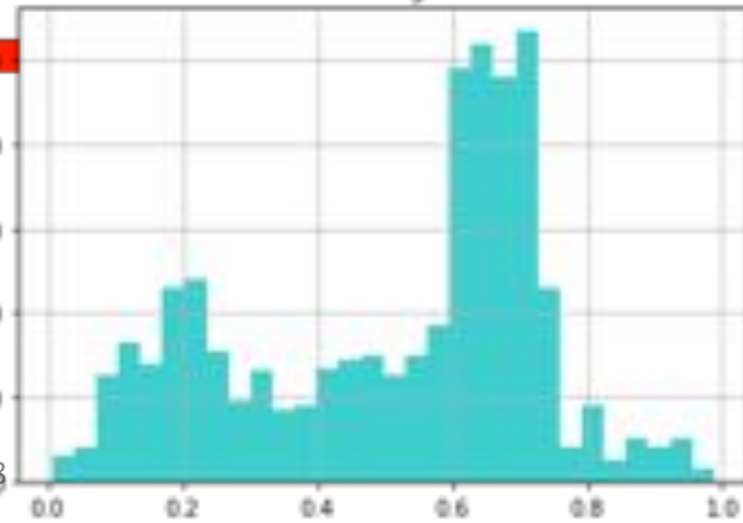
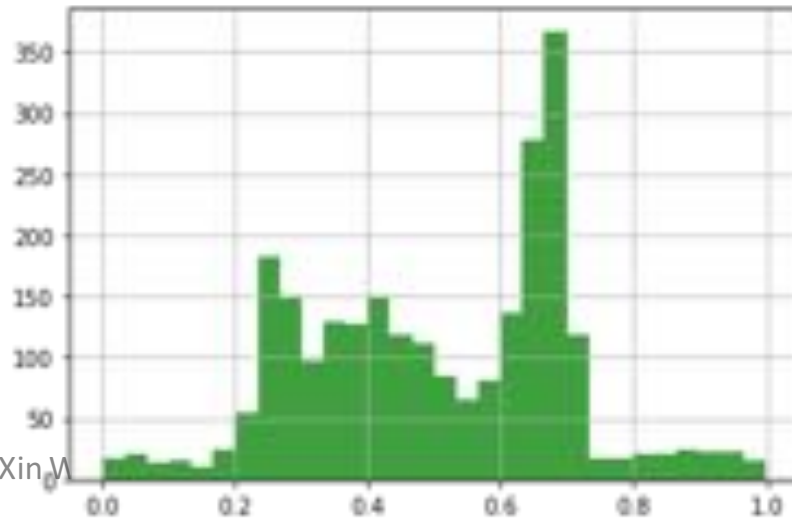
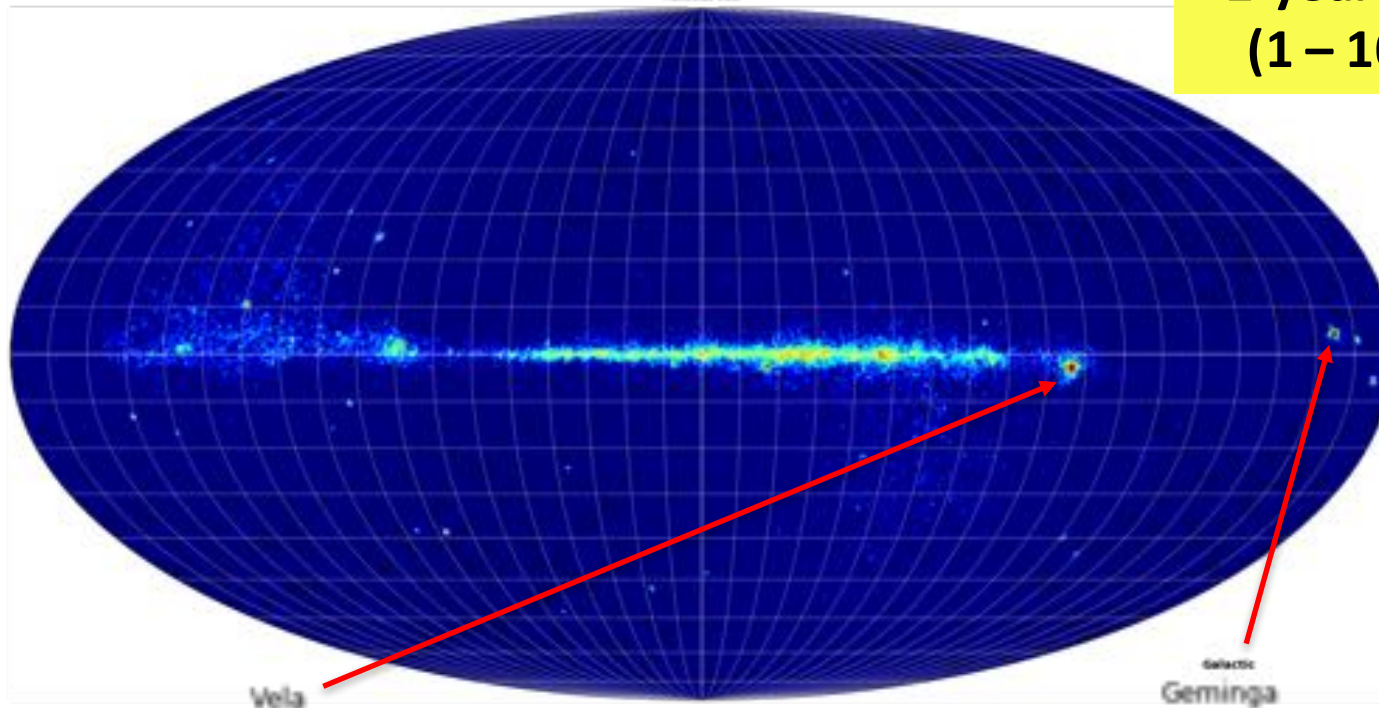
DAMPE proton flux up to 100 TeV in progress

Another spectral hardening > 1 TeV?  
and a softening > 20 TeV?

# Photon detection with DAMPE

- What are those tungsten plates for?

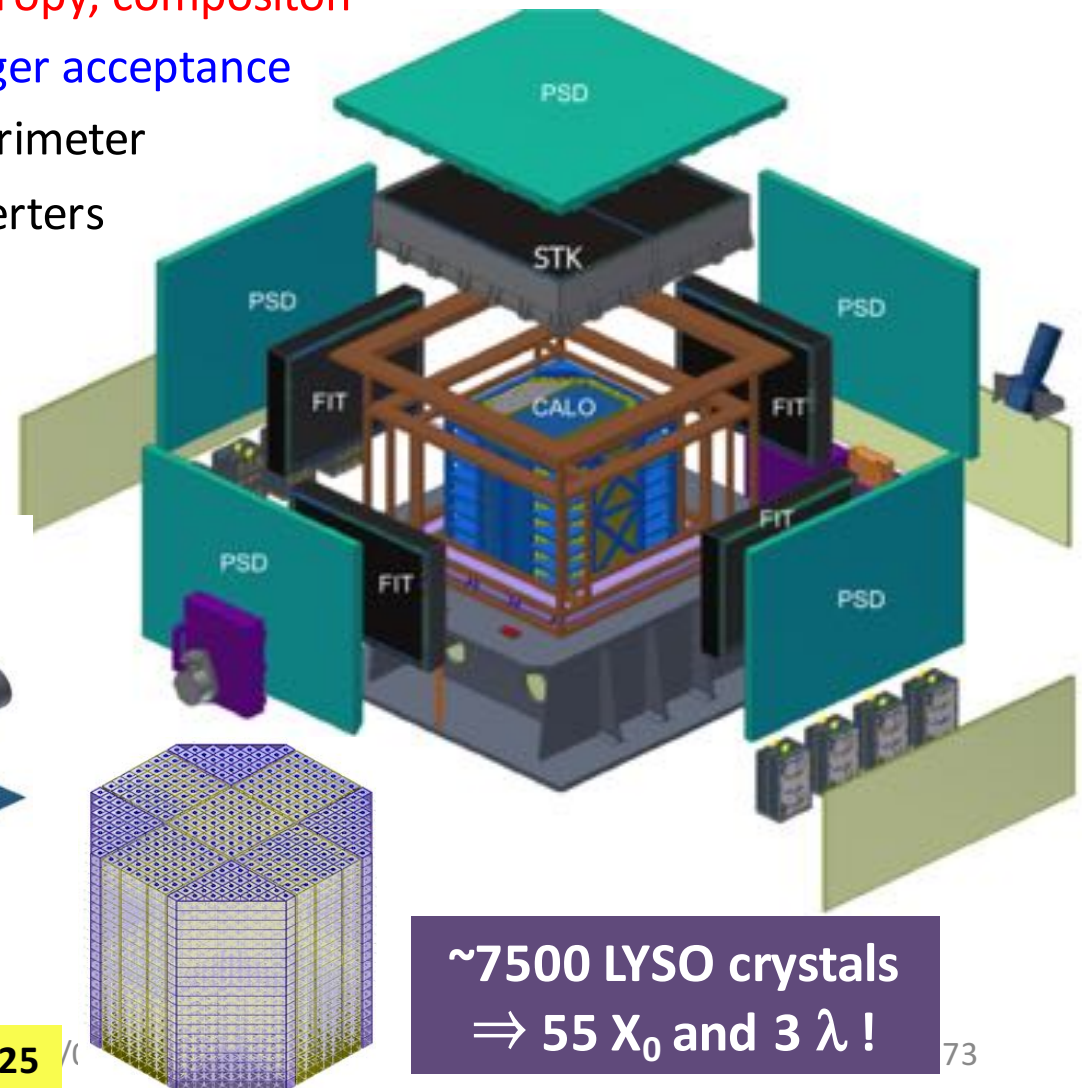
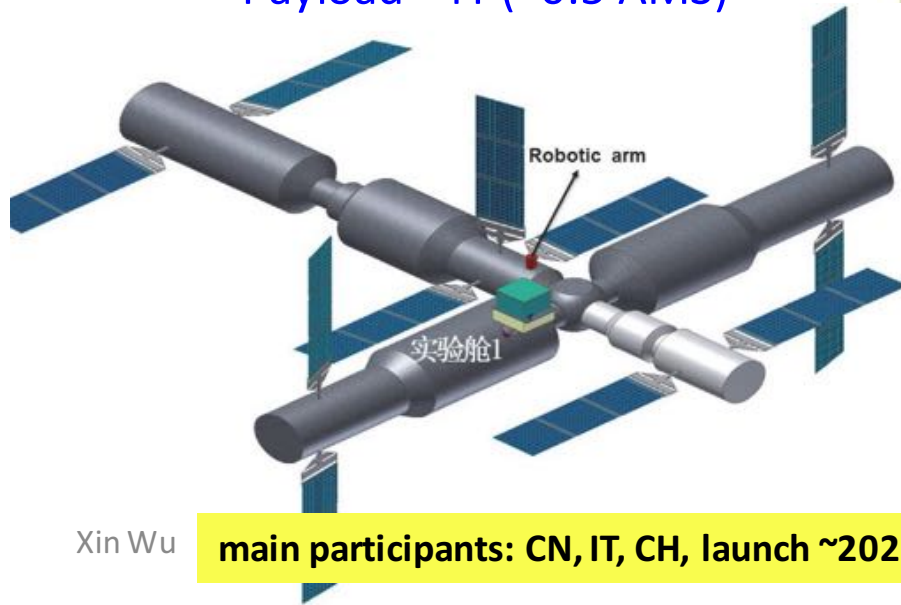
2-year sky map  
(1 – 100 GeV)





# Next: HERD (High Energy Radiation Detection facility)

- Next generation high energy particle detector on board the Chinese Space Station
  - Cosmic-ray physics at TeV - PeV, DM search, high energy  $\gamma$ -ray astronomy
  - CR source identification, anisotropy, composition
  - Similar to DAMPE, but with larger acceptance
    - LYSO cube 3D imaging calorimeter
    - Si/Fiber tracker, with converters
    - Anti-coincidence detector
    - Charge measurements
  - 5-side sensitive  $\Rightarrow \sim 3 \text{ m}^2\text{sr}$
  - Payload  $\sim 4\text{T}$  ( $\sim 0.5 \text{ AMS}$ )



**$\sim 7500$  LYSO crystals  
 $\Rightarrow 55 X_0$  and  $3 \lambda$  !**

# Conclusions

- DAMPE is working extremely well since launched more than 2 years ago
  - A precise electron + positron flux in the TeV region has been measured
    - A clear spectral break has been observed at  $\sim 1$  TeV  $\rightarrow$  **a new piece of puzzle to understand many mysteries in cosmic ray physics!**
  - Results on nuclei measurements (proton flux to 100 TeV!) coming soon
  - Photon detection capability is demonstrated. Need more statistics to profit the excellent energy resolution at high energy
- Space is the new frontier of particle physics
  - Still an exploratory science  $\Rightarrow$  ground breaking measurements are expected
- Experimentally challenging but many opportunities
  - Opportunities to apply latest particle detection technologies to space
  - Opportunities to develop specialized and multi-purpose space detector concepts
  - Close interplay between particle physics, nuclear physics, astrophysics, cosmology, solar physics, space weather, space radiation dosimetry, planetary explorati...

Particles in space: exciting sciences, broad interests, advanced technologies!